

EVALUATION OF THE AIRPACT2 AIR QUALITY FORECAST SYSTEM
FOR THE PACIFIC NORTHWEST

By

ABDULLAH AL MAHMUD

A thesis submitted in partial fulfillment of
the requirements for the degree of

MASTER OF SCIENCE IN ENVIRONMENTAL ENGINEERING

WASHINGTON STATE UNIVERSITY
Department of Civil & Environmental Engineering

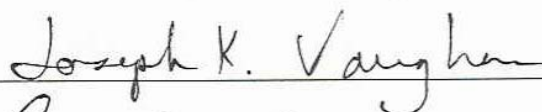
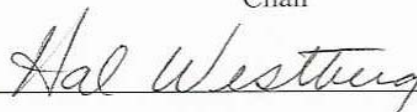
DECEMBER 2005

To the Faculty of Washington State University:

The members of the Committee appointed to examine the thesis of ABDULLAH AL MAHMUD find it satisfactory and recommended that it be accepted.



Chair



ACKNOWLEDGMENTS

I would like to take the opportunity to express my deepest sense of gratitude to my advisor Professor Brian Lamb for his continuous support, encouragement and guidance during my Master's work at Washington State University. I would also like to thank Professor Hal Westberg, Dr. Joe Vaughan, and Dr. Guangfeng Jiang for being in my thesis committee, and for their guidance, comments and suggestions. My special gratitude goes to Dr. Vaughan for acquainting me with the AIRPACT2 forecast system, and helping with the UNIX computing.

I want to recognize all the help I received from my colleagues: Jack Chen, Jeremy Avise, and Ying Xie at the Laboratory for Atmospheric Research air quality modeling group. I also thank my office mates for keeping the serenity our office at Dana 340. I appreciate the help I received from the CEE department office: thanks to Vicki Ruddick, Maureen Clausen and Tom Weber for their help.

Many thanks to the outside collaborators: colleagues from the University of Washington, Department of Ecology, Oregon Department of Environmental Quality, and Puget Sound Clean Air Agency for sharing their resources, and data with us.

Finally, I wish to thank my wife for her support and love, and my parents for their continuous encouragement in my education.

EVALUATION OF THE AIRPACT2 AIR QUALITY FORECAST SYSTEM
FOR THE PACIFIC NORTHWEST

Abstract

by Abdullah Al Mahmud, M.S.
Washington State University
December 2005

Chair: Brian K. Lamb

AIRPACT2 is a numerical photochemical air quality modeling system that generates daily forecasts of hourly gas-phase mixing ratios of ozone (O_3) and related species, including air toxic compounds, and particulate concentrations for the Pacific Northwest. The performance of the AIRPACT2 system has been evaluated in this work. The current AIRPACT2 system, which employs the second-generation CALGRID photochemical model, is undergoing conversion to utilize the third-generation CMAQ photochemical model. In anticipation of this change, an intercomparison between the CALGRID and the CMAQ model performances has also been completed. For both models, the forecast performance was assessed against observations from September and October 2003 using statistical measures including mean bias (MB), fractional bias (FB), mean error (ME), and fractional error (FE).

The system predicted O_3 quite accurately during an O_3 episode that occurred during early September; but over-estimated O_3 during non-episode periods later in the month. Although the CMAQ model produced performance results similar to the CALGRID model for the episode, CMAQ also predicted O_3 quite well for non-episodes and for urban sites as compared to CALGRID. The current AIRPACT2 system yielded the following monthly statistics: MB of 14 ppb and FB of 40% for urban sites, and MB of 8 ppb and FB of 22% for semi-urban/rural sites, respectively. Using CMAQ in AIRPACT2 improved these statistics: MB of 0 ppb and FB of -

4% for urban sites, and MB of 1 ppb and FB of 6% for semi-urban/rural sites. Both CALGRID and CMAQ captured the temporal patterns of the air toxic compounds benzene, acetaldehyde, formaldehyde, perchloroethylene and 1,3-butadiene correctly; however, both models over-estimated ambient levels, except for perchloroethylene. The degree of over-estimation was generally within the bounds of predicted levels within a 3 x 3 grid-cell matrix around the monitoring site. CMAQ predicted mixing ratios of formaldehyde and acetaldehyde more accurately than did CALGRID. For fine particulate matter (PM_{2.5}), both CALGRID and CMAQ captured the PM_{2.5} concentrations during the morning rush hour reasonably well, but overall under-estimated 24-hr average concentrations. As CALGRID only treats primary emissions of PM_{2.5}, the current system under-estimated PM_{2.5} at all sites.

TABLE OF CONTENTS

ACKNOWLEDGMENTS iii

ABSTRACT..... iv

LIST OF TABLES ix

LIST OF FIGURES xi

ATTRIBUTION..... xiv

CHAPTER 1

INTRODUCTION 1

 1.1 Overview of research 1

 1.2 Air quality models and forecasting 3

 1.3 AIRPACT2 system design..... 6

 1.3.1 MM5 version 3..... 6

 1.3.2 CALMET version 5 6

 1.3.3 MCIP version 2.2..... 7

 1.3.4 SMOKE version 2.0..... 8

 1.3.5 CALGRID version 1.6..... 9

 1.3.6 Initial and boundary conditions 10

 1.4 Model evaluation 11

 References..... 16

CHAPTER 2

EVALUATION OF THE AIRPACT2 AIR QUALITY FORECAST SYSTEM FOR THE
PACIFIC NORTHWEST..... 32

Abstract..... 33

2.1 Introduction.....	34
2.2 System design	36
2.3 Modeling domain and observation network	37
2.4 Evaluation methods.....	38
2.5 Results and discussions.....	39
2.5.1 Simulations of meteorological parameters.....	40
2.5.2 Simulations of O ₃	43
2.5.3 Simulations of air toxics	46
2.5.4 PM _{2.5} prediction	48
2.6 Conclusion	50
2.7 Acknowledgments.....	51
References.....	52
 CHAPTER 3	
EVALUATION OF THE AIRPACT2 AIR QUALITY FORECAST SYSTEM AND THE	
COMMUNITY MULTI-SCALE AIR QUALITY (CMAQ) MODEL FOR THE PACIFIC	
NORTHWEST	79
Abstract.....	80
3.1 Introduction.....	82
3.2 System design, modeling domain, and observation network.....	83
3.3 Results and discussions.....	86
3.3.1 Simulations of O ₃	86
3.3.2 Simulations of air toxics	89
3.3.3 PM _{2.5} prediction	91

3.4 Conclusion	93
3.5 Acknowledgments.....	94
References.....	95
APPENDIX I	120
Table 1: List of air quality monitoring stations	121

LIST OF TABLES

CHAPTER 1

Table 1:	Current photochemical models and attributes. Adapted from Russell and Dennis (2000).....	24
Table 2:	Web-based air quality forecasting systems around the world.	25
Table 3:	Air quality index (AQI) designed by the AIRNow project of the United States Environmental Protection Agency (USEPA) (http://www.epa.gov/airnow/).....	26
Table 4:	MM5 and MCIP vertical sigma levels, and the approximate MCIP sigma level height above the surface. Further details are available at: http://pah.cert.ucr.edu/rmc/	27
Table 5:	List of modeled hydrocarbon species in the AIRPACT2 system.	28
Table 6:	Initial Concentrations (IC) and Boundary Conditions (BC) for all lateral boundaries used in the CALGRID model.....	29
Table 7:	National Ambient Air Quality Standards (NAAQS). This can be found at the website of the United States Environmental Protection Agency (http://www.epa.gov).	30
Table 8:	Definition of the statistical measures for model evaluation. Measures in italic are used in this study.....	31

CHAPTER 2

Table 1:	Performance statistics for CALMET wind speed predictions using data obtained from September 4-30, 2003. Max and min represent statistics based on the maximum and minimum wind speeds within the 3 x 3 grid-cell matrix.	73
Table 2:	Performance statistics for predictions of temperature of CALMET based on the data obtained from September 4 to September 30, 2003.....	74
Table 3:	O ₃ prediction performance statistics for September 2003 based on 8-hr daily maximum mixing ratios. Results in max and min columns represent performance statistics based on the maximum and minimum O ₃ mixing ratios predicted within the 3 x 3 grid-cell around the monitor.	75
Table 4:	Performance statistics for O ₃ predictions during an episode (September 2-5, 2003) and a non-episode (September 18-21, 2003) periods.....	76

Table 5: Ratio analysis of air toxics relative to benzene measured at Seattle Beacon Hill site. 77

Table 6: Performance statistics for AIRPACT2 for PM_{2.5} predictions (September 1-15, 2003). 78

CHAPTER 3

Table 1: CMAQ Initial Conditions (ICON) and Boundary Conditions (BCON) for the western boundary. 112

Table 2: CMAQ O₃ prediction performance statistics for September 2003. Statistical measures were calculated using 8-hr daily maximum mixing ratios with a 20 ppb of observed O₃ cutoff. Results in max and min columns represent the statistics for the maximum and the minimum O₃ mixing ratios predicted within the 3 x 3 grid-cell matrix. 113

Table 3: Performance statistics for CALGRID and CMAQ for O₃ prediction. 114

Table 4: First order reactions for primary air toxics, and their rate constants incorporated in the CMAQ chemical mechanisms. 115

Table 5: Ratio of air toxics compounds relative to benzene at Seattle Beacon Hill, WA. 116

Table 6: List of aerosol species treated in CMAQ that account for total PM_{2.5} concentration. 117

Table 7: Performance statistics of CMAQ for PM_{2.5} predictions. Note that 24-hr average data were calculated using hourly PM_{2.5} concentration from September 1 to September 14, 2003). 118

Table 8: Performances of CALGRID and CMAQ models in predicting PM_{2.5} concentrations. 119

LIST OF FIGURES

CHAPTER 1

- Figure 1: Example outputs from the AIRPACT2 operations (a) hourly O₃ forecast (b) monthly average benzene mixing ratio 20
- Figure 2: Schematic diagram of AIRPACT2 showing meteorological, emission, and photochemical components. Square boxes represent input and output files, and rounded boxes represent programs in the AIRPACT2 system. 21
- Figure 3: Flow diagram of the diagnostic wind model in CALMET. Winds derived from MM5 are introduced as the initial guess field (A) and as observations (C). Adapted from CALMET User’s Guide by Scire *et al.* (2000)..... 22
- Figure 4: Relationship between data and processors in SMOKE. Square and rounded boxes represent input-output files and processors, respectively (adapted from Houyoux *et al.*, 2004) 23

CHAPTER 2

- Figure 1: Schematic diagram of the AIRPACT2 system showing major meteorological, emission, and photochemical components..... 55
- Figure 2: Domain of the AIRPACT2 system. The locations of the air quality monitoring stations in WA and OR used for evaluation in this study are shown. Surface elevations are in meters..... 56
- Figure 3: Plots showing time series of modeled and observed hourly wind speeds at eight sites in WA during an elevated O₃ period. Error bars associated with modeled wind speeds represent the maximum and the minimum wind speeds within the 3 x 3 grid-cell matrix..... 57
- Figure 4: Frequency distributions of modeled and observed wind directions at six monitoring stations in WA. Note that the frequency distributions were calculated from hourly observed and corresponding modeled data points from September 4 through to September 18, 2003..... 58
- Figure 5: Diurnal time series of the difference between modeled and observed wind directions. Hourly average measured and modeled data from eight monitoring stations were used to calculate the difference plot..... 59
- Figure 6: Vertical profiles of predicted and measured wind speeds at Salem, OR for (a) episode and (b) non-episode at 0000 PST, and (c) episode and (d) non-episode) at 2000 PST..... 60

Figure 7:	Profiles of modeled and observed temperature at Salem, OR at 0000 PST: (a) episode and (b) non-episode, and at 1200 PST: (c) episode and (d) non-episode.	61
Figure 8:	Hourly time series of O ₃ mixing ratios of the episode (September 2-5, 2003), and the non-episode (September 18-21, 2003) periods at monitoring sites in WA and OR.	66
Figure 9:	A Q-Q plot of O ₃ modeled and observed 8-hr daily maximum data points (un-paired in time and space) for September 2003 within 15 sites with a cutoff at 20 ppb of observed O ₃ . The solid line represents 1:1 relationship between modeled and observed O ₃ . The broken lines around the modeled data points show the maximum and the minimum within the 3 x 3 grid-cell matrix	67
Figure 10:	8-hr daily max observed and corresponding modeled 8-hr max O ₃ within 15 sites (paired in time).	68
Figure 11:	Modeled cloud cover during a non-episode period (September 18-21, 2003) at 1200 PST; outputs were taken from MM5-MCIP cloud fraction calculations.	69
Figure 12:	24-hr average modeled and observed air toxics mixing ratios for selected days in September and October 2003 at Seattle Beacon Hill site. Error bars associated with the modeled air toxics represent the maximum and minimum levels within the 3 x 3 grid-cell matrix.	70
Figure 13:	Time series of 24-hr average PM _{2.5} modeled and observed concentrations. The error bars associated with the modeled concentration represent the maximum and minimum modeled concentrations of PM _{2.5} within the 3x3 grid-cell matrix. The shaded time period corresponds to an observed high O ₃ period.	71
Figure 14:	(a) Modeled and observed average hourly concentrations of PM _{2.5} using data from 12 sites for September 1-15, 2003, and (b) for September 8-15, 2003. Error bars are showing the maximum and minimum modeled concentrations within the 3x3 grid-cell matrix.	72

CHAPTER 3

Figure 1:	Schematic diagram of the modified AIRPACT2 forecast system. Rounded boxes represent main models/processors and square boxes represent input/output files.	98
Figure 2:	Major components in the CMAQ modeling system (<i>adapted from Ching and Byun, 1999</i>). Circles represent processors and boxes represent main models.	99
Figure 3:	Hourly O ₃ mixing ratios during the episode (September 2-5, 2003), and the non-episode (September 18-21, 2003) periods for sites in WA and OR.	104

Figure 4:	A Q-Q plot of O ₃ modeled and observed data points (unpaired in time and space) for September 2003. The solid line represents 1:1 relationship between modeled and observed O ₃	105
Figure 5:	8-hr daily maximum observed and corresponding modeled 8-hr daily maximum O ₃ within 15 sites (paired in time). Dashed lines represent linear trend lines for CALGRID (open circles) and CMAQ (open triangles).....	106
Figure 6:	Scatter plot of observed versus modeled data points: CALGRID (open circles) and CMAQ (open diamonds). Note that the data are paired in time and space. Dashed lines represent linear trend lines of modeled O ₃	107
Figure 7:	24-hr average modeled and observed air toxics mixing ratios at Seattle Beacon Hill. Error bars associated with CMAQ modeled air toxics represent the maximum and the minimum levels within the 3 x 3 grid-cell matrix.....	108
Figure 8:	Time series of 24-hr average PM _{2.5} modeled and observed concentrations. The plot is based on average data obtained from 12 monitoring stations in WA during September 1-14, 2003. The error bars associated with the modeled concentrations represent the maximum and the minimum modeled concentrations of PM _{2.5} within the 3 x 3 grid-cell matrix.....	109
Figure 9:	Diurnal patterns of modeled and observed concentrations of PM _{2.5} . Error bars show the maximum and the minimum modeled concentrations of PM _{2.5} within the 3 x 3 grid-cell matrix.....	110
Figure 10:	Partial contributions of aerosol species to the fine particulate mass (PM _{2.5}). Note that each species includes both the Aitkin (<i>i</i> th) mode and the accumulation (<i>j</i> th) mode particles.	111

ATTRIBUTION

This thesis consists of three chapters. Chapter 1 contains an overview of the research, an introduction to air quality forecasting, and a literature review on model evaluation. Chapter 2 presents the performance evaluation of the current AIRPACT2 system for the Pacific Northwest, and Chapter 3 presents an inter-comparison between the performances of the CALGRID and the CMAQ models. While I am the primary author of the entire thesis, I received much help from my advisor, Professor Brian Lamb, and other committee members in preparing this thesis.

CHAPTER 1

INTRODUCTION

1.1 Overview of research

This thesis includes two main chapters that present different aspects of the performance evaluation of the Air Indicator Report for Public Access and Community Tracking version 2 (AIRPACT2) air quality forecast system for the Pacific Northwest (<http://www.airpact.wsu.edu>). AIRPACT2 is a numerical photochemical modeling system that predicts hourly mixing ratios of ozone and related gaseous species, a number of selected reactive air toxic tracers, and concentrations of primary particulates for a 24-hr period in advance. The model domain encompasses Vancouver, BC on the north and Salem, OR on the south and extends west beyond the Pacific coast and east beyond the crest of the Cascade Mountain range. In the current configuration, AIRPACT2 employs CALMET version 5 (Scire *et al.*, 2000) and MCIP version 2.2 (Byun *et al.*, 1999a) to process outputs from the Mesoscale Meteorological model MM5 version 3 (Dudhia *et al.*, 2002), emissions are processed by the SMOKE processor version 2.0 (Houyoux *et al.*, 2004), and the chemistry and transport are treated using the CALGRID model version 1.6 (Scire *et al.*, 1989). AIRPACT2 runs automatically on a daily basis to produce 24-hr forecasts and results are displayed on a public website. Chapter 2 presents an evaluation of the current AIRPACT2 system in terms of the statistical performance in predicting mixing ratios of gaseous species ozone (O₃), the air toxic compounds formaldehyde, acetaldehyde, 1,3-butadiene, benzene, and perchloroethylene, and concentrations of primary fine particulates (PM_{2.5}). The chapter also discusses the strengths and weaknesses of the modeling system, and seeks to identify areas where improvements are needed.

During the summer, 2005, the current AIRPACT2 system was under going conversion to AIRPACT3 to take the advantage of the-state-of-the-science photochemical model CMAQ version 4.4 (Byun and Ching, 1999b) as a replacement for the CALGRID model in the system, and to expand the model domain to include all of Idaho, Oregon, Washington and a portion of southwestern Canada. As a preliminary analysis of the change from CALGRID to CMAQ, the CALGRID model was replaced with the CMAQ model in AIRPACT2 and the performance analysis described in Chapter 2 for the CALGRID version of AIRPACT2 was repeated. Results from this analysis using CMAQ are described in Chapter 3. The AIRPACT2 system with CMAQ was also run for the same time period of September 2003 and some selected days in October 2003 for the same domain. The findings from this study should be regarded as a pre-development study for the AIRPACT3 system.

The motivation of this research primarily came from the need to understand how well the AIRPACT2 system using either the CALGRID or CMAQ photochemical models simulated air quality conditions in the Pacific Northwest. This system evaluation is important because of the large economic, public health, and the ecosystem health impacts associated with the use of air quality modeling results (Chang and Hanna, 2004). So, it is crucial that the AIRPACT2 system be evaluated before the forecast results are used by regulatory agencies in a decision making process. It is also inherently important to a modeling system to have confidence in predicted results; the modeling system should deliver predictions as accurately as possible. Therefore, the research outcomes from this study were aimed at better understanding of the forecasting abilities of the AIRPACT2 system for different gaseous and particulate species in the Pacific Northwest.

1.2 Air quality models and forecasting

Air quality models are powerful tools to predict the fate of pollutant gases or aerosols upon their release into the atmosphere (Chang and Hanna, 2004). These models play a pivotal role in both scientific investigations of how pollutants evolve and behave in the atmosphere and air quality management policy development processes. Numerous photochemical models are currently available in the scientific communities, and in the hands of the regulatory agencies. Air quality models are viewed as an inexpensive option for air quality management as opposed to expensive measurement campaigns over a large area. Table 1 contains a list of currently available major air quality models of urban to regional scales. Although these models vary in their designs and applications, they share many commonalities. In particular, these are based on solving the same species conservation equations describing the formation, transport and fate of air pollutants, including components for processing emissions, meteorology, topography, air quality observations and chemistry. A detailed description of an air quality model formulation can be found in the work of Russell and Dennis (2000). Over the last 30 years or so, the photochemical models have evolved from rather crude representations of the physics of the atmosphere, and the chemistry of species to the more comprehensive current state. Photochemical models are now able to predict more accurately than was possible during the early stage of the development process. The understanding of the physics and chemistry modules in air quality models, however, are not complete yet, and these models still have some degree of inaccuracy in representing the real world.

Together with the advanced computational abilities, the latest photochemical models show good promise in air quality forecasting using meteorological models, and emission processors. Research institutes and regulatory agencies around the world have developed several

fully or quasi-operational air quality forecasting systems to predict primarily O₃ pollution. Table 2 contains a list of web-based air quality forecasting systems in North America, Europe, and Australia. The list is not meant to be exhaustive, rather instructive of currently available air quality forecasting initiatives around the world. These systems provide near-real time forecasting for 24-72 hours in advance. The forecast results are usually expressed in the form of an air quality index (AQI) specific to the national air quality standards of a country. An example of an AQI used in the United States is given in Table 3.

AIRNow (<http://airnow.gov>) is the largest national air quality forecasting network in the United States. The United State Environmental Protection Agency (US EPA), National Oceanic & Atmospheric Administration (NOAA), National Park Services (NPS), tribal, state, and local agencies developed the AIRNow website to provide the public with easy access to national air quality information (AIRNow, 2005). This website offers daily AQI forecasts as well as near-real time AQI scores for over 300 cities across the US, and provides links to more detailed state and local air quality websites. For example, the University of Maryland provides detailed air quality forecast for the Washington DC, Baltimore, and Western MD areas (http://www.atmos.umd.edu/~forecaster/ozone_fcst.html). Other state level air quality forecasting system include the Maine Department of Environmental Quality air quality forecast (<http://www.maine.gov/dep/air/ozone/>), the Massachusetts Department of Environmental Protection air quality forecast (<http://www.mass.gov/dep/bwp/ozone/dailyoz.htm>), and the Tennessee Department of Environment and Conservation air quality forecast (<http://www.tennessee.gov/environment/apc/ozone/>). There are also county level air quality management activities such as Maricopa County, AZ air quality forecast system (<http://www.maricopa.gov/aq/airday.asp>) and the Puget Sound Clean Air Agency, WA air

quality forecast system (<http://www.pscleanair.org/>). The ability of air quality forecasting of a state level agency is variable. For example, the state of Massachusetts operates O₃ forecast during the O₃ months from May up to September 30. Forecast systems of many local agencies operate mainly for O₃ and PM_{2.5} species. It is important to recognize that most of these forecast operations are based upon combinations of weather forecasts, statistical regression analyses of weather and pollutant patterns, and expert opinion. The use of advanced numerical photochemical forecast systems is relatively new and not yet in widespread use.

The AIRPACT2 system is a regional scale near-real time operational air quality forecast system for the Pacific Northwest. The detailed description of the forecast system is given in the next section. The original AIRPACT system was developed during the years from 2000 to 2001 with the objectives of (a) providing air-quality managers in the Puget Sound region with timely forecasts of air pollution episodes and (b) allowing for the potential notification of sensitive populations (Vaughan *et al.*, 2004). In September, 2003, the AIRPACT system was updated to AIRPACT2 by incorporating air toxic compounds and expanding the domain to include parts of southern BC, Canada in the north, Cascade Mountain Regions, WA in the east, and Salem, OR areas in the south. The results from AIRPACT2 could have several implications in air quality management, and protecting public health and the ecosystem health. Daily results could be used by the sensitive population to plan their activities, and by the regulatory agencies to provide an air quality advisory to the public. The long-term simulation results could also be used by the agencies to develop air quality policies. Figure 1 shows model outputs depicting these two major aspects of AIRPACT2 applications for the Pacific Northwest.

1.3 AIRPACT2 system design

Figure 2 illustrates major components and data flow in the current AIRPACT2 system. Details of the AIRPACT system can also be found in Vaughn *et al.* (2004). Following is a summary of the descriptions of the system components:

1.3.1 MM5 version 3

The PSU/NCAR fifth generation Mesoscale Meteorological model version 3 (MM5 v3) is the base meteorological model in AIRPACT2. The data used in AIRPACT2 flow from the MM5 (4-km resolution) runs carried out at the University of Washington (<http://www.atmos.washington.edu/mm5rt/>). The model utilizes 38 full-sigma vertical levels, and it is run on a non-hydrostatic mode in order to limit pressure gradient force errors over the complex terrain. MM5 uses the United States Geological Survey (USGS) 1-km terrain and land-use data. The following physics options are included in MM5: CCM2 radiation scheme, Reisner 2 mixed moisture scheme, Kain-Fritsch Cumulus cloud scheme, MRF PBL scheme, and 5-layer Soil Model scheme (Dudhia *et al.*, 2002). It adopts the terrain following pressure dependent σ coordinate in the vertical direction. The MM5 run is initialized with the National Center for Environmental Prediction (NCEP) Global Forecasting System (GFS) model at 00Z hours. The lateral boundary conditions (BC) are also extracted from the MM5-GFS initialization. Table 4 shows vertical layer stratification in the MM5 model with MCIP layers and corresponding heights above ground.

1.3.2 CALMET version 5

The CALMET meteorological model includes a diagnostic wind field generator including objective analysis; parameterized treatments of slope flows, kinematic terrain effects, terrain

blocking effects, and a divergence minimization procedure; and a micro-meteorological model for overland and over-water boundary layers (Scire *et al.*, 2000). The main role of CALMET in AIRPACT2 is to generate mass-consistent three-dimensional wind vectors, and extract temperature and short-wave radiation from MM5 outputs suitable for mobile and biogenic emission processing in the SMOKE processor. Figure 3 shows the step-wise process of CALMET three-dimensional wind generation.

The diagnostic CALMET model can produce detailed wind fields portraying observations quite accurately. In a study of the performance of the MM5-CALMET modeling pair, Chandrasekar *et al.* (2003) found that wind speeds as well as the wind components are better simulated by the MM5 ingested CALMET fields than the MM5 wind speed and their components alone for a 4-km resolution. They suggested that utilizing the prognostic meteorological model output as input for a diagnostic model provides an attractive option for generating accurate meteorological inputs for air quality modeling studies, especially for long-term simulations, i.e. periods lasting from several weeks to a year. In another study, Barna and Lamb (2000) reported that the performance of the MM5-CALMET pair and hence the performance of the CALGRID model could be improved with an observational nudging technique even in a complex terrain.

1.3.3 MCIP version 2.2

Most meteorological models are not built for air quality modeling purposes. As a result, the Meteorology-Chemistry Interface Processor (MCIP) was developed to deal with issues related to data format translation, conversion of units of parameters, diagnostic estimations of parameters not provided by the meteorological model, extraction of data for appropriate window domains, and reconstruction of meteorological data on different grid and layer structures (Byun

et al., 1999a). In the AIRPACT2 system, MCIP extracts planetary boundary layer (PBL) and surface layer parameters and cloud information from the MM5 outputs. MCIP also windows out the AIRPACT2 domain from the bigger MM5 domain and collapses the MM5 vertical layers into the desired number of layers used in the CALGRID model. MCIP writes the bulk of its two- and three-dimensional meteorological and geophysical output data in a transportable binary format using the Models-3 input/output applications program interface (I/O API) library. In AIRPACT2, the parameters extracted with MCIP are combined with CALMET winds into a single file used as input to CALGRID.

1.3.4 SMOKE version 2.0

The purpose of the Sparse Matrix Operator Kernel Emission (SMOKE) emission processor is to convert the resolution of the data in an emission inventory to the resolution needed by an air quality model (Houyoux *et al.*, 2004). SMOKE transforms inventory emissions from area, mobile, point and biogenic sources into hourly gridded and speciated emissions. The mobile and the biogenic source emissions are processed with the MOBILE6 (US EPA, 1997) model and the BEIS3 (Guenther *et al.*, 1993) model, respectively within the SMOKE framework. SMOKE provides a variety of speciation schemes such as SAPRC90 (Carter, 1990), RADM2 (Stockwell *et al.*, 1990) and CBIV (Gery *et al.*, 1989) suitable for different air quality models. SMOKE also provides with flexible format options for the output data. Data can be structured either in the ASCII format or in the Models-3 I/O API Network Common Data Form (NetCDF) format. In the AIRPACT2 system, SMOKE processes the emissions from area, mobile and biogenic sources with a modified version of the SAPRC97 (Carter, 1997) speciation scheme. However, the point source emissions are processed separately outside of SMOKE in the CALGRID modeling framework using the SAPRC97 scheme. In AIRPACT2, SMOKE provides

the output data in the NetCDF format for use in the CALGRID model. Figure 4 depicts the programs involved in the SMOKE emissions processing, and options for output formats.

1.3.5 CALGRID version 1.6

CALGRID is an Eulerian photochemical transport and dispersion model, which includes modules for horizontal and vertical advection/diffusion, dry deposition, and one of the State Air Pollution Research Center (SAPRC) family of photochemical mechanisms (Scire *et al.*, 1989). The model solves the species conservation equation using quasi-steady-state approximation (QSSA) method for each specie (C_i), at every grid cell, at every time step:

$$\frac{\partial C_i}{\partial t} + U \frac{\partial C_i}{\partial x} + V \frac{\partial C_i}{\partial y} + w \frac{\partial C_i}{\partial z} = \frac{\partial}{\partial x} \left(K_x \frac{\partial C_i}{\partial x} \right) + \frac{\partial}{\partial y} \left(K_y \frac{\partial C_i}{\partial y} \right) + \frac{\partial}{\partial z} \left(K_z \frac{\partial C_i}{\partial z} \right) + R + D + S$$

(A) (B1) (B2) (B3) (C1) (C2) (C3) (D) (E) (F)

where,

- (A) is the time rate of change of chemical specie i
- (B1,2) are horizontal components of the advection term
- (B3) is the vertical advection
- (C1,2) are the horizontal diffusion terms
- (C3) is the vertical diffusion term
- (D) accounts for chemical reactions of the specie i
- (E) is the deposition term for the specie i
- (F) is the source (emission) of the specie i

In the above equation, the diffusion coefficients K_x , K_y and K_z are parameterized from the turbulent fluxes using a first order closure scheme. These are calculated from meteorological data, and depend on atmospheric stability and location of a grid-cell in the domain. The dry deposition (term E) is calculated from a three-step resistance model accounting for: aerodynamic, boundary layer, and canopy resistances. The chemical reaction (term D) accounts for either addition or loss of the chemical specie i . The horizontal advective/diffusion equation is solved by a high-order chapeau function scheme, which conserves mass exactly, prohibits negative concentrations, and exhibits very little numerical diffusion (Scire *et al.*, 1989).

Chemical mechanisms are approximations to real-world chemistry, and in the AIRPACT2 system, CALGRID version 1.6 employs a modified version of the SAPRC97 chemical mechanism. A list of model hydrocarbon and particulate species is given in Table 5. The molecular weights of the particulate tracers were arbitrarily set to a value of 30.0 to handle the concentration conversion process.

The CALGRID model has been used widely in the United States and overseas in air quality modeling studies. The model has been shown to provide acceptable simulations for ozone. Jiang *et al.* (1998) found that the model performance met EPA guidelines for photochemical modeling, but exhibited some discrepancies compared to observations. The model under-estimated the four-day average peak ozone levels, predictions were generally in agreement with observations during the daytime at most sites, but missed the nighttime low O_3 mostly at inland sites in the Lower Fraser Valley, BC areas.

1.3.6 Initial and boundary conditions

In AIRPACT2, the initial condition (ICON) and the boundary condition (BCON) files are provided as inputs to the CALGRID three-dimensional chemistry and transport model. A user

defined IC template option is chosen in the CALGRID code. This option assumes the same concentrations at all grid-cells for each chemical specie in the three-dimensional structure at the beginning of each simulation. The BC file, on the other hand, is generated from the ICON file for grid-cells surrounding the domain. The IC and BC used in the AIRPACT2 system is given in Table 6.

1.4 Model evaluation

Model evaluation is a necessary part in the iterative cycle of model development, testing and confidence building (Russell and Dennis, 2000). An essential objective of a performance evaluation is to define the level of acceptability and usefulness of a model for a particular task, and to show that the model results are the “right answers for the right reasons”. It is also critical that a photochemical model should not only simulate observations as accurately as possible, but also pass a series of tests designed to ensure that the apparently accurate results are not produced by a combination of compensating errors. A definition of model evaluation is given by Russell and Dennis (2000) as follows:

“Assessment of the adequacy and correctness of the science represented in the model through comparison against empirical data, such as laboratory tests, in situ tests and the analysis of natural analogs. Evaluation is a process of model confirmation relative to current understanding. Multiple, confirmatory evaluations can never demonstrate the veracity of a model: confirmation is a matter of degree. However, an evaluation can raise doubts about the science in a model.”

Regulatory agencies use three-dimensional photochemical models such as UAM-V (Morris *et al.*, 1991), CAM_x (ENVIRON, 1997), CMAQ (US EPA, 2000), MAQSIP (Odman and Ingram, 1996; Kasibhatla and Chameides, 2000), etc. as the primary tools for developing

strategies to control air pollutants to below the National Ambient Air Quality Standards (NAAQS); the NAAQS for various pollutants are given in Table 7. Model evaluation is important because of huge economic, human health, and ecosystem impacts associated with model results. Recently, there has been much interest in air quality forecasting using photochemical models (e.g., McHenry, 2004; Vaughn *et al.*, 2004; Cope *et al.*, 2004; Hogrefe *et al.*, 2001), and most of these forecast systems are in their early stages of fully or quasi-operational use and/or in research mode. Discussions of the evaluation of air quality models as well as of the development of general evaluation methods have been presented by many scientists in recent years (e.g., Seigneur *et al.*, 2000; McNally and Tasche, 1993; Hanna *et al.*, 1993; Russell and Dennis, 2000); however, standard evaluation procedures and performance standards still do not exist in the air quality modeling community. It is important to recognize that efforts to develop evaluation methods and guidelines have been aimed at models used for simulation of historic short-term episodes where the meteorological model is often tuned to match available observations. Typically, a comprehensive evaluation process should include evaluations of meteorological, emission, and the chemistry and transport components of a forecast system. How air quality models are evaluated, and what are the issues that need to be addressed in an evaluation process are discussed later in this section.

Fundamentally, there can be three components to the evaluation of air quality models: scientific, statistical, and operational (Chang and Hanna, 2004). In a scientific evaluation, the model algorithms, physics, assumption, and codes are examined in detail for their accuracy, efficiency and sensitivity. So, the scientific evaluation requires an in-depth knowledge of the model. In a statistical evaluation approach, model outputs are compared with observations, and the model performance is expressed in the form of statistical measures. The third component of

a model evaluation is considered to be associated more with the application of the model itself; how easy it is to use the model, are there errors in the user's guide- are some of the typical questions answered in an operational evaluation. It is critical to define the goal of the evaluation process; different goals could lead to focusing on different variables and use of different performance measures. Most of the model evaluation works found in literature primarily dealt with the performance evaluation using statistical measures. Evaluation approaches differed in these studies, with varying evaluation periods, statistical measures, selection of modeled species and the level of concentrations. These studies, nevertheless, shared one thing in common in that they studied historic pollution episodes rather than evaluating model performance over a long period of time. Table 8 contains a list of the most used statistical measures in model performance evaluation studies. In addition to using such statistics, evaluation results could also be presented in percentiles to give a confidence interval for the results (e.g., Tilmes *et al.*, 2002)

In most of the evaluation studies, researchers typically presented statistical measures for domain average results where observations are taken from sparsely located monitoring stations throughout the domain. The results from this kind of averaging sometimes obscure the poor and/or good performances of a model in a particular area within the domain. Davis *et al.* (2000) suggested that a block of grid-cells covering an area of interest within the domain could be selected for evaluation. The authors conducted the performance evaluation of the Regional Oxidant Model (ROM) model in predicting O₃ for the Lake Michigan region by selecting blocks of grid-cells within the domain, and they found that the model performance was variable; better agreement with observations in the central Illinois and worse in the lake areas.

Evaluation of a three-dimensional, multi-layer photochemical model is generally carried out for the results found in the first layer of the model because regulatory agencies are mostly

interested in pollutant concentrations in this layer, and also, measured data are usually available for this layer. However, Duclaux *et al.* (2002) suggested that a comprehensive evaluation should also include model results from vertical layers. The authors argued that ground-based data are highly dependent on the location of monitoring stations. In their work, they found that the LIDAR estimated PBL heights differed significantly from the model calculated PBL heights resulting in inaccurate concentrations of PM_{2.5} and O₃ at the ground level. Although vertical profile measurements are difficult to obtain for many locations in the domain, models should also be evaluated for vertical predictions with as much measured data as possible.

In addition to evaluate performance in predicting O₃, researchers also studied O₃ precursors species such as NO_x and VOCs (e.g., Kumar *et al.*, 1994; Pilinis *et al.*, Jiang *et al.*, 1997, Arnold *et al.*, 2003) – a mechanistic approach of model evaluation. Studying the precursors could provide insight to the mechanisms associated with O₃ productions and losses in the model algorithms. Arnold *et al.* (2003) performed a diagnostic evaluation of the CMAQ air quality model using observations from the Southern Oxidant Study (SOS), examining surface indicator ratios of [O₃]/NO_x] and [NO_z]/NO_y] to understand the simulations of processes in the model. Sensitivity analysis also provides a better understanding of the model mechanisms. Changing input parameters such as meteorology and emissions could delineate any flows in the processes that might contribute to inaccurate predictions. O'Neill and Lamb (2005) used a processes analysis method to track hourly O₃ production and loss for each simulation. A model's ability to predict PM_{2.5} and its precursors and associated particulate should also be investigated mechanistically.

Researchers evaluated model performances using a variety of averaging periods including 1-hr mean, 8-hr mean, 8-hr max, 1-hr daily max, daily mean, and weekly mean. For example,

Hanna *et al.* (1996) evaluated the model performance for the Lake Michigan areas using 1-hr daily maximum modeled and observed O₃. The authors argued that the primary concern of emissions control strategies is the peak 1-hr average O₃ concentration for a given day anywhere within the geographic domain. It is worth mentioning that, in most studies, evaluation statistics were applied to a data series filtered by a threshold value. Usually, the cutoff level for O₃ varied between 20 ppb and 60 ppb. While it is true that regulatory agencies are mostly concerned with high O₃ levels; it is also true that choosing a higher cut-off level tends to improve the model performance statistics.

To summarize, model evaluation is an important part of a model development process. A specific goal of an evaluation task needs to be determined so that the usefulness of the model is clearly defined. There is a variety of statistical measures available for use in an evaluation work. However, one should choose statistics that give a meaningful interpretation of the model performance. It gives a clearer picture of the performance of a model when most of the recommendations discussed are tried in an evaluation study.

References

- AIRNow, 2005. National Air Quality Forecast System, United States Environmental Protection Agency (USEPA) (<http://airnow.gov>).
- Arnold, J., Dennis, R., and Tonnesen, G., 2003. Diagnostic evaluation of numerical air quality models with specialized ambient observations: testing the Community Multiscale Air Quality modeling system (CMAQ) at selected SOS 95 ground sites. *Atmospheric Environment* **37**, 1185–1198.
- Atlas, E., and Ridley, B. 1996. The Mauna Loa Observatory Photochemistry Experiment: Introduction, *Journal of Geophysical Research* **101 (D9)**, 14531-14541.
- Barna, M., and Lamb, B., 2000. Improving ozone modeling in regions of complex terrain using observational nudging in a prognostic meteorological model. *Atmospheric Environment* **34**, 488-9-4906
- Barna, M., Lamb, B., O'Neil, S., Westberg, H., Figueroa-Kaminsy, C., Otterson, S., Bowman, C., and DeMay, J., 2000. Modeling Ozone formation and transport in the Cascadian Region of the Pacific Northwest. *Journal of Applied Meteorology* **39**, 349-366.
- Byun, D., Pleim, J., Tang, R., and Bourgeois, A. 1999a. Meteorology Chemistry Interface Processor (MCIP) for MODEL-3 Community Multiscale Air Quality (CMAQ) Modeling System. United States Environment Protection Agency, EPA/600/R-99/030.
- Byun, D., and Ching, J. (Eds.), 1999b. Science algorithms of the EPA Models-3 Community Multiscale Air Quality (CMAQ) Modeling System. EPA Report No. EPA-600/R-99/030, Office of Research and Development, US Environmental Protection Agency, Washington, DC.
- Carter W., 1990. A detailed mechanism for the gas-phase atmospheric reactions of organic compounds. *Atmospheric Environment* **24A (3)**, 481-518.
- Carter, W, Luo, D., and Malkina, I., 1997. Environmental chamber studies for development of an updated photochemical mechanism for VOC reactivity assessment. Final report prepared for California Air Resources Board under Contract 92-345 by Center for Environmental Research and Technology, University of California, Riverside, pp-213.
- Chandrasekar, A., Philbrick, R., Clark, R., Doddridge, B., and Georgopoulos, P., 2003. Evaluating the performance of a computationally efficient MM5/CALMET system for developing wind field inputs to air quality models. *Atmospheric Environment* **37**, 3267-3276.
- Chang, J, and Hanna, S., 2004. Air quality performance evaluation. *Meteorology and Atmospheric Physics* **87**, 167-196.
- Chang, J., Brost, R., Isakson, I., Madronic, S., Middleton, P., Stockwell, W., Walcek, C., 1987. A three-dimensional Eulerian acid deposition model: physical concepts and formulation. *Journal of Geophysical Research* **92**, 14681-14700.
- Cope, M., Hess, G., Lee, S., Tory, K., Azzi, M., Carras, J., Lilley, W., Mannis, P., Nelson, P., Ng, L., Puri, K., Wong, N., Walsh, S., and Young, M., 2004. The Australian air quality forecasting system. Part I: Project description and early outcomes. *Journal of Applied Meteorology* **43**, 649-662.
- Davis, J., Nychka, D., and Bailey, B., 2000. A comparison of regional oxidant model (ROM) output with observed ozone data. *Atmospheric Environment* **34**, 2413 – 2423.

- Duclaux, O., Frejafon, E., Schmidt, H., Thomasson, A., Mondelain, D., Yud, J., Guillaumond, C., Puele, C., Savoie, F., Ritter, P., Boche, J., and Wolf, J., 2002. 3D-air quality model evaluation using the Lidar technique. *Atmospheric Environment* **36**, 5081-5095.
- Dudhia, J., Gill, D., Guo, Y., Manning, K., Bourgeois, A., Wang, W., and Bruyere, C. 2002. PSU/NCAR Mesoscale Modeling System Tutorial Class Notes and User's Guide: *MM5 Modeling System Version 3*. Mesoscale and Microscale Meteorology Division, National Center for Atmospheric Research, Boulder, CO.
- ENVIRON, 1997. User's Guide to the Comprehensive Air Quality Model with Extensions (CAMx). Available from ENVIRON International Corporation, 101 Rowland Way, Novato, CA 94945.
- Finlayson-Pitts, B., and Pitts, J. 2000. Chemistry of the upper and lower atmosphere. Academic Press, USA.
- Gery, M., Whitten, G., Killus, J., and Dodge M., 1989. A photochemical kinetics mechanism for urban and regional scale computer modeling. *Journal of Geophysical Research* **104(D3)**, 3555-3576.
- Guenther, A., Zimmerman, P., Harley, P., Monson, R., and Fall, R., 1993. Isoprene and monoterpene emission rate variability: model evaluations and sensitivity analysis. *Journal of Geophysical Research* **98**, 12,609-12,617.
- Hanna, S., Chang, J., and Strimaitis, D. 1993. Hazardous gas model evaluation with field observations. *Atmospheric Environment* **27A**, 2265-2285.
- Hanna, S., Moore, G., and Fernau, M., 1996. Evaluation of photochemical grid models (UAM-IV, UAM-V, AND the HE ROM/UAM-IV couple) using data from the Lake Michigan Ozone Study (LMOS). *Atmospheric Environment* **30(19)**, 3265-3279.
- Hass, H., 1991. Description of the EURAD chemistry transport module (CTM) version 2. In: Ebel, A., Neubauer, F.M., Speth, P. (Eds.), Report 83. Institute of Geophysics and Meteorology, University of Cologne, Cologne, Germany.
- Hogrefe, C., Rao, S., Kasibhatla, P., Kallos, G., Tremback, C., Haoe, W., Olerud, D., Xiu, A., McHenry, J., and Alapaty, K., 2001. Evaluating the performance of regional-scale photochemical modeling systems: Part I-meteorological predictions. *Atmospheric Environment* **35**, 4159-4174.
- Houyoux, M., Vukovich, J., Brandmeyer, J., Seppanen, C., and Holland, A., 2004. SMOKE user manual version 2. Carolina Environmental Program, NC.
- Jiang, W., Singleton, D., Hedley, M., and McLaren, R., 1997. Sensitivity of ozone concentrations to VOC and NOx emissions in the Canadian Lower Fraser Valley. *Atmospheric Environment* **31(4)**, 627-638.
- Jiang, W., Hedley, M., and Singleton, D., 1998. Comparison of the MC2/CALGRID and SAIMM/UAM-V photochemical modeling systems in the Lower Fraser Valley, British Columbia. *Atmospheric Environment* **32(17)**, 2969-2980.
- Jiang, G., 2001. Photochemical air quality modeling in the Puget Sound region. PhD dissertation, Washington State University, Department of Chemistry, Pullman, WA.
- Kasibhatla, P., and Chameides, W.L., 2000. Seasonal modeling of regional ozone pollution in the eastern United States. *Geophysical Research Letters* **27**, 1415-1418.
- Killin, R., Simonich, S., Jaffe, D., DeForest, C., and Wilson, G., 2004. Transpacific and regional atmospheric transport of anthropogenic semi-volatile organic compounds to Cheeka Peak Observatory during the spring of 2002. *Journal of Geophysical Research* **109**, D23S24

- Kumar, N; Russell, A., Tesche, T., and McNally, D., 1994. Evaluation of CALGRID using two different ozone episodes and comparisons to UAM. *Atmospheric Environment* **28(17)**, 2823-2845.
- McHenry, J., Ryan, W., Seaman, N., Coats, C., Pudykiewicz, J., Arunachalam, S., and Vukovich, J., 2004. A real-time Eulerian photochemical model forecast system. *Bulletin of the American Meteorological Society* **85**, 525-548
- McNally, D. and Tesche, T. 1993. MAPS sample products, Alpine Geophysics, 16225 W. 74th Dr., Golden, CO 80403.
- McRae, G., Seinfeld, J., 1983. Development of a Second- Generation Mathematical Model for urban air pollution-II, Evaluation of model performance. *Atmospheric Environment* **17**, 501-522.
- Millet, D., Goldstein, A., Allan, J., Bates, T., Boudries, H., Bower, K., Coe, H., Ma, Y., McKay, M., Quinn, P., Sullivan, A., Weber, R., and Worsnop, D., 2004. Volatile organic compound measurements at Trinidad Head, California, during ITCT 2K2: analysis of sources, atmospheric composition, and aerosol residence times. *Journal of Geophysical Research* **109**, D23S16.
- Morris, R., Myers, T., Douglas, S., Yocke, M., and Mirabella, V., 1991. Development of a nested-grid urban airshed model and application to Southern California. In: Proceedings, 84th Annual Meeting of the Air and Waste Management Association, Vol. 5 Ozone, June 16-21, 1991, Vancouver, British Columbia, Canada. Air and Waste Management Association, Pittsburgh, Pennsylvania, Paper No. 91-66.8., 15.
- O'Neill, S., and Lamb, B., 2005. Intercomparison of the Community Multi-Scale Air Quality model and CALGRID using process analysis. *Environmental Science and Technology* **39**, 5742-5753.
- Odman, M., and Ingram, C., 1996. Multiscale Air Quality Simulation Platform (MAQSIP): source code documentation and validation. Technical Report ENV-96TR002-v1.0, MCNC Environmental Programs, Research Triangle Park, NC 27709, 83.
- Pilinis, C., Kassomenos, P., and Kallos, G., 1993. Modeling of photochemical pollution in Athens, Greece. Application of the RAMS-CALGRID modeling system. *Atmospheric Environment* **27B**, 353-370.
- Reynolds, S., Seinfeld, J., and Roth, P., 1973. Mathematical modeling of photochemical air pollution C1, Formulation of the model. *Atmospheric Environment* **7**, 1033-1061.
- Russell, A. and Dennis, R., 2000. NARSTO critical review of photochemical models and modeling. *Atmospheric Environment* **34**, 2283-2324
- Scire, J, Yamartino, R., Carmichael, G., and Chang, Y., 1989. CALGRID: A Mesoscale Photochemical Grid Model Volume II: User's Guide, California Air Resources Board, CA.
- Scire, J., Robe, F., Fernau, M., and Yamartino, R. 2000. A user's guide for the CALMET meteorological model version 5. Earth Tech, Concord, MA.
- Seigneur, C., Pun, B., Pai, P., Louis, J., Solomon, P., Emery, C., Moris, R., Zahniser, M., Worsnop, D., Koutrakis, P., White, W., and Tombach, I. 2000. Guidance for the performance evaluation of three-dimensional air quality modeling systems for particulate matter and visibility. *Journal of Air Waste Management Association* **50**, 588-599.
- Stockwell, W., Middleton, P., Chang, J., and Tang, X., 1990. The second-generation regional acid deposition model chemical mechanism for regional air quality modeling. *Journal of Geophysical Research* **95 (D10)**, 16,343-16,367.

- Timles, S., Brandt, J., Flatoy, F., Bergstrom, R., Flemming, J., Langer, J., Christensen, J., Frohn, L., Hov, O., Jacobsen, I., Reimer, E., Stern, R. and Zimmermann, J., 2002. Comparison of five Eulerian air pollution forecasting systems for the summer of 1999 using the German ozone monitoring data. *Journal of Atmospheric Chemistry* **42**, 91–121.
- U.S. Environmental Protection Agency. 1991. Guideline for regulatory applications of the Urban Airshed Model. EPA-450/4-91-013, U.S. Environmental Protection Agency, Research Triangle Park, NC 27711.
- United States Environmental Protection Agency (US EPA), 2000. Models-3 Home Page available online at <http://www.epa.gov/asmdnerl/models3/>.
- Vaughan, J., Lamb, B., Frei, C., Wilson, R., Bowman, C., Figueroa-Kaminsky, C., Otteson, S., Boyer, M., Mass, C., Albright, M., Koenig, J., Collingwood, A., Gilroy, M., and Maykut, N. 2004. A numerical daily air quality forecast for the Pacific Northwest. *Bulletin of the American Meteorological Society* **85**, 549-561.
- Yamartino, R., Scire, J., Carmichael, G., Chang, Y., 1992. The CALGRID mesoscale photochemical grid model CI, Model formulation. *Atmospheric Environment* **26**, 1493-1512.

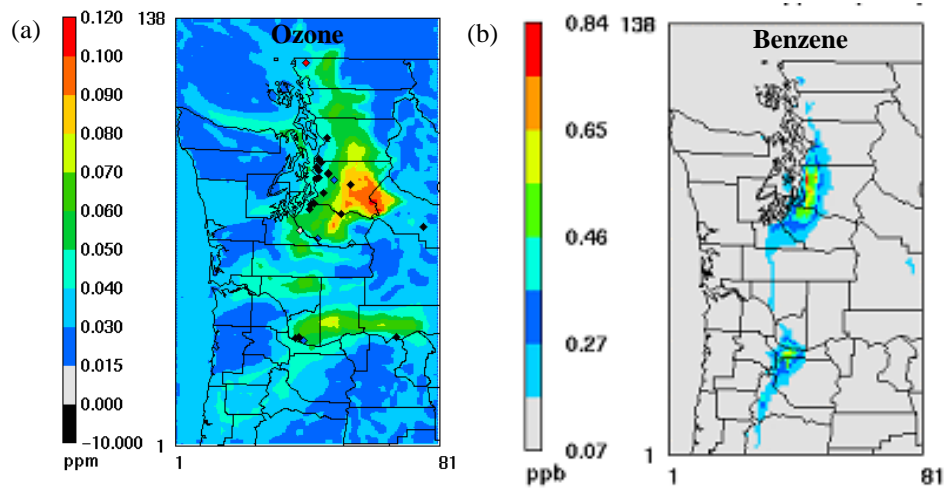


Figure 1: Example outputs from the AIRPACT2 operations (a) hourly O₃ forecast (b) monthly average benzene mixing ratio

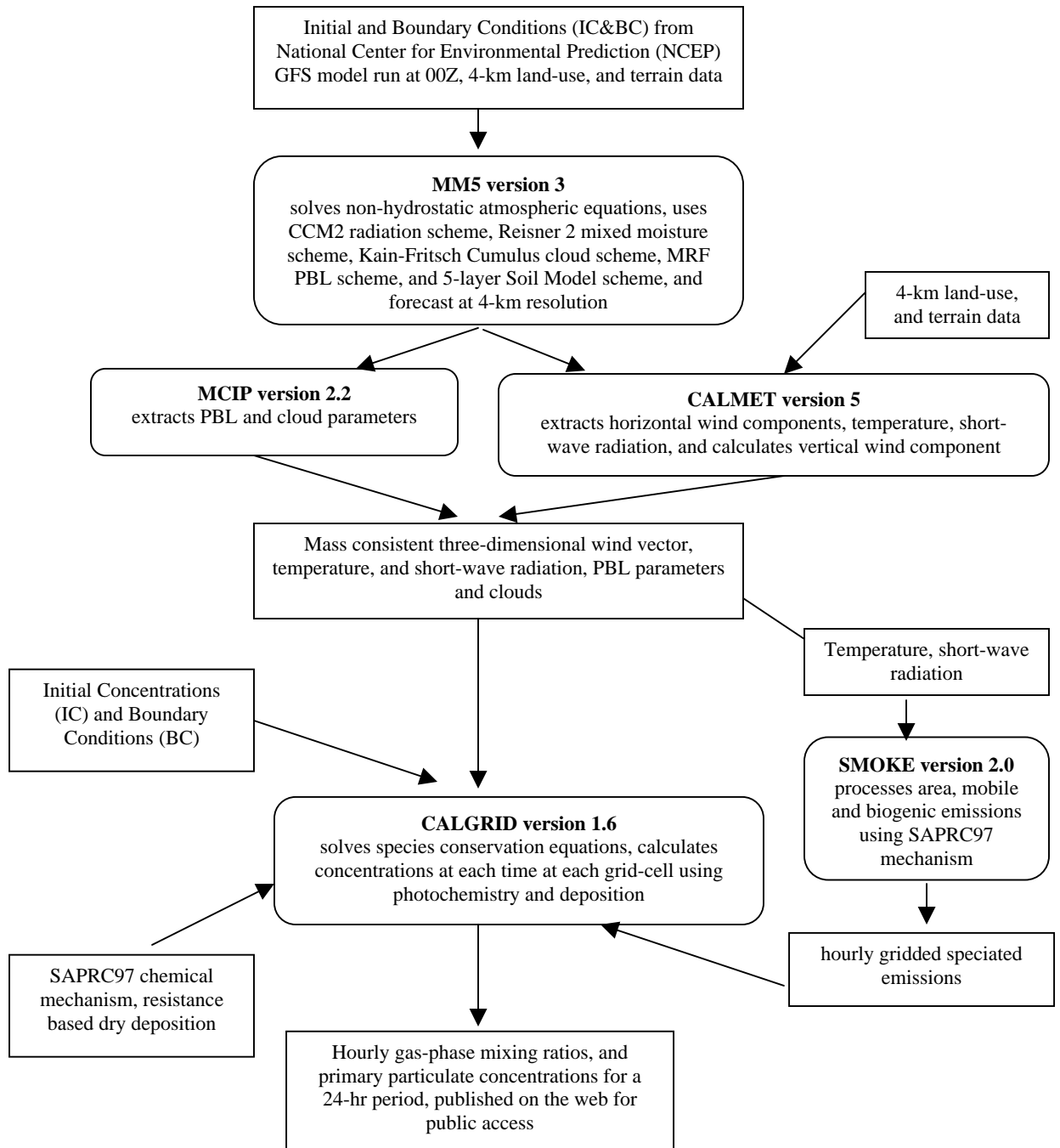


Figure 2: Schematic diagram of AIRPACT2 showing meteorological, emission, and photochemical components. Square boxes represent input and output files, and rounded boxes represent programs in the AIRPACT2 system.

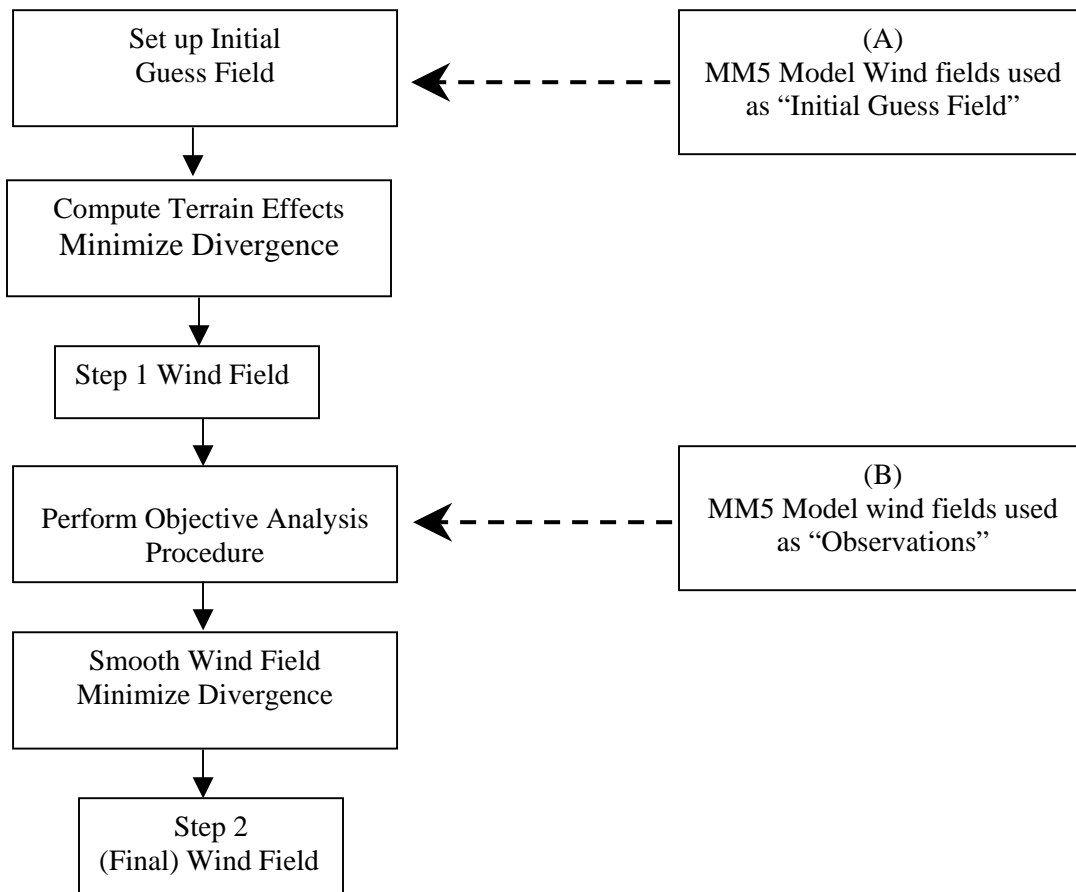


Figure 3: Flow diagram of the diagnostic wind model in CALMET. Winds derived from MM5 are introduced as the initial guess field (A) and as observations (C). Adapted from CALMET User's Guide by Scire *et al.* (2000).

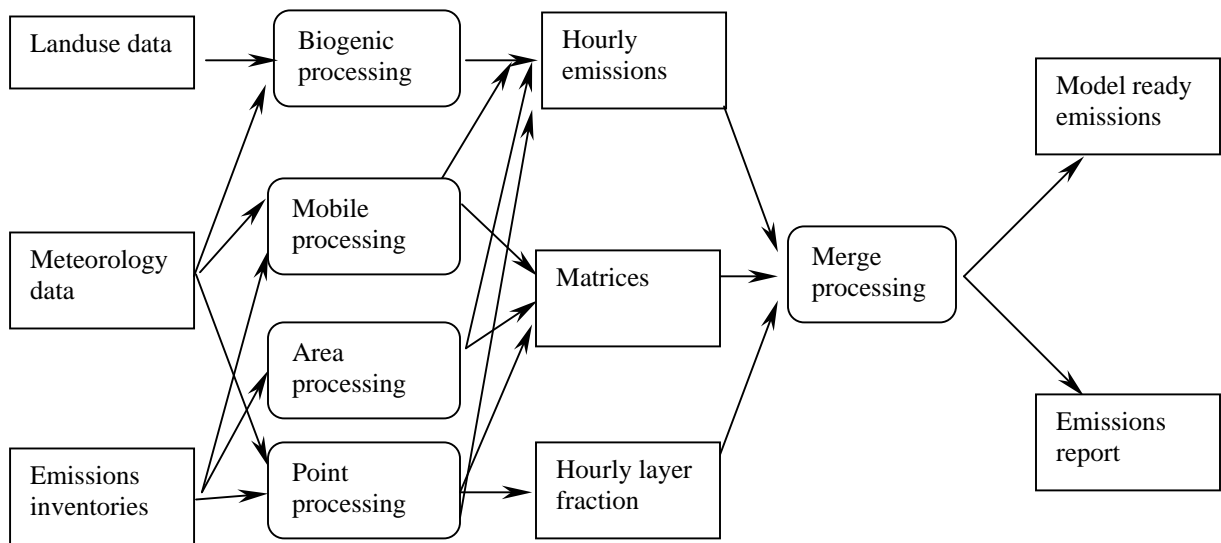


Figure 4: Relationship between data and processors in SMOKE. Square and rounded boxes represent input-output files and processors, respectively (adapted from Houyoux *et al.*, 2004)

Table 1: Current photochemical models and attributes. Adapted from Russell and Dennis (2000).

Model	Full name/reference	Model type	Chemical mechanism	Typical applications
(a) <u>Urban scale</u> UAM-IV	Urban Air-shed Model, version IV (Reynolds <i>et al.</i> , 1973)	Eulerian, multilayer	CB-IV (Gery <i>et al.</i> , 1989)	US regulatory model
CIT	California Institute of Technology model (McRae and Seinfeld, 1983)	Eulerian, multilayer	SAPRC (Carter, 1990)	O ₃ , PM, deposition
CALGRID	California Air Resources Board Grid Model (Yamartino <i>et al.</i> , 1992)	Eulerian, multilayer	CB-IV, SAPRC	O ₃ , PM, deposition
EKMA	Empirical kinetics modeling approach (NRC, 1991)	Box model	CB-IV, SAPRC, RADM	Used for understanding chemistry
(b) <u>Regional Scale</u> RADM	Regional acid deposition model (Chang <i>et al.</i> , 1987)	Eulerian, multilayer	RADM2 (Stockwell <i>et al.</i> , 1990)	Acid deposition and O ₃
ROM	Regional oxidant model (Lamb, 1983)	Eulerian, 3 layer	CB-IV	O ₃
EURAD	European Air Dispersion Model (Hass, 1991)	Eulerian, multilayer	RADM2	Acid deposition, O ₃
(c) <u>Multi-scale</u> MAQSIP	Multiscale air quality simulation Program (Odman and Ingram, 1996)	Eulerian, multilayer	CB-IV	O ₃ , PM
EURAD	European Air Dispersion Model (Hass, 1991)	Eulerian, multilayer	RADM2	Acid deposition, O ₃
UAM-V	Urban Airshed Model -V (Morris <i>et al.</i> , 1991)	Eulerian, multilayer	CB-IV	O ₃
URM	Urban-to-regional multiscale model (Kumar <i>et al.</i> , 1994)	Eulerian, multilayer	SAPRC	O ₃
MODELS-3/CMAQ	Community multiscale air quality model (Byun and Ching, 1999)	Eulerian, multilayer	CB-IV, SAPRC, RADM2	O ₃ , PM, acid deposition

Table 2: Web-based air quality forecasting systems around the world.

System	Main photochemical model(s)	Predicted species	Status	Organization
AIRNow ^a	Various	O ₃ , PM _{2.5}	Operational/ Quasi-operational	United State Environment Protection Agency
Australian Air Quality Forecasting System (AAQFS) ^b	Modified version of CIT model	O ₃ , oxides nitrogen and sulfur, CO, PM ₁₀ , benzene, and tracers	Operational	Environmental Protection Authority, Victoria, Australia
UK Air Pollution Forecasting ^c	NAME III (Numerical Atmospheric-dispersion Modelling Environment)	O ₃ , oxides nitrogen and sulfur, CO and PM ₁₀ .	Operational	The Met Office, United Kingdom
THOR Forecast system ^d	Long Range Transport Model (DEHM) Urban Background Model (UBM)	Several species	Operational	National Environmental Research Institute, Denmark
Canadian Air Quality Forecast ^e	CHRONOS (Canadian Hemispheric and Regional Ozone and NO _x System)	O ₃ , PM _{2.5} , CO	Operational (Research)	Environment Canada
European air quality forecast ^f	EURAD	O ₃	Quasi-operational	Rhenish Institute for Environmental Research, University of Cologne, Germany

a. <http://airnow.gov/>

b. <http://www.epa.vic.gov.au/Air/AAQFS/default.asp>

c. <http://www.airquality.co.uk/archive/index.php>

d. http://www2.dmu.dk/1_Viden/2_miljoe-tilstand/3_luft/4_udsigt/default_en.asp

e. http://www.msc-smc.ec.gc.ca/aq_smog/index_e.cfm

f. http://db.eurad.uni-koeln.de/index_e.html?/prognose/description_e.html

Table 3: Air quality index (AQI) designed by the AIRNow project of the United States Environmental Protection Agency (USEPA) (<http://www.epa.gov/airnow/>)

Air Quality Index Levels of Health Concern	Numerical Value	Meaning
Good	0-50	Air quality is considered satisfactory, and air pollution poses little or no risk.
Moderate	51-100	Air quality is acceptable; however, for some pollutants there may be a moderate health concern for a very small number of people who are unusually sensitive to air pollution.
Unhealthy for Sensitive Groups	101-150	Members of sensitive groups may experience health effects. The general public is not likely to be affected.
Unhealthy	151-200	Everyone may begin to experience health effects; members of sensitive groups may experience more serious health effects.
Very Unhealthy	201-300	Health alert: everyone may experience more serious health effects.
Hazardous	> 300	Health warnings of emergency conditions. The entire population is more likely to be affected.

Table 4. MM5 and MCIP vertical sigma levels, and the approximate MCIP sigma level height above the surface. Further details are available at: <http://pah.cert.ucr.edu/rmc/>

MM5 sigma levels	MCIP sigma levels	Height of MCIP sigma level above surface (m)
1.00	1.00	0
0.995	0.995	35
0.99	0.99	53
0.985		
0.98	0.98	105
0.97	0.97	177
0.96	0.96	248
0.95		
0.94	0.94	357
0.93		
0.92	0.92	503
0.91		
0.90	0.90	652
0.88		
0.86	0.86	880
0.83	0.83	1150
0.80	0.80	1390
0.77		
0.74	0.74	1760
0.71		
0.68		
0.64		
0.60	0.60	2650
0.56		
0.52		
0.48		
0.44	0.44	4180
0.40		
0.36		
0.32		
0.28		
0.24	0.24	6390
0.20		
0.16		
0.12		
0.08		
0.04		
0.00	0.00	10315

Table 5: List of modeled hydrocarbon species in the AIRPACT2 system.

Modeled species	Names	MW (g/mole)
<u>Gaseous species</u>		
ACET	Acetone	58.08
ALK1	Lumped Alkane 1	68.58
ALK2	Lumped Alkane 2	108.0
ARO1	Lumped Aromatic 1	95.52
ARO2	Lumped Aromatic 2	115.76
BALD	Benzaldehyde	106.13
CCHO	Acetaldehyde	44.05
CRES	Cresol	108.14
GLY	Glyoxal	58.04
HCHO	Formaldehyde	30.03
ISOP	Isoprene	68.12
MEK	Methyl Ethyl Ketone	72.11
MGLY	Methyl Glyoxal	72.07
NPHE	Nitro-phenol	139.11
OLE1	Lumped Olefin 1	54.39
OLE2	Lumped Olefin 2	68.42
OLE3	Lumped Olefin 3	116.43
PHEN	Phenol	94.11
<u>Particulates</u>		
DSPM	Diesel Soot Particulate Matter	30.0
PM2_5	Particulate Matter 2.5	30.0
WSPM	Wood Stove Particulate Matter	30.0
<u>Added primary air toxic species</u>		
AALD	Acetaldehyde	44.06
BENZ	Benzene	78.1
BUTD	1,3-Butadiene	54.09
FORM	Formaldehyde	30.03
PERC	Perchloroethylene	165.9
PHNT	Phenanthrene	178.23

Table 6: Initial Concentrations (IC) and Boundary Conditions (BC) for all lateral boundaries used in the CALGRID model.

Model Species	Species name	Initial and Boundary concentrations in ppm_v	Reference
ACET	Acetone	0.001	Millet <i>et al.</i> (2004)
BALD	Benzaldehyde	0.00001	Finlayson Pitts and Pitts (2000)
BENZ	Benzene	0.0001	Millet <i>et al.</i> (2004)
BUTD	1,3-Butadiene	0.00002	Finlayson Pitts and Pitts (2000)
CCHO	Acetaldehyde	0.003	Jiang (2001)
CCOOH	Acetic acid	0.0005	Finlayson Pitts and Pitts (2000)
CO	Carbon monoxide	0.17000	Millet <i>et al.</i> (2004)
CO2	Carbon-dioxide	359	Atlas <i>et al.</i> (1996)
ETHE	Ethene	0.00005	Killin <i>et al.</i> (2004)
GLY	Glyoxal	0.00001	Finlayson Pitts and Pitts (2000)
HCHO	Formaldehyde	0.0002	Atlas <i>et al.</i> (1996)
HCOOH	Formic acid	0.0003	Finlayson Pitts and Pitts (2000)
HNO3	Nitric acid	0.0001	Jiang (2001)
HO2.	Hydroperoxide Radicals	0.0003	Atlas <i>et al.</i> (1996)
HO2H	Hydrogen peroxide	0.002	Finlayson Pitts and Pitts (2000)
HONO	Nitrous acid	0.00005	Finlayson Pitts and Pitts (2000)
ISOP	Isoprene	0.0003	Jiang (2001)
MEK	Methyl-ethyl ketone	0.0001	Millet <i>et al.</i> (2004)
MGLY	Methylglyoxyl	0.00002	Finlayson Pitts and Pitts (2000)
MVK	Methyl vinyl ketone	0.00001	Millet <i>et al.</i> (2004)
NO2	Nitrogen dioxide	0.0002	Finlayson Pitts and Pitts (2000)
O3	Ozone	0.04	Jiang (2001)
OLE1	Lumped olefins 1	0.0004	Jiang (2001)
OLE2	Lumped olefins 2	0.0005	Jiang (2001)
PERC	Perchloroethylene	0.00001	Killin <i>et al.</i> (2004)
PM2_5	Particulate matter	0.002	Killin <i>et al.</i> (2004)
PPN	Peroxy propanoil nitrate	0.00004	Finlayson Pitts and Pitts (2000)
RCHO	Propanaldehyde	0.00020	Finlayson Pitts and Pitts (2000)

Table 7: National Ambient Air Quality Standards (NAAQS). This can be found at the website of the United States Environmental Protection Agency (<http://www.epa.gov>).

Pollutant	Primary Standards	Averaging Period	Secondary Standards
Carbon monoxide (CO)	9 ppm (10 mg/m ³)	8-hr ¹	None
	35 ppm (40 mg/m ³)	1-hr ¹	None
Lead (Pb)	1.5 µg/m ³	Quarterly average	Same as Primary
Nitrogen Dioxide (NO ₂)	0.053 ppm (100 µg/m ³)	Annual arithmetic mean	Same as Primary
Particulate Matter (PM ₁₀)	50 µg/m ³	Annual arithmetic mean ²	Same as Primary
	150 µg/m ³	24-hr ¹	
Particulate Matter (PM _{2.5})	15.0 µg/m ³	Annual arithmetic mean ³	Same as Primary
	65.0 µg/m ³	24-hr ⁴	
Ozone (O ₃)	0.080 ppm	8-hour ⁵	Same as primary
Sulfur Oxides (SO ₂)	0.03 ppm	Annual arithmetic mean	N/A
	0.14 ppm	24-hour ¹	N/A
	N/A	3-hour ¹	0.5 ppm (1300 µg/m ³)

¹ Not to be exceeded more than once per year.

² To attain this standard, the 3-year average of the weighted annual mean PM₁₀ concentration at each monitor within an area must not exceed 50 µg/m³

³ To attain this standard, the 3-year average of the weighted annual mean PM_{2.5} concentrations from single or multiple community-oriented monitors must not exceed 15.0 ug/m³.

⁴ To attain this standard, the 3-year average of the 98th percentile of 24-hour concentrations at each population-oriented monitor within an area must not exceed 65 ug/m³.

⁵ To attain this standard, the 3-year average of the fourth-highest daily maximum 8-hour average ozone concentrations measured at each monitor within an area over each year must not exceed 0.08 ppm.

Table 8: Definition of the statistical measures for model evaluation. Measures in *italic* are used in this study.

Statistics	Formula	Reference
Mean Bias Error (MBE) or <i>Mean Bias (MB)</i>	$\frac{1}{N} \sum_{i=1}^N (C_{\text{mod}i} - C_{\text{obs}i}) \text{ in ppm or } \mu\text{g}/\text{m}^3$	McHenry <i>et al.</i> , 2004
Normalized Mean Bias (NMB)	$\frac{\sum_{i=1}^N (C_{\text{mod}i} - C_{\text{obs}i})}{\sum_{i=1}^N C_{\text{obs}i}} \text{ in } \%$	O'Neill, 2002 Barna and Lamb, 2000
Fractional Mean Bias (FMB) or <i>Fractional Bias (FB)</i>	$\frac{1}{N} \sum_{i=1}^N \frac{(C_{\text{mod}i} - C_{\text{obs}i})}{(C_{\text{mod}i} + C_{\text{obs}i})} \text{ in } \%$	Cope <i>et al.</i> , 2004 Hanna <i>et al.</i> , 2004
Mean Absolute Gross Error (MAGE) or <i>Mean Error (ME)</i>	$\frac{1}{N} \sum_{i=1}^N (C_{\text{mod}i} - C_{\text{obs}i}) \text{ in ppm or } \mu\text{g}/\text{m}^3$	McHenry <i>et al.</i> , 2004
Normalized Mean Error (NME)	$\frac{\sum_{i=1}^N C_{\text{mod}i} - C_{\text{obs}i} }{\sum_{i=1}^N C_{\text{obs}i}} \text{ in } \%$	
Mean Absolute Fractional Error (MAFE) or <i>Fractional Error (FE)</i>	$\frac{1}{N} \sum_{i=1}^N \frac{ (C_{\text{mod}i} - C_{\text{obs}i}) }{(C_{\text{mod}i} + C_{\text{obs}i})} \text{ in } \%$	
Root Mean Square Error (RMSE)	$\left[\frac{1}{N} \sum_{i=1}^N (C_{\text{mod}i} - C_{\text{obs}i})^2 \right]^{1/2}$	Barna and Lamb, 2000 O'Neill, 2002 McHenry <i>et al.</i> , 2004 Hanna <i>et al.</i> , 2004 Cope <i>et al.</i> , 2004
Index of Agreement (IA)	$1 - \frac{\sum_{i=1}^N (C_{\text{mod}i} - C_{\text{obs}i})^2}{\sum_{i=1}^N (C_{\text{mod}i} - \bar{C}_{\text{obs}} + C_{\text{obs}i} - \bar{C}_{\text{obs}})^2}$	Barna and Lamb, 2000 O'Neill, 2002
Standard Deviation of Residuals (SD _R)	$\left[\frac{1}{N} \sum_{i=1}^N (C_{\text{mod}i} - C_{\text{obs}i} - MBE)^2 \right]^{1/2}$	Hogrefe <i>et al.</i> , 2001

CHAPTER 2

EVALUATION OF THE AIRPACT2 AIR QUALITY FORECAST SYSTEM

FOR THE PACIFIC NORTHWEST

Abdullah Mahmud, Joe Vaughan, Jack Chen, Jeremy Avise, Brian Lamb and Hal Westberg

Laboratory for Atmospheric Research

Department of Civil & Environmental Engineering

Washington State University, WA 99164-2910

Abstract

AIRPACT2, a numerical photochemical air quality modeling system that generates daily forecasts of hourly gas-phase species mixing ratios, including air toxics, and primary particulate concentrations for the Pacific Northwest, was evaluated in this study. The statistical performance of the forecast system was assessed using observations from the months of September and October 2003. Mean bias (MB), fractional bias (FB), mean error (ME), and fractional error (FE) were used to describe the modeling performance. The AIRPACT2 system showed varying abilities to simulate observations of ozone (O_3), the air toxic compounds formaldehyde, acetaldehyde, benzene and perchloroethylene, and primary fine particulate matter ($PM_{2.5}$). Meteorological parameters such as wind speed, wind direction, and temperature were also investigated in line with the forecast system evaluation.

Simulations of wind speed and direction, and temperature by the meteorological component in the AIRPACT2 system showed reasonable agreement with observations, although localized variations in those parameters were not portrayed quite accurately at a few sites. The system showed better O_3 forecasting abilities during an O_3 episode as compared to non-episode periods. An average MB of 14 ppb and FB of 40%, and MB of 8 ppb and FB of 22% were found for urban sites and semi-urban/rural sites, respectively. The system captured the general temporal and spatial patterns of O_3 fairly well. One in six day, 24-hr average measured air toxic mixing ratios were available from one Seattle monitoring site. The system captured the temporal pattern of most air toxics correctly. However, mixing ratios of the air toxic compounds, except for perchloroethylene, were over-estimated. Because the AIRPACT2 system treats primary emissions of $PM_{2.5}$ only, the system under-estimated fine particulate concentrations at all sites.

2.1 Introduction

Recently, there has been much interest in the development of chemical weather forecasting capabilities (McHenry *et al.*, 2004) using numerical models (e.g., Vaughan *et al.*, 2004; Mass *et al.*, 2003; Elbir, 2003; Cope *et al.*, 2004). The Air Indicator Report for Public Access and Community Tracking version 2 (AIRPACT2) is a numerical air quality forecasting system that has been developed for the Pacific Northwest. The system produces hourly mixing ratios of gas-phase species including air toxics, and concentrations of particulates in advance of a 24-hr period. The daily forecast results are published on the website at <http://www.airpact.wsu.edu> for general access. Although the Pacific Northwest is not known to have severe air quality problems, there is regional concern with the potential impacts of with increasing population and industries in the region as reported by several other studies (e.g., O'Neill, 2002; Barna *et al.*, 2000; Jiang *et al.*, 2003). Thus, the original AIRPACT system was developed during the years from 2000 to 2001 with the objectives of (a) providing air-quality managers in the Puget Sound region with timely forecasts of air pollution episodes and (b) allowing for the potential notification of sensitive populations (Vaughan *et al.*, 2004). Later, with increasing interest among federal and state regulatory agencies, the modeling system was updated to AIRPACT2 in September 2003 by incorporating air toxic species, and expanding the modeling domain to extend from north of Vancouver, BC to south of Portland, OR.

In the past, simulations of historic air pollution episodes in the Pacific Northwest have been carried out to better understand roles of emissions, chemistry, and transport of different chemical species (e.g., Barna *et al.*, 2000; Barna and Lamb, 2000; Barna *et al.*, 2001; O'Neill, 2002; Chen, 2002; Jiang *et al.*, 2003; O'Neill and Lamb, 2005) in an air quality modeling system. However, the implementation of the daily air quality forecasting system, AIRPACT2, is

a novel one for this region. Although Vaughan *et al.* (2004) presented preliminary evaluation of the original AIRPACT system, no such evaluation was carried out for AIRPACT2 until this study. Evaluation of model performance is a matter of great interest and it becomes particularly important for air quality modeling (Elbir, 2003) because of the complexities associated with atmospheric processes. The system evaluation is also important because of the large economic, public health, and ecosystem impacts associated with the use of air quality modeling results (Chang and Hanna, 2004).

Discussions of the evaluation of air quality models as well as of the development of general evaluation methods have been presented by many scientists in recent years (e.g., Seigneur *et al.*, 2000; McNally and Tasche, 1993; Hanna *et al.*, 1993); however, standard evaluation procedures and performance standards still do not exist in the air quality modeling community. There can be three components to the evaluation of air quality models: scientific, statistical, and operational (Chang and Hanna, 2003). A scientific evaluation usually deals with the model algorithms, underlying physics, assumption, and codes for their accuracy, efficiency and sensitivity. This kind of evaluation process requires an in-depth knowledge of the modeling system. In a statistical evaluation approach, model outputs are compared with observations, and the model performance is expressed in the form of statistical measures. The third component of a model evaluation is considered to be associated more with the application of the model itself; how easy it is to use the model, are there errors in the user's guide - are some of the typical questions answered in an operational evaluation. It is also important to define the goal of the evaluation process; different goals could lead to different variables being evaluated and different performance measures being used. In this study, a mainly statistical evaluation of the modeling

system has been performed with an objective to understand the system performances in simulating gas-phase species, such as O₃ and air toxics, and fine particulate matter (PM_{2.5}).

2.2 System design

A schematic diagram of the AIRPACT2 system is given in Figure 1. The detailed system design has been discussed elsewhere (Vaughan *et al.*, 2004), and also, has been described in Chapter 1 of this thesis. The major components of the system are the PSU/NCAR fifth generation Mesoscale Meteorological model, MM5 version 3 (Dudhia *et al.*, 2002) coupled with the diagnostic three-dimensional wind-field model, CALMET version 5 (Scire *et al.*, 2000) and meteorology-chemistry interface processor, MCIP version 2.2 (Byun *et al.*, 1999), the emissions processor, SMOKE version 2.0 (Houyoux *et al.*, 2004), and the Eulerian photochemical grid model, CALGRID version 1.6 (Yamartino *et al.*, 1992).

In AIRPACT2, meteorological parameters are processed by CALMET and MCIP from MM5 hourly outputs. CALMET extracts only the horizontal wind components from the MM5 data then calculates the vertical wind component from the continuity equation to generate a mass consistent three-dimensional wind field. It also extracts temperature and short-wave radiation components suitable for mobile and biogenic emission processing by SMOKE. In a previous MM5-CALMET-CALGRID simulation study in the Pacific Northwest, O'Neill and Lamb (2005) found that the results of CALGRID O₃ simulations are much more realistic if using the planetary boundary layer (PBL) heights directly extracted by MCIP from MM5 than using the heights calculated by CALMET. So, in the AIRPACT2 system MCIP was also incorporated to extract the PBL parameters. The following PBL parameters are extracted by MCIP, which replace those calculated by CALMET in the final output file: friction velocity, convective

velocity scale, PBL height, air temperature, Monin-Obukhov length, roughness length, and terrain elevation.

SMOKE processes emissions from area, mobile, and biogenic sources. The BEIS3 (Guenther *et al.*, 1993) biogenic emissions module provides biogenic emissions while MOBILE6 (US EPA, 1997) produces mobile source emissions within the SMOKE framework. The emission inventory provided by Washington Department of Ecology based on NET96 is used in AIRPACT2. Unlike other emission sources, the point source emissions are processed without SMOKE within the CALGRID modeling system using the SAPRC97 (Carter *et al.*, 1997) chemical speciation scheme.

The CALGRID model solves species conservation equations for 50 chemical species and 102 chemical reactions using the quasi-steady-state-approximation (QSSA). The model assumes clear-sky photolysis, which is a reasonable assumption for photochemical events, and includes the SAPRC97 chemical mechanism. There are 13 vertical layers of variable depth distributed over the first 5000 m above ground. The initial condition (IC) and the boundary condition (BC) used are two fixed-value input files in the modeling system. The initial and the boundary concentrations of different species were obtained from the work of Jiang (2001), and findings from literature. The details of the model IC and BC can be found in Chapter 1 of this thesis.

2.3 Modeling domain and observation network

The modeling domain depicted in Figure 2 encompasses an area from Vancouver, BC in the north to Salem, OR in the south, and from the Pacific coast in the west to beyond the crest of the Cascade Mountain Range, WA in the east. The domain is represented by 81 (E-W) x 138 (N-S) grid cells with 4-km spacing. Figure 2 also shows the locations of the air quality monitoring stations within the domain.

Washington Department of Ecology (ECOLOGY) has a network of several air quality monitoring stations throughout WA, whose data automatically flow into their central database. Oregon Department of Environmental Quality (ODEQ) also has a similar monitoring network, although it is not currently fully automated. In this study, observations of O₃, air toxics and PM_{2.5} data have been extracted from an archived database from a total of 25 AQ monitoring stations in WA and OR. A list of the monitoring stations in WA and OR can be found in APPENDIX I. The monitoring stations have been categorized as “urban” and “semi-urban/rural” sites in this study. Most of the stations are located near and around the Seattle and Portland metropolitan areas, with other stations sparsely located within the domain.

2.4 Evaluation methods

AIRPACT2 was evaluated using observations from ECOLOGY, ODEQ, and the United State Environmental Protection Agency’s (USEPA’s) Urban Air Toxics Measurement Campaign in Seattle, WA. Data from a total of 15 urban, and semi-urban/rural monitoring stations were used for O₃, and from 12 stations for PM_{2.5}. Due to a limited availability of continuous measurements in 2003, data from only one urban monitoring station were used for air toxics evaluation. O₃ and PM_{2.5} simulations were evaluated for September 2003, and air toxics simulations were evaluated using one in six day observation for the months of September and October 2003. Observations of surface layer wind speed, wind direction, and temperature from eight meteorological monitoring stations, and upper air data from one location were also used to evaluate the meteorological component of the AIRPACT2 system.

In order to compare predicted results with observations, hourly modeled mixing ratios of gaseous species and concentrations of particulates from the first layer of the modeling domain were extracted. The extraction process involved conversion of geographic coordinates of the

locations of the monitoring stations to corresponding grid-cell numbers, determination of eight other grid-cells around the monitoring station, and extraction of cell volumetric concentrations of that 3 x 3 grid-cell mask. This was done in order to compensate for the known level of uncertainty in predicted wind fields. Finally, observations were compared with corresponding modeled cell mixing ratios and concentrations, and with the maximum and the minimum within the nine grid-cells.

The evaluation process applied the following model performance metrics:

$$\text{Mean Bias: } \frac{1}{N} \sum_{i=1}^N (C_{mi} - C_{oi}) \text{ [ppb or ug/m}^3\text{]}$$

$$\text{Fractional Bias: } \frac{1}{N} \sum_{i=1}^N \left(\frac{C_{mi} - C_{oi}}{\left(\frac{C_{mi} + C_{oi}}{2} \right)} \right) \text{ [x 100\%]}$$

$$\text{Mean Error: } \frac{1}{N} \sum_{i=1}^N |C_{mi} - C_{oi}| \text{ [ppb or ug/m}^3\text{]}$$

$$\text{Fractional Error: } \frac{1}{N} \sum_{i=1}^N \left(\frac{|C_{mi} - C_{oi}|}{\left(\frac{C_{mi} + C_{oi}}{2} \right)} \right) \text{ [x 100\%]}$$

Where C_m : modeled concentration

C_o : observed concentration

$i - N$: number of data points

2.5 Results and discussions

This section includes findings of prediction capabilities of CALMET/MCIP in simulating meteorological parameters, and CALGRID in simulating gas-phase species, and particulates in the AIRPACT2 modeling system. It also presents discussions on the findings of different simulation results. It is worth emphasizing that the model re-runs for September - October 2003

were carried out with the current modeling configurations. Model control parameters were not modified for this study. The results were analyzed using evaluation statistics for each species over a specific time period, and by carefully inspecting and interpreting time series of simulated and observed hourly data.

2.5.1 Simulations of meteorological parameters

A critical component of any air pollution modeling study is the representation of the meteorology within the model domain, since an accurate air quality simulation requires an accurate portrayal of the three-dimensional wind fields (Barna and Lamb, 2000). Meteorological parameters such as temperature, wind speed and direction, and planetary boundary layer (PBL) heights play critical roles in production, transport, and distribution of primary and secondary pollutants in the atmosphere. As a result, inaccurate representations of meteorological parameters could contribute to inaccurate predictions of gas-phase species and particulates. Although evaluation of the meteorological models in this study was not the primary objective in this study, an attempt was made to characterize the performance of the meteorological models in the AIRPACT2 system in order to explain findings of simulations of other species later. Details of the meteorological model, MM5 solutions, and its performance to simulate observations in the Pacific Northwest have been discussed by Barna and Lamb (2000).

Meteorological performance was evaluated through a step-wise process: modeled wind components and temperature were extracted from the first layer of the CALMET output files, wind speed and direction were calculated for each monitoring site, and finally, the modeled wind speed and direction were compared against observations from eight monitoring sites in WA. Vertical profiles of the modeled meteorological parameters were also investigated using observations from only one site at Salem, OR.

Table 1 contained the performance statistics for the MM5/CALMET in the AIRPACT2 system in simulating wind speeds at and around the monitoring stations. Wind speeds were generally over-estimated, except at Seattle Beacon Hill and Wishram, where wind speeds were under-estimated. Although average FB of 19% and FE of 37% indicate a reasonable model performance, performances at individual sites were quite variable. The model performed the worst at Tacoma, which is an urban site, as indicated by relatively higher biases and errors compared to other sites. Surprisingly, wind speeds were best simulated at Seattle Beacon Hill, which is also an urban site and sits on a steep hill above the Seattle city center. The maximum daily mean wind speed of 5.4 m/s was measured at Wishram, which is located in the Columbia River Gorge southeast of Seattle. Interestingly, this is where the model most under-estimated wind speed; MB was -2.2 m/s. Figure 3 shows hourly time series of wind speed at different sites for the time period of September 4-6, 2003. It can be seen from this figure that the diurnal patterns of measured wind speeds are portrayed quite well at all sites, except at North Bend, where the modeled results (even the maximum and minimum within the nine grid-cells), missed the diurnal pattern. On the other hand, measured hourly wind speeds were found within the maximum and minimum range of modeled values at most sites. Wind speeds were slightly better simulated at nighttime than daytime. Unlike wind speed, simulations of wind direction were slightly less variable. Figure 4 shows the frequency distribution (in %) of modeled and measured wind directions at six different sites. The predominant modeled and observed wind directions were found to be southwesterly (181-270 degree) and/or northwesterly (271-360 degree) at most sites. Modeled wind directions showed reasonable agreement with observations at most sites, except at North Bend, which also showed poor prediction of wind speeds. A difference plot between modeled and measured wind directions in Figure 5 shows that the variation of wind

direction was within a 10-15 degree window average during a 24-hr period. The model performance results for wind speed and direction, however, need to be carefully interpreted. Both the magnitude and direction of wind can be highly influenced by very localized phenomena such as sea breeze and nighttime drainage flow, and by the local topographic features that are not resolved by the current system resolution. Thus it is significant that an average modeled wind speed over a 4-km x 4-km grid-cell was compared to a measured value at a point location.

The modeled temperatures were also compared with observations in this study. Results in Table 2 reveal that the modeled temperatures were in reasonably good agreement with measured temperatures as indicated by the low biases and errors. The average measured temperature was 62 °F among the sites. Like wind speed, temperature was also under-estimated at the Columbia Gorge Wishram site. The model over-estimated temperatures primarily in urban sites i.e. Seattle Beacon Hill and Vancouver.

Wind speed and temperature vertical profiles were compared with observations. There are only two upper air stations within the domain and only one of these (Salem) is along the urbanized I-5 corridor. Profile observations were gathered from the Salem, OR station and the daily 0000 PST and 1200 PST profile data were compared with the modeled data for the same time. Figure 6 shows modeled and observed wind speed profile at 0000 PST and 1200 PST and for time periods during both O₃ episode and non-episode days. In general, the model predicted higher wind speeds at midday and lower at midnight. The vertical wind speed profile hardly matched with observations. This, perhaps, was due to different heights of measured and modeled data points. In the AIRPACT2 system, layers below 1000 m are more highly resolved than upper layers. As a result, the shapes of the modeled profiles looks different at higher altitudes compared to observed profiles.

2.5.2 Simulations of O₃

O₃ is a secondary pollutant, which is generated in the atmosphere through chemical reactions. Because of its impact on human health and on ecosystem dynamics, O₃ is one of the most studied air pollutants in the atmosphere. Consequently, many photochemical models have emerged as means to predict O₃ mixing ratios over the years. Yet, the success of these models in predicting O₃ is highly variable, and largely depends on the accurate representations of the precursor species such as NO_x and VOCs, and the meteorological parameters such as the horizontal and vertical temperature profiles, the mixing length heights, and the wind vectors. In this study, the performance of the CALGRID photochemical model in the AIRPACT2 system has been evaluated. From a regulatory perspective, 8-hr daily max O₃ mixing ratios were used to calculate the model performance statistics. In order to generate 8-hr daily max statistics, a cutoff at 20 ppb of observed O₃ was applied to include O₃ mixing ratios 20 ppb and above in both modeled and observed data. The choice of the cutoff value for model evaluation was the same as adopted by Jiang *et al.* (1998), but below the suggested level of 40 ppb by Ian *et al.* (2003). The model performance was studied at each site for the month of September 2003, and average statistics were calculated for urban and semi-urban/rural sites. The performance was also studied for an episode and a non-episode periods.

Table 3 contains O₃ prediction performance statistics for the month of September 2003. The system showed variable performances at different monitoring sites. So, it is equally important to look at statistics for individual sites as well as to the average statistics while interpreting the results. On average, the system performed relatively better in semi-urban/rural sites than urban sites. Average MB of 14 ppb and FB of 40% were found at urban sites as compared to MB of 8 ppb and FB of 24% at semi-urban/rural sites. The positive biases and

errors indicate that the system generally over-estimated O₃ mixing ratios. However, the MB and FB found in this study are quite comparable with the results reported by McHenry *et al.* (2004). As expected, the urban sites usually showed lower 8-hr daily maximum ambient O₃ compared to semi-urban/rural sites. The highest 8-hr daily maximum of 89 ppb was measured at Paradise located at 1700 on the side of Mt Rainier, which is a 120 km downwind of the Seattle metropolitan areas. Sites located within the Vancouver/Portland area in the southern part of the domain, which includes Sauvie Island, Vancouver, Wishram, Milwaukie, Carus, and Turner, usually showed higher levels of O₃ compared to other monitoring sites near Seattle in the middle and northern parts of the domain. The system also predicted higher O₃ at sites in the southern part of the domain compared to the Seattle region.

Although biases and errors of O₃ predictions over the entire month of September 2003 provided good estimates of overall performance of the system, their calculations might obscure good and/or poor simulations during an O₃ episode and/or non-episode period. So, the evaluation statistics were also applied to episode and non-episode cases in order to understand the system performance in detail. A four-day episode period from September 2 through to September 5, 2003, and a non-episode period from September 18 through to September 21, 2003 were selected for this study. Table 4 shows performance statistics for episode and non-episode periods. The system performed relatively better during the O₃ episode than during the non-episode period. The system slightly under-estimated O₃ mixing ratios during the episode at most sites while it over-estimated at all sites during the non-episode period. This was further investigated using time series at individual sites.

Figure 8 depicts time series of hourly O₃ mixing ratios during the episode and the non-episode cases for each site. It can clearly be seen that the diurnal pattern of O₃ was captured by

the system quite well for both cases. During the episode, modeled daily peak O₃ mixing ratios closely matched with observations at most sites; however, the daily peaks were under-estimated during the non-episode period. The time series plots also reveal that the system failed to depict nighttime O₃ titration. Issaquah and North Bend are the two sites where O₃ titration by local on-road emissions at night was clearly seen from measurements; but the system did not capture this behavior. Jiang *et al.* (2003) also reported similar findings using the CALGRID photochemical model for the Pacific Northwest. Although observed nighttime O₃ levels during September were not significant, differences between the modeled and observed mixing ratios largely contributed to bias and error calculations. The system's inability to represent nighttime O₃ might be caused by errors in nighttime emissions and/or by incorrect treatment of vertical mixing during stable nighttime conditions. Pleim *et al.* (2005) described similar behavior and suggested a modification of the vertical diffusivity as a function of landuse to correct this problem.

A Q-Q plot of modeled and observed 8-hr daily max O₃ mixing ratios from all sites in Figure 9 shows that the system simulated observations relatively better at higher O₃ than for observations approximately below 50 ppb. This was further corroborated by the plot of the 8-hr daily maximum modeled and observed mixing ratios within all sites in figure 10.

The CALGRID model utilizes the clear-sky assumption for photolysis. So, the general over-predictions during the non-episode period (September 18-21, 2003) were further investigated by looking at the MCIP cloud cover outputs for that time period. Figure 11 shows that the most parts of the domain were overcast at noon on the 18th and 19th of September 2003, resulting in unfavorable conditions for O₃ productions in the environment. However, the system primarily over-estimated O₃ mixing ratios at all sites. In addition, it can also be seen that at noon

on September 21, 2003, the sky was relatively clearer in most parts in the domain, and so the predicted peak O₃ seemed to match better with the observations.

To summarize, the ability of the AIRPACT2 system to predict O₃ mixing ratios was found to be variable. The system performed better during episode days compared to non-episode days. O₃ mixing ratios higher than 50 ppb were usually simulated more accurately than low O₃. Poor performances during nighttimes and during non-episode days could be attributed to localized traffic related emissions that were not considered in the model emissions, inaccuracies of vertical diffusivities for complex areas within the domain, and cloud covers that are not taken into account in CALGRID. In this research, the role of boundary condition O₃ mixing ratios was also tested. It was found that O₃ modeled mixing ratios usually increased by approximately 3 ppb, if the boundary O₃ was increased by 5 ppb. Therefore, it should also be recognized that boundary conditions for O₃, VOCs and NO_x can also influence model predictions.

2.5.3 Simulations of air toxics

There has been growing interest in air toxics in recent years because of the potential adverse health effects. Simulation of air toxics with the AIRPACT2 system is, however, new and unique to the AIRPACT2 system. Although there have been measurements in the United States, modeling air toxics species using a sophisticated three-dimensional grid modeling system is relatively new in the modeling community. In an early modeling study, the US EPA conducted a nation-wide air toxics exposure study using a modified version of a Gaussian dispersion model, the Human Exposure Model (HEM) in 1998. The modeling work included point, mobile and area emission sources of air toxics, and secondary formation of some selected air toxics using first-order decay and a simple deposition algorithm. Study results of long-term

averages of air toxics over the entire US, and the level of human exposure were used as a benchmark for developing the Air Toxics Program for the US EPA.

In this study, modeled gas-phase air toxics mixing ratios were extracted for those days when observations were available. Ambient toxics mixing ratios were obtained over a 24-hr period on every sixth day from an urban site in Seattle Beacon Hill, WA. To increase the size of the comparison data set, modeled data were also extracted for October 2003. Model performance for simulations of acetaldehyde, formaldehyde, benzene, 1,3-butadiene, and perchloroethylene was evaluated. The system captured the trend of air toxics correctly as shown in Figure 12, although mixing ratios, except for perchloroethylene, were over-predicted. It is noteworthy, however, that the observed concentrations generally falls within the max-min range of modeled mixing ratios for the 3 x 3 matrix of grid cells around the Beacon Hill site. This level of agreement suggests that the modeling system, including the emission inventory, generally captures the correct behavior of air toxics and also suggests that wind direction variability and the terrain feature of the site are not completely resolved with the model.

This systematic discrepancy was further investigated by a ratio analysis of different species. Table 5 shows the ratios of air toxics to benzene, a relatively non-reactive species in the atmosphere. The closeness between the ratios of modeled and observed air toxics suggests that the system simulated the real world chemistry of formaldehyde, benzene and 1,3-butadiene better than those of acetaldehyde and perchloroethylene. In addition to primary emissions, formaldehyde and acetaldehyde are also formed in the atmosphere through series of hydrocarbon oxidation reactions. The system portrayed the secondary formation of these compounds quite well; yet, less accurately for acetaldehyde. The discrepancies between the ratios of emissions and modeled mixing ratios suggest that the system included the secondary formation of these

compounds in the chemical mechanisms. However, the process of secondary formation of acetaldehyde might have not been included as accurately as for formaldehyde. The systematic over-prediction of air toxics could also be attributed to emissions and/or the to the sub-grid effects as the monitoring site is located close to a major emission source, the interstate I-5 corridor.

In general, the system seemed to have air toxics chemistry incorporated correctly as indicated by the average modeled and observed mixing ratio time series, and by the ratio analysis. The systematic over-estimations of mixing ratios might have been due to sub-grid effects i.e. Seattle Beacon Hill site is located very close to a major source of mobile emissions from the I-5 corridor and/or by the influence of the local topographic as it was found that most of the air toxics measurements fell within the max-min modeled mixing ratio range of the 3 x 3 grid-cell matrix.

2.5.4 PM_{2.5} prediction

The AIRPACT2 system treats primary PM_{2.5} as an unreactive tracer because CALGRID does not account for particle growth or the secondary formation of particulates in the atmosphere. As a result, modeled concentrations of PM_{2.5} account for the primary emission sources mostly from diesel particulate matter (DSPM) and woodstove particulate matter (WSPM). However, in this study, emissions from woodstove were not included in the PM_{2.5} primary emissions because of the fairly warm temperatures of approximately 60 °F in and around Seattle areas during September 2003. So, concentrations predicted by the system are based primarily on direct PM_{2.5} emissions of which approximately 75% is DSPM. Hourly measured concentrations from 12 monitoring sites in WA and corresponding modeled concentrations were considered to calculate a 24-hr average performance statistics of the modeling system. Table 6

contains the performance results of the system in predicting $PM_{2.5}$. The system showed variable performances, although it under-estimated $PM_{2.5}$ concentrations at all sites. It showed an average MB of $-4 \mu\text{g}/\text{m}^3$ and a FB of -38% during the study period. The model performed relatively well at the Bellevue site as indicated by lower MB and FB, where average measured $PM_{2.5}$ concentration was $8 \mu\text{g}/\text{m}^3$. The highest 24-hr average concentrations of $12 \mu\text{g}/\text{m}^3$ of $PM_{2.5}$ were measured at sites in Seattle Duwamish Valley and Tacoma areas, and the system performed poorly in these sites. The findings, however, were quite expected as measured $PM_{2.5}$, which includes both the primary and the secondary $PM_{2.5}$ as opposed to the system, which includes primary $PM_{2.5}$ only.

Figure 13 shows the 24-hr average time-series plot of modeled and observed $PM_{2.5}$ concentrations from 12 sites in the domain (September 1-15, 2003). It is interesting to notice that the occurrences of high concentrations of $PM_{2.5}$ in the atmosphere coincided with the O_3 episode (please refer to Figure 8). It is likely that the formation of secondary $PM_{2.5}$ was favored during the episode (September 2-5, 2003). As the system does not account for secondary formation of $PM_{2.5}$, the predicted low concentrations came as no surprise.

In order to understand how the system behaved during the day, the diurnal patterns of modeled and observed $PM_{2.5}$ were also constructed. Using data from all sites from September 1 through to September 15, average hourly concentrations of $PM_{2.5}$ were calculated. Figure 14(a) shows that the system predicted the early hour $PM_{2.5}$ peak concentrations between 5 AM and 10 AM quite close to the measured levels. However, the system missed the traffic induced late afternoon rush-hour peak in between 4 PM and 8 PM $PM_{2.5}$ levels, and consistently under-estimates at other hours during the day. This indicates that the emissions of primary $PM_{2.5}$ might not be quite correct for the afternoon period given that the model only handles primary $PM_{2.5}$

emissions, and assumes fairly consistent atmospheric mixing during that time. As it was found high observed concentrations during ozone episode (September 2 –5), the diurnal pattern of $PM_{2.5}$ concentrations was recalculated using data from September 8 to September 15. Figure 14(b) clearly shows that the modeled concentrations were not effected by great deal by changing the averaging time period, and the morning hour (between 5 to 10 AM) measured peak $PM_{2.5}$ concentration was found within the modeled range of max-min of the 3 x 3 grid-cell matrix. Hence, it could be argued that the emission inventory used in AIRPACT2 is correct, and the system performed reasonably well in predicting primary emissions, which are freshly emitted from traffic sources, during morning hours. However, it fails to simulate observations correctly as time progresses during the day. It should also be remembered that measured $PM_{2.5}$ concentrations could be influenced by fugitive fine particles from local activities that could not be resolved in the modeled emissions.

2.6 Conclusion

The forecasting performance of the AIRPACT2 system for O_3 , air toxics including formaldehyde, acetaldehyde, benzene, 1,3-butadiene, and perchloroethylene, fine particulate matter ($PM_{2.5}$) and key meteorological parameters such as wind speed, wind direction and temperature for the month of September and October 2005 was evaluated. It was found that the system simulated observed O_3 mixing ratios fairly well during the episode, and captured the temporal patterns correctly. High levels of O_3 were better simulated than low levels. The system also captured the trends of air toxics, although it over-estimated mixing ratios. $PM_{2.5}$ concentrations were under-predicted by the system, as CALGRID does not account for secondary formation of $PM_{2.5}$ aerosols in the atmosphere. The predictions of wind speeds were

quite variable at different sites. On the other hand, modeled wind direction and temperature were close to observed levels.

These results demonstrate that AIRPACT2 shows good promise for forecasting O₃ and air toxics for the Pacific Northwest. Also, as AIRPACT2 is currently undergoing a conversion from CALGRID to CMAQ, modeling of PM_{2.5} is expected to improve, because unlike CALGRID, CMAQ can handle particle growth and the secondary formation of PM_{2.5} in the atmosphere. So, generally speaking, the AIRPACT2 system should have an improved forecasting for the Pacific Northwest in the future.

2.7 Acknowledgments

The authors would like to thank the NW-AIRQUEST for funding this study. Support was also provided from Boeing Corporation endowment funds to Washington State University. The authors thank Sally Otterson and colleagues from the Washington Department of Ecology and staff from the Oregon Department of Environmental Quality for collaboration to compile the AIRPACT2 emission inventory and Cliff Mass and colleagues at the University of Washington for assistance in accessing the MM5 forecast system.

References

- Allan, J., K., Bower, K., Coe, H., Boudries, H., Jayne, J., Canagaratna, M., Millet, D., Goldstein, A., Quinn, P., Weber, R., and Worsnop, D. 2004. Submicron aerosol composition at Trinidad Head, California, during ITCT 2K2: its relationship with gas phase volatile organic carbon and assessment of instrument performance, *Journal of Geophysical Research* **109**, D23S24.
- Atlas, E., and Ridley, B. 1996. The Mauna Loa Observatory Photochemistry Experiment: Introduction, *Journal of Geophysical Research* **101 No. D9**, pp 14531-14541.
- Barna, M., and Lamb, B. 2000. Improving ozone modeling in regions of complex terrain using observational nudging in a prognostic meteorological model. *Atmospheric Environment* **34**, 488-9-4906
- Barna, M., Lamb, B., and Westberg, H., 2001. Modeling the effects of VOC/NO_x emissions on ozone synthesis in the Cascadia airshed of the Pacific Northwest, *Journal of Air Waste Management Association* **51**,1021-1034.
- Barna, M., Lamb, B., O'Neil, S., Westberg, H., Figueroa-Kaminsy, C., Otterson, S., Bowman, C., and DeMay, J., 2000. Modeling Ozone formation and transport in the Cascadian Region of the Pacific Northwest. *Journal of Applied Meteorology* **39**, 349-366.
- Byun, D., Pleim, J., Tang, R., and Bourgeois, A. 1999. Meteorology Chemistry Interface Processor (MCIP) for MODEL-3 Community Multiscale Air Quality (CMAQ) Modeling System. United States Environment Protection Agency, EPA/600/R-99/030.
- Carter, W, Luo, D., and Malkina, I., 1997. Environmental chamber studies for development of an updated photochemical mechanism for VOC reactivity assessment. Final report prepared for California Air Resources Board under Contract 92-345 by Center for Environmental Research and Technology, University of California, Riverside, pp-213.
- Chang, J., and Hanna, S. 2004. Air quality model performance evaluation. *Meteorology and Atmospheric Physics* **87**, 167-196.
- Cope, M., Hess, G., Lee, S., Tory, K., Azzi, M., Carras, J., Lilley, W., Mannis, P., Nelson, P., Ng, L., Puri, K., Wong, N., Walsh, S., and Young, M. 2004. The Australian air quality forecasting system. Part I: Project description and early outcomes. *Journal of Applied Meteorology* **43**, 649-662.
- Dudhia, J., Gill, D., Guo, Y., Manning, K., Bourgeois, A., Wang, W., and Bruyere, C. 2002. PSU/NCAR Mesoscale Modeling System Tutorial Class Notes and User's Guide: *MM5 Modeling System Version 3*. Mesoscale and Microscale Meteorology Division, National Center for Atmospheric Research, Boulder, CO.
- Elbir, T. 2003. Comparison of model predictions with the data of an urban air quality monitoring network in Izmir, Turkey. *Atmospheric Environment* **37**, 2149-2157.
- Guenther, A., Zimmerman, P., Harley, P., Monson, R., and Fall, R., 1993. Isoprene and monoterpene emission rate variability: model evaluations and sensitivity analysis. *Journal of Geophysical Research* **98**, 12,609-12,617.
- Hanna, S., Chang, J., and Strimaitis, D. 1993. Hazardous gas model evaluation with field observations. *Atmospheric Environment* **27A**, 2265-2285.
- Houyoux, M., Vukovich, J., Brandmeyer, J., Seppanen, C., and Holland, A. 2004. SMOKE user manual version 2. Carolina Environmental Program, NC.

- Ian, J., Anderson, B., and Wilson, R. 2003. Base Case Development (Air Quality and Meteorology). Particulate Matter/Regional Haze/Ozone Modeling Workshop, Santa Fe, New Mexico, June 5, 2003.
- Jiang, G., Lamb, B., and Westberg, H. 2003. Using back trajectories and process analysis to investigate photochemical ozone production in the Puget Sound Region. *Atmospheric Environment* **37**, 1489-1502.
- Jiang, W., Hedley, M., and Singleton, D., 1998. Comparison of the MC2/CALGRID and SAIMM/UAM-V photochemical modeling systems in the Lower Fraser Valley, British Columbia. *Atmospheric Environment* **32(17)**, 2969-2980.
- Mass, C., Albright, M., Ovens, D., Steed, R., Gritmit, E., Eckel, T., Lamb, B., Vaughan, J., Westrick, K., Storck, P., Coleman, B., Hill, C., Maykut, N., Gilroy, M., Ferguson, S., Yetter, J., Sierchio, J., Bowman, C., Stender, D., Wilson, R., and Brown, W., 2003. Regional environmental prediction over the Pacific Northwest. *Bulletin of the American Meteorological Society* **84**, 1353-1366.
- McHenry, J., Ryan, W., Seaman, N., Coats, C., Pudykiewicz, J., Arunachalam, S., and Vukovich, J. 2004. A real-time Eulerian photochemical model forecast system. *Bulletin of the American Meteorological Society* **85**, 525-548
- McNally, D. and Tesche, T. 1993. MAPS sample products, Alpine Geophysics, 16225 W. 74th Dr., Golden, CO 80403.
- O'Neill, S. 2002. Modeling ozone and aerosol formation and transport in the Pacific Northwest and calculating fractional source contributions to downwind receptors. PhD dissertation, Department of Civil and Environmental Engineering, Washington State University.
- O'Neill, S., and Lamb, B., 2005. Intercomparison of the Community Multi-Scale Air Quality model and CALGRID using process analysis. *Environmental Science and Technology* **39**, 5742-5753.
- Pleim, J., and Mathur, R., 2005. Diagnostic evaluation, sensitivity analyses, and new development in the Eta/CMAQ air quality forecast system. Paper presented at the 7th Conference on Atmospheric Chemistry organized by the American Meteorological Society. January 10-13, 2005. San Diego, CA.
- Scire, J., Robe, F., Fernau, M., and Yamartino, R. 2000. A user's guide for the CALMET meteorological model version 5. Earth Tech, Concord, MA.
- Scire, J., Yamartino, R., Carmichael, G., and Chang, Y., 1989. CALGRID: A Mesoscale Photochemical Grid Model Volume II: User's Guide, California Air Resources Board, CA.
- Seigneur, C., Pun, B., Pai, P., Louis, J., Solomon, P., Emery, C., Moris, R., Zahniser, M., Worsnop, D., Koutrakis, P., White, W., and Tombach, I. 2000. Guidance for the performance evaluation of three-dimensional air quality modeling systems for particulate matter and visibility. *Journal of Air Waste Management Association* **50**, 588-599.
- U.S. Environmental Protection Agency. 1991. Guideline for regulatory applications of the Urban Airshed Model. EPA-450/4-91-013, U.S. Environmental Protection Agency, Research Triangle Park, NC 27711.
- U.S. Environmental Protection Agency. 1997. Development of speed correction cycles, US EPA assessment and modeling division, national vehicle fuel and emissions laboratory, 2565 Plymouth Road, Ann Arbor, MI, EPA Report no. M6.SPD.001.
- U.S. Environmental Protection Agency. 1998. APPENDIX B: Modeled Outdoor Concentrations of Hazardous Air Pollutants: Analysis of Data from the Cumulative Exposure Project for

the Urban Area Source Program May 1998 prepared by Daniel Axelrad, Tracey Woodruff, Jane Caldwell, Raquel Morello-Frosch, and Arlene Rosenbaum (http://www.epa.gov/ttn/atw/urban/appx_b1.pdf)

Vaughan, J., Lamb, B., Frei, C., Wilson, R., Bowman, C., Figueroa-Kaminsky, C., Otteson, S., Boyer, M., Mass, C., Albright, M., Koenig, J., Collingwood, A., Gilroy, M., and Maykut, N. 2004. A numerical daily air quality forecast for the Pacific Northwest. *Bulletin of the American Meteorological Society* **85**, 549-561.

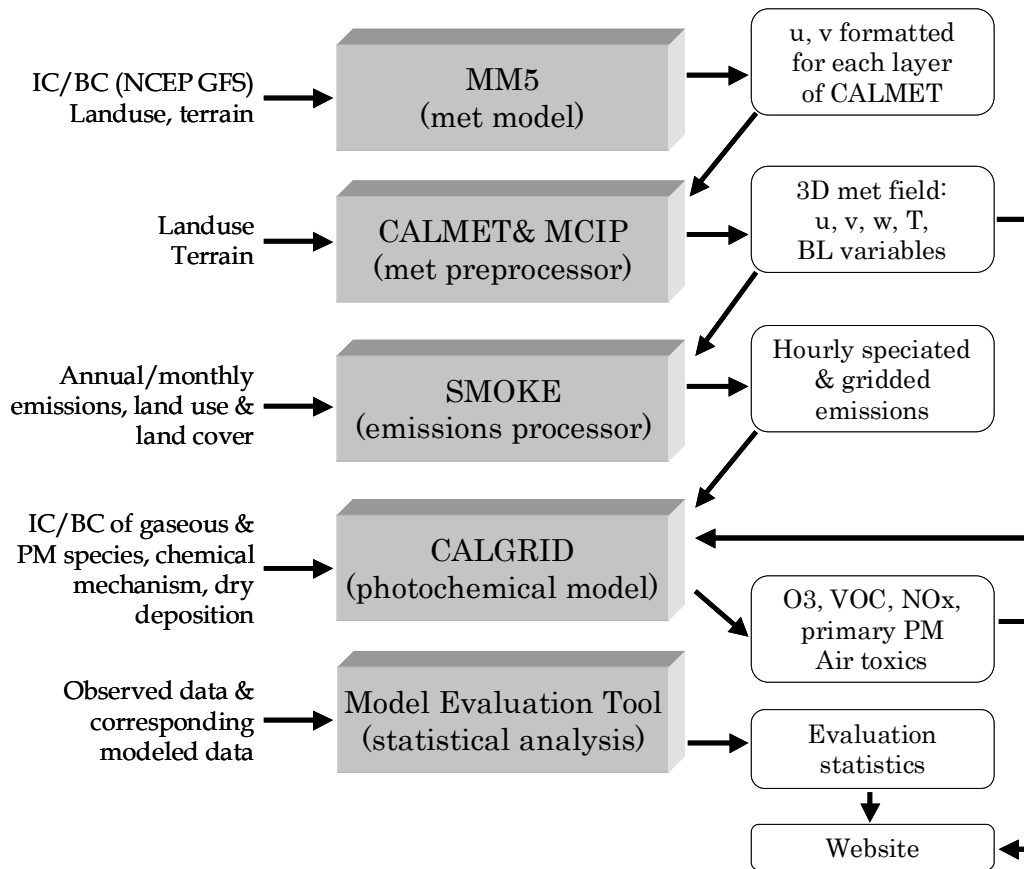


Figure 1: Schematic diagram of the AIRPACT2 system showing major meteorological, emission, and photochemical components.

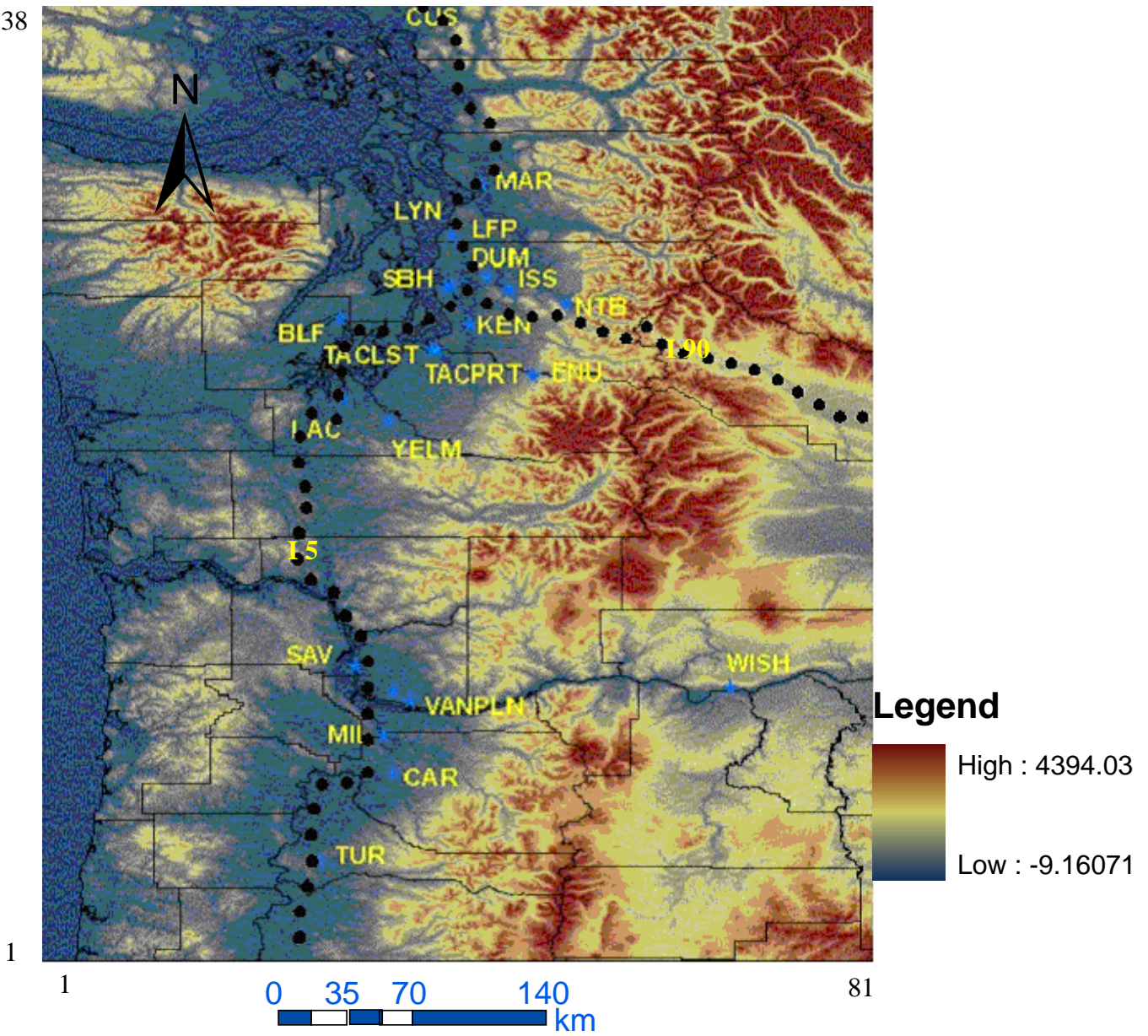


Figure 2: Domain of the AIRPACT2 system. The locations of the air quality monitoring stations in WA and OR used for evaluation in this study are shown. Surface elevations are in meters.

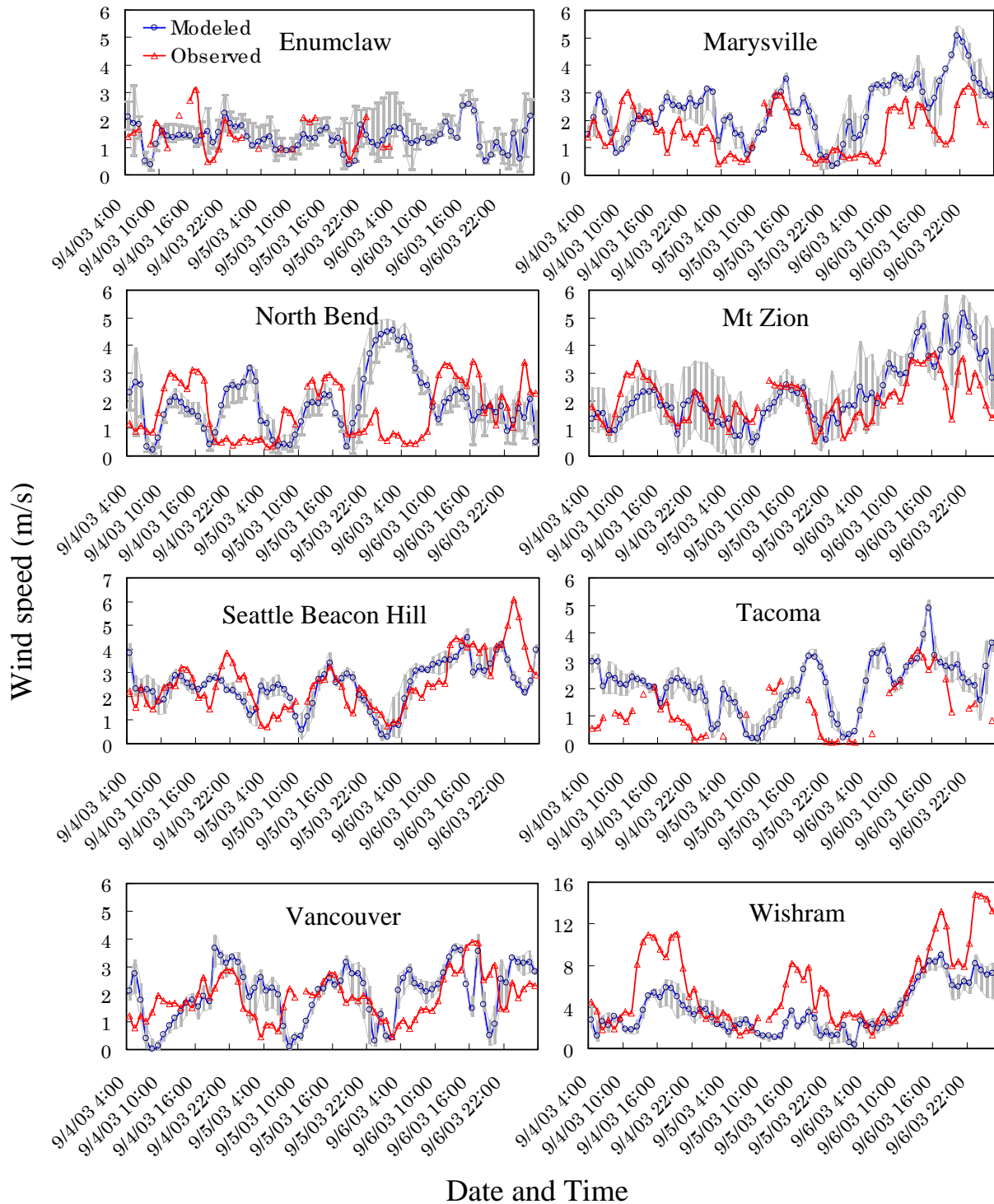


Figure 3: Plots showing time series of modeled and observed hourly wind speeds at eight sites in WA during an elevated O_3 period. Error bars associated with modeled wind speeds represent the maximum and the minimum wind speeds within the 3 x 3 grid-cell matrix.

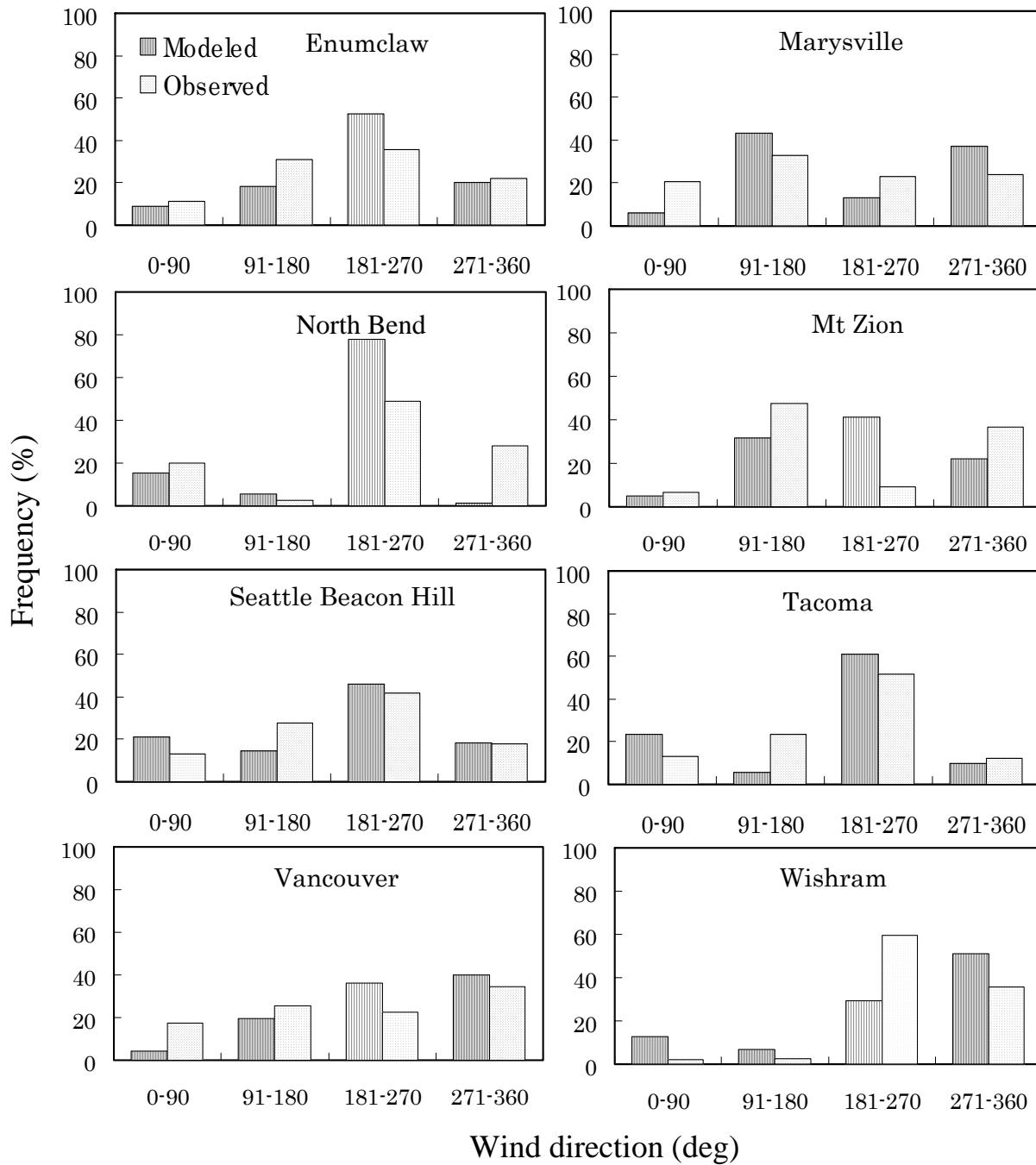


Figure 4: Frequency distributions of modeled and observed wind directions at six monitoring stations in WA. Note that the frequency distributions were calculated from hourly observed and corresponding modeled data points from September 4 through to September 18, 2003.

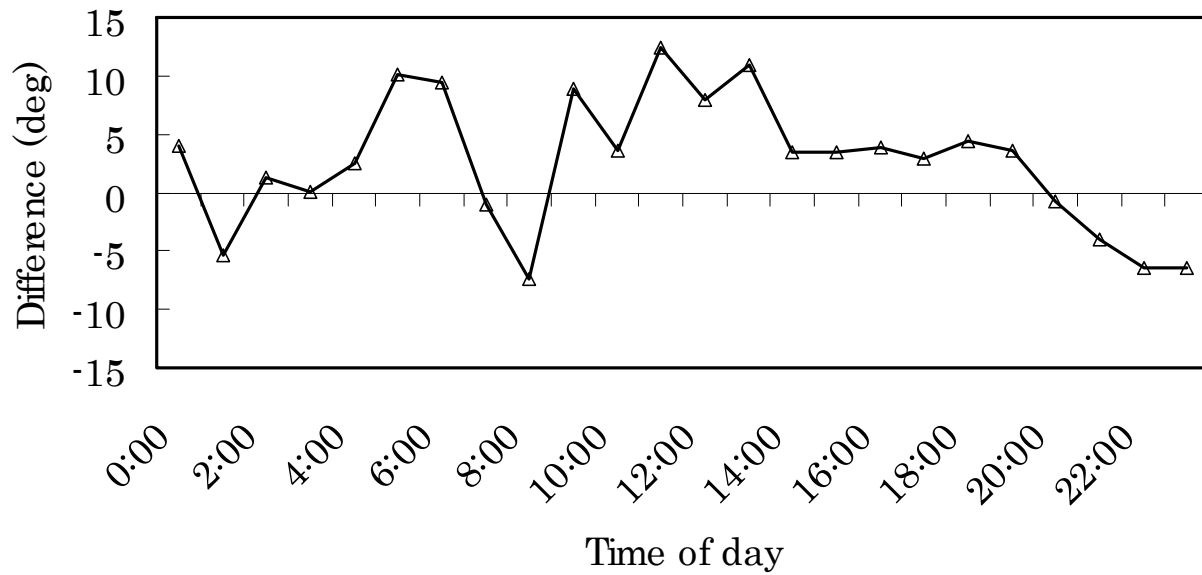


Figure 5: Diurnal time series of the difference between modeled and observed wind directions. Hourly average measured and modeled data from eight monitoring stations were used to calculate the difference plot.

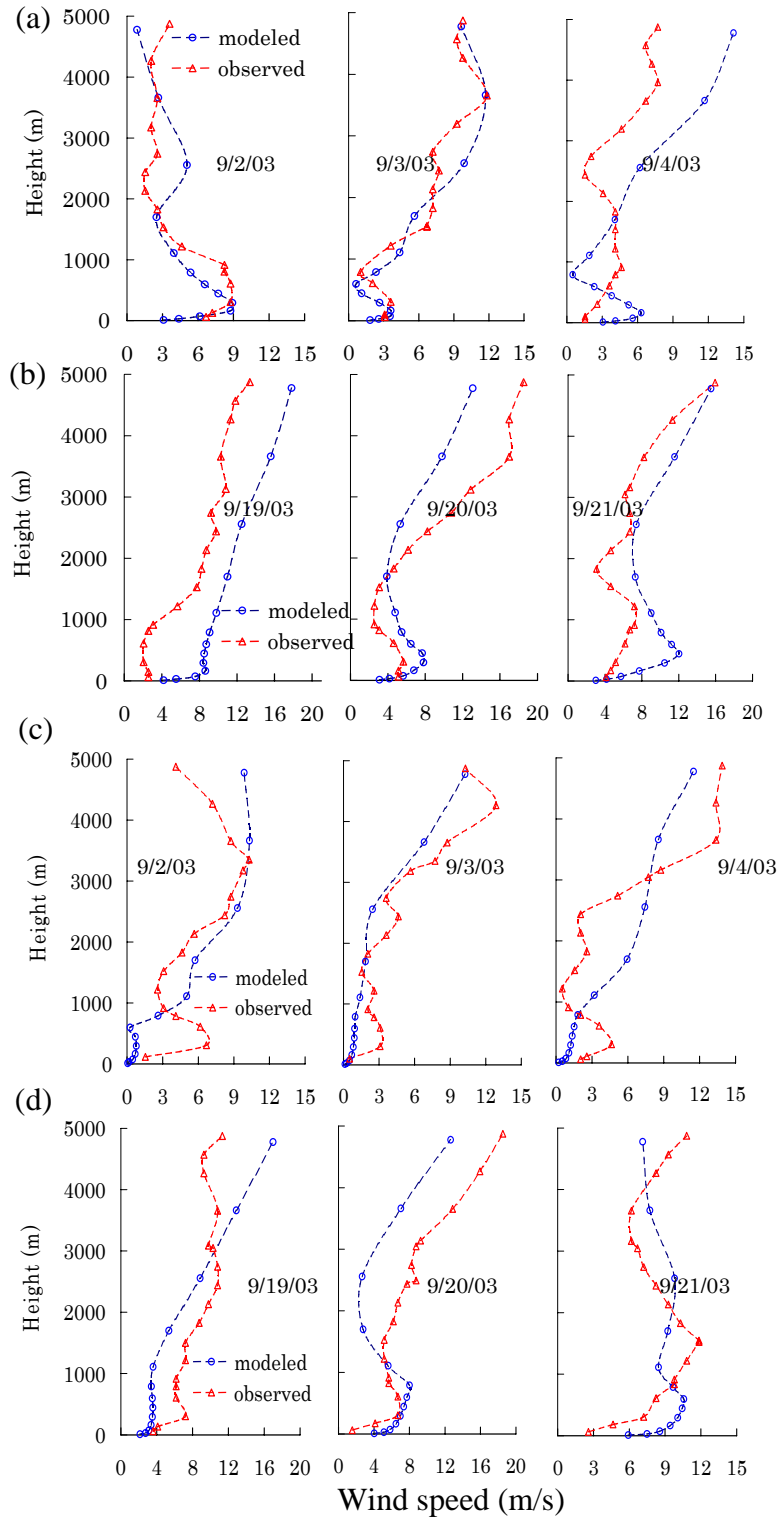


Figure 6: Vertical profiles of predicted and measured wind speeds at Salem, OR for (a) episode and (b) non-episode at 0000 PST, and (c) episode and (d) non-episode) at 2000 PST

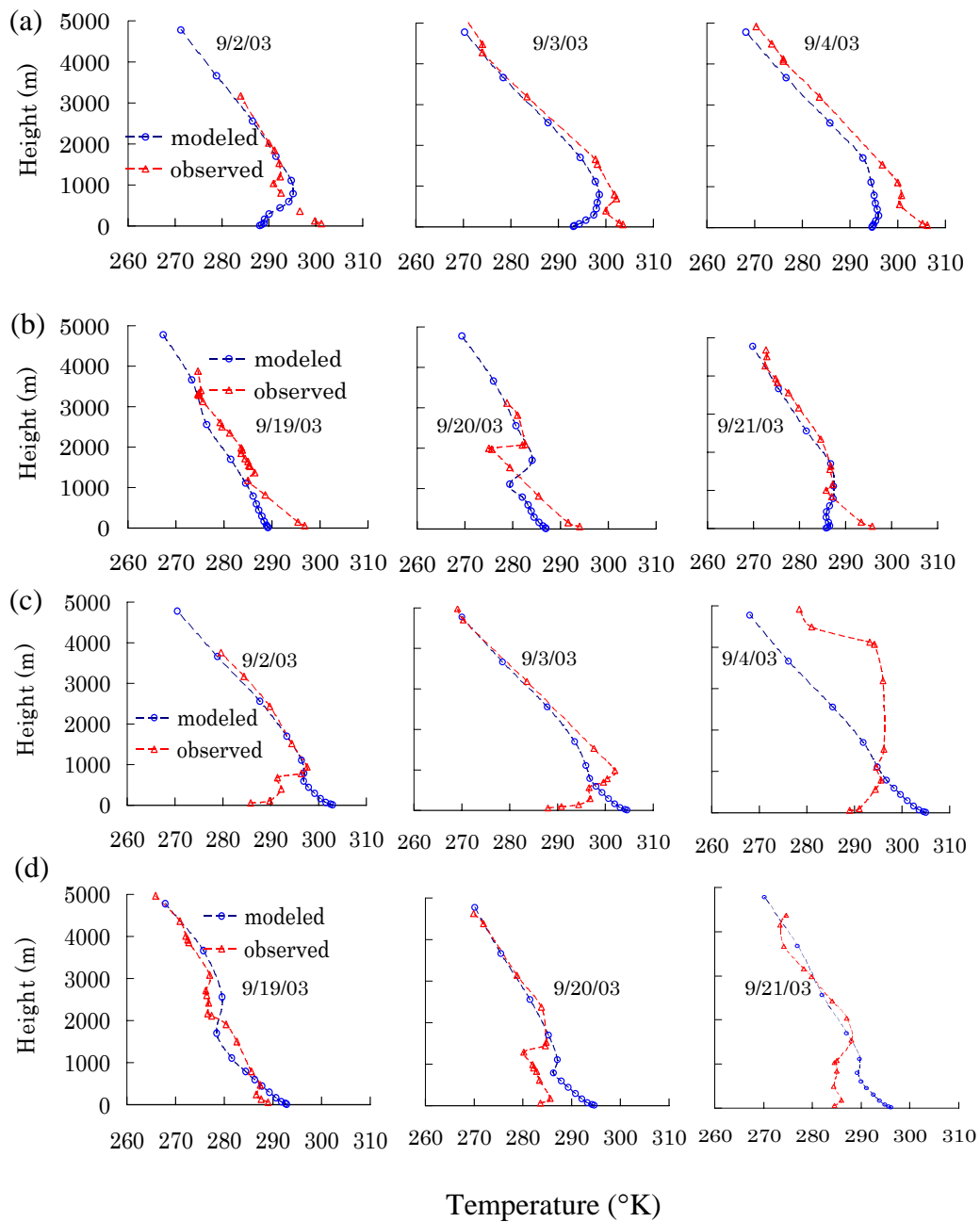


Figure 7: Profiles of modeled and observed temperature at Salem, OR at 0000 PST: (a) episode and (b) non-episode, and at 1200 PST: (c) episode and (d) non-episode.

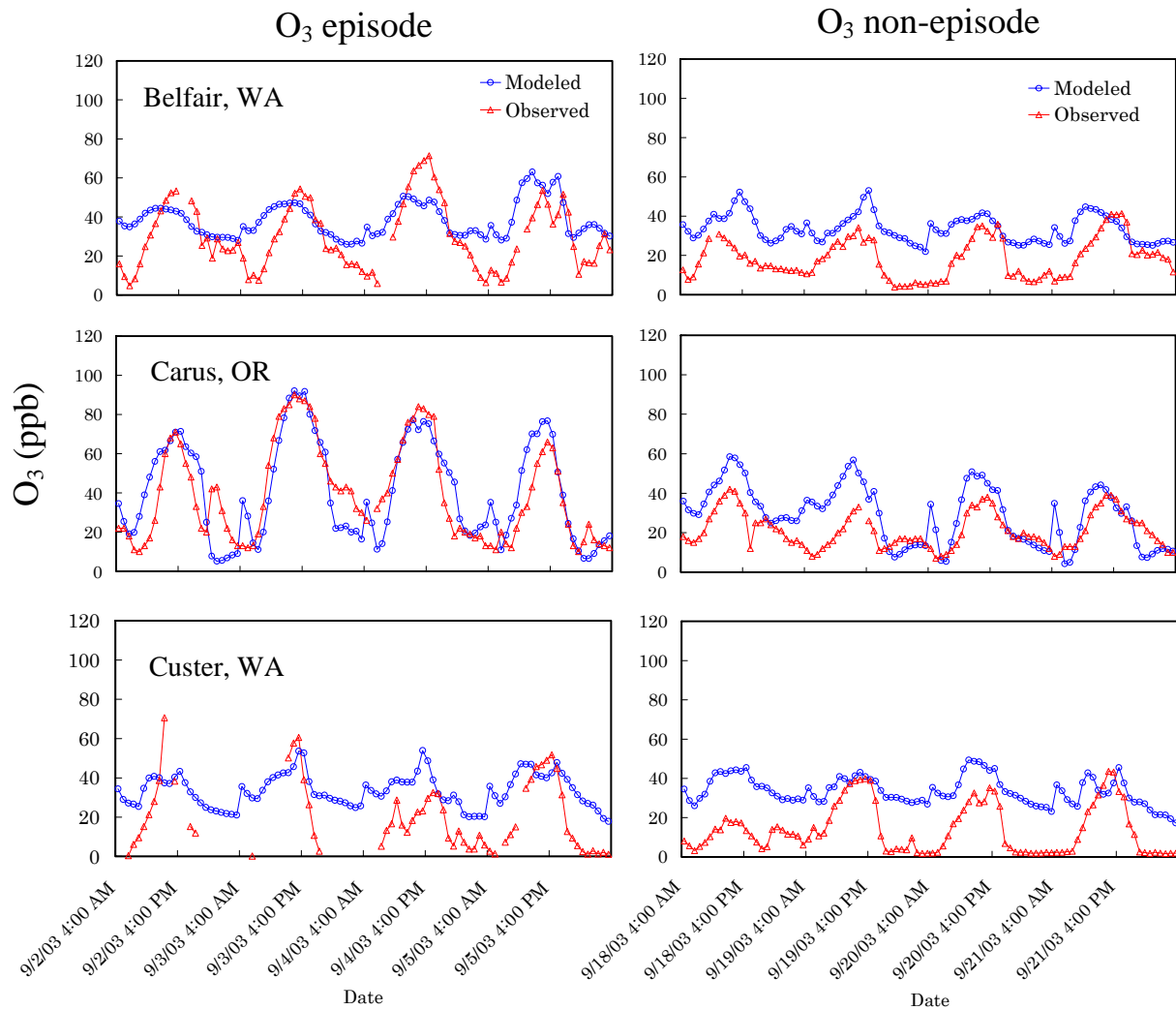


Figure 8 (cont.): Hourly time series of O₃ mixing ratios of the episode (September 2-5, 2003), and the non-episode (September 18-21, 2003) periods at monitoring sites in WA and OR.

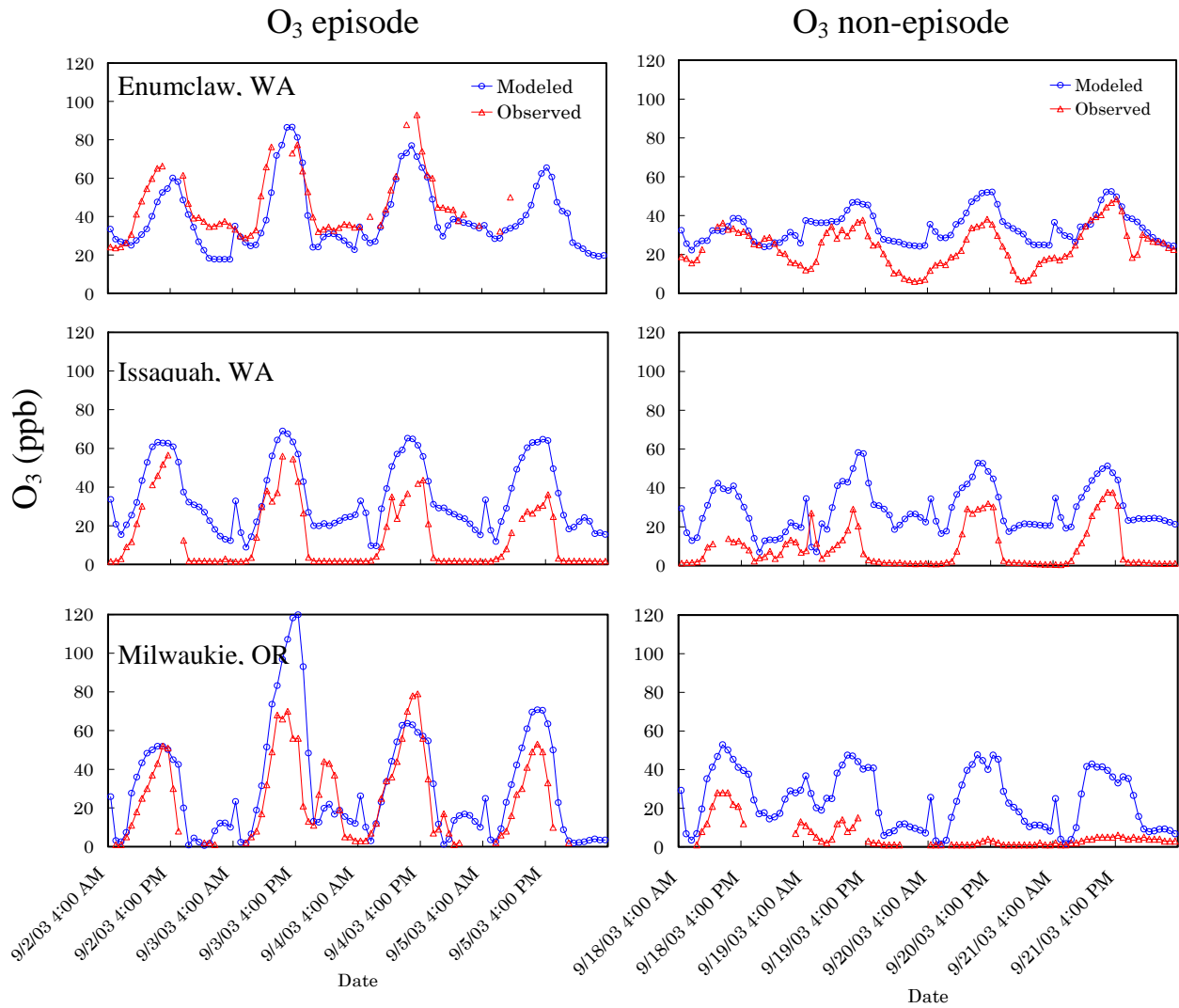


Figure 8 (cont.): Hourly time series of O₃ mixing ratios of the episode (September 2-5, 2003), and the non-episode (September 18-21, 2003) periods at monitoring sites in WA and OR.

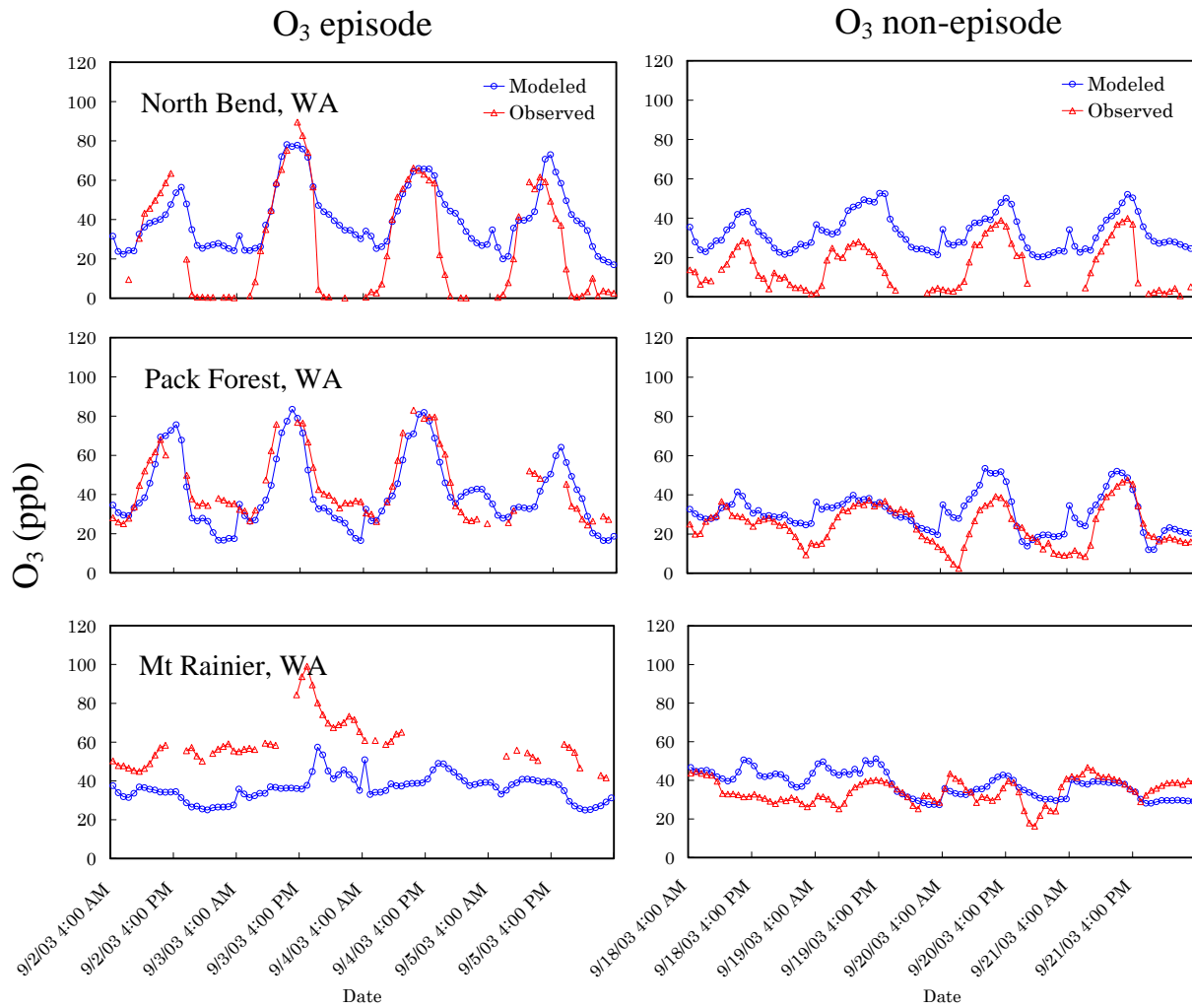


Figure 8 (cont.): Hourly time series of O₃ mixing ratios of the episode (September 2-5, 2003), and the non-episode (September 18-21, 2003) periods at monitoring sites in WA and OR.

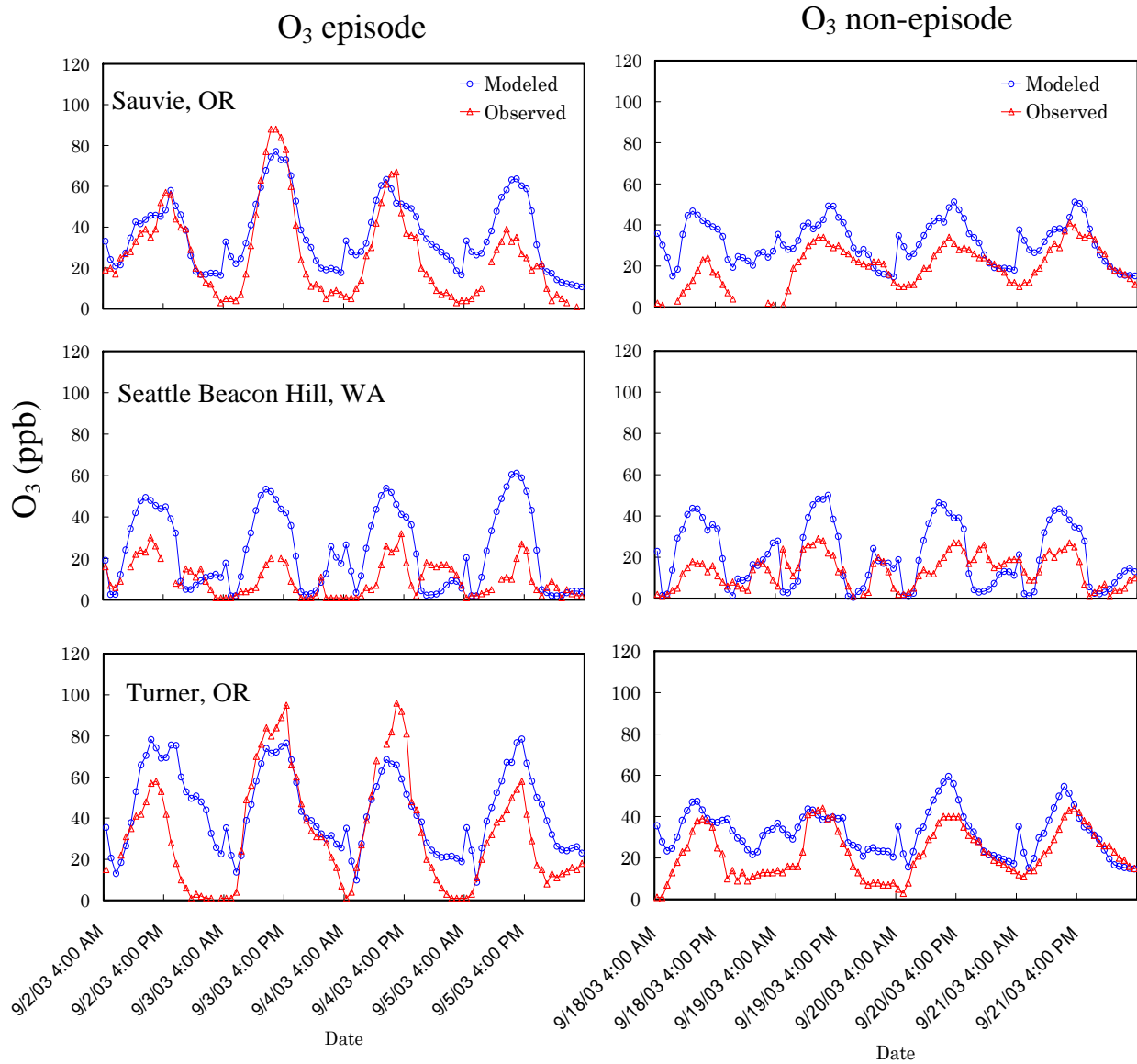


Figure 8 (cont.): Hourly time series of O₃ mixing ratios of the episode (September 2-5, 2003), and the non-episode (September 18-21, 2003) periods at monitoring sites in WA and OR.

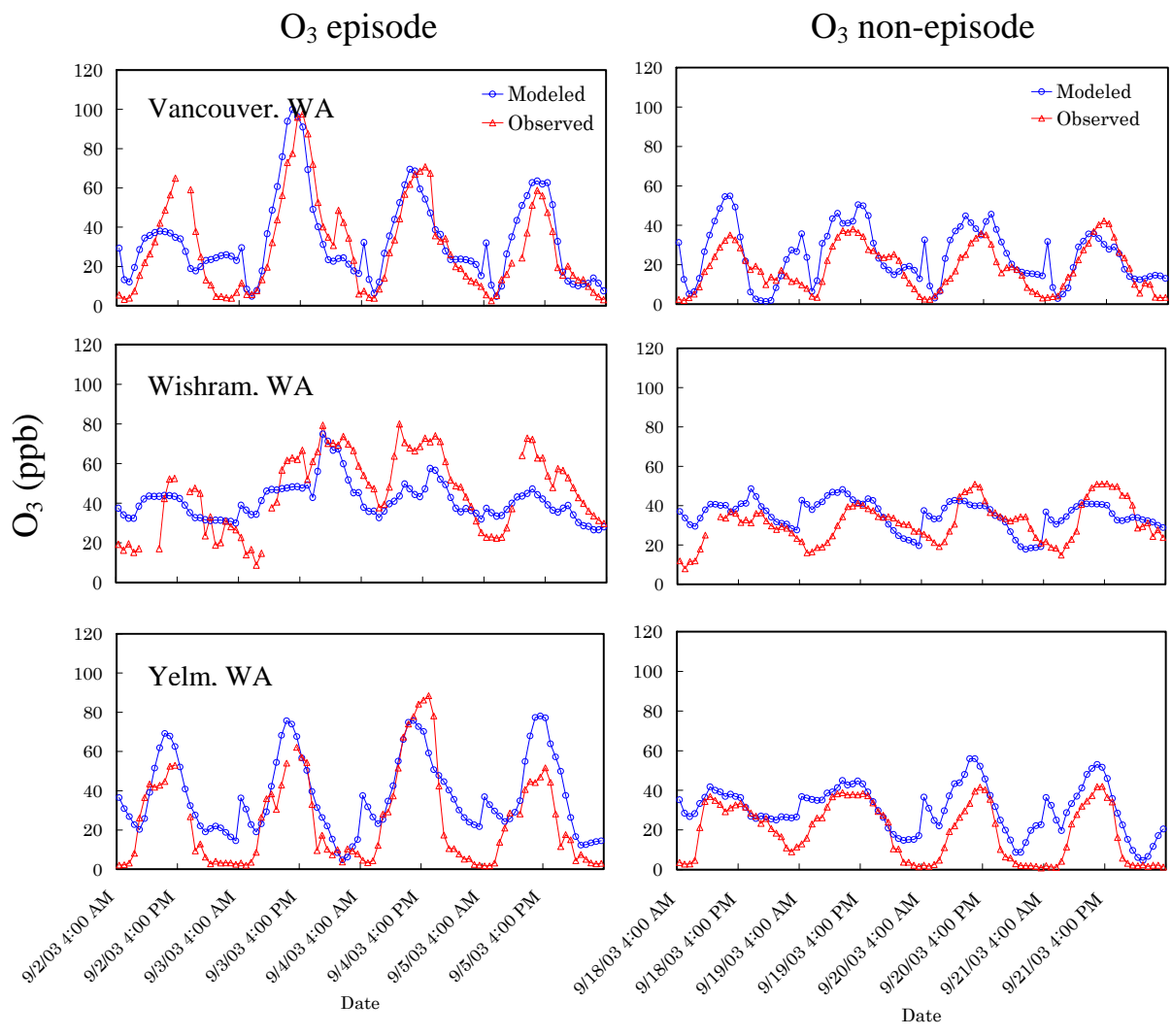


Figure 8: Hourly time series of O₃ mixing ratios of the episode (September 2-5, 2003), and the non-episode (September 18-21, 2003) periods at monitoring sites in WA and OR.

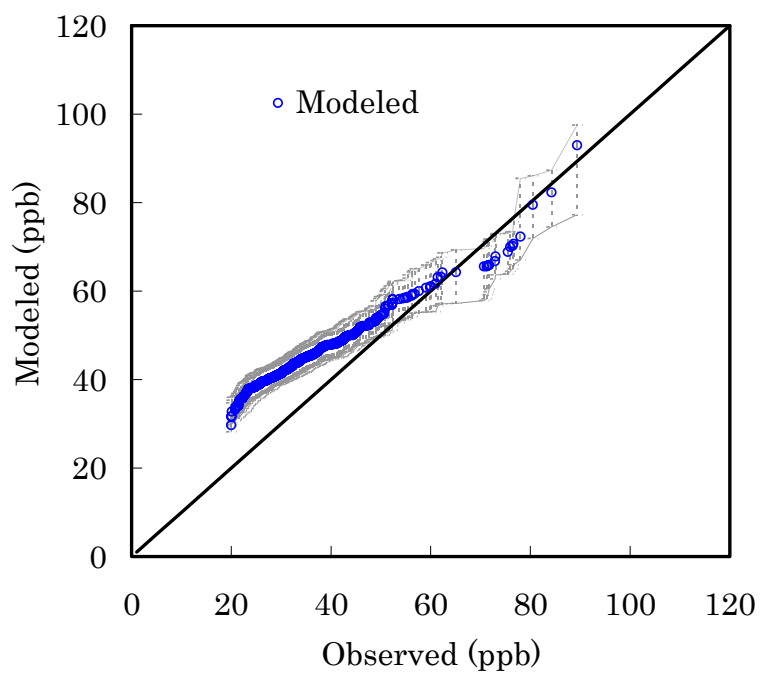


Figure 9: A Q-Q plot of O₃ modeled and observed 8-hr daily maximum data points (un-paired in time and space) for September 2003 within 15 sites with a cutoff at 20 ppb of observed O₃. The solid line represents 1:1 relationship between modeled and observed O₃. The broken lines around the modeled data points show the maximum and the minimum within the 3 x 3 grid-cell matrix

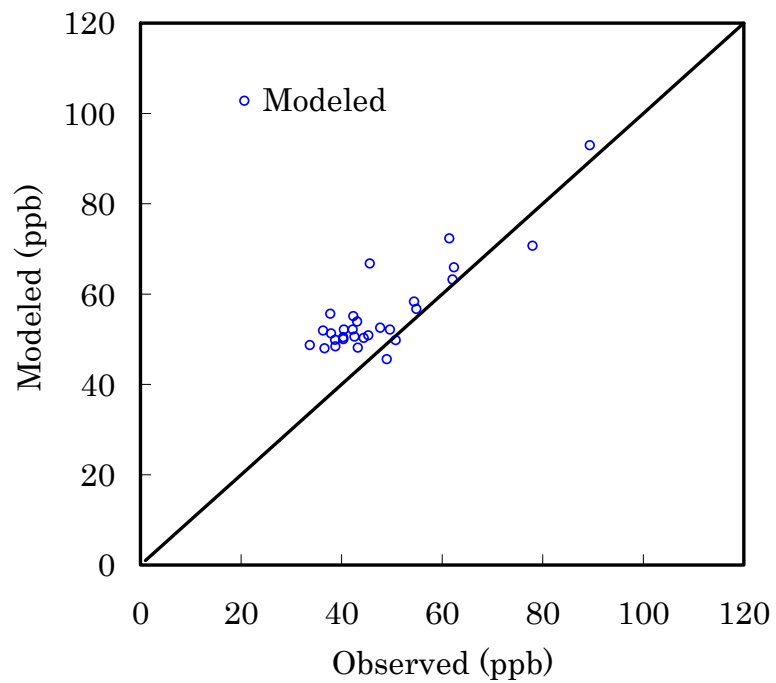


Figure 10: 8-hr daily max observed and corresponding modeled 8-hr max O₃ within 15 sites (paired in time).

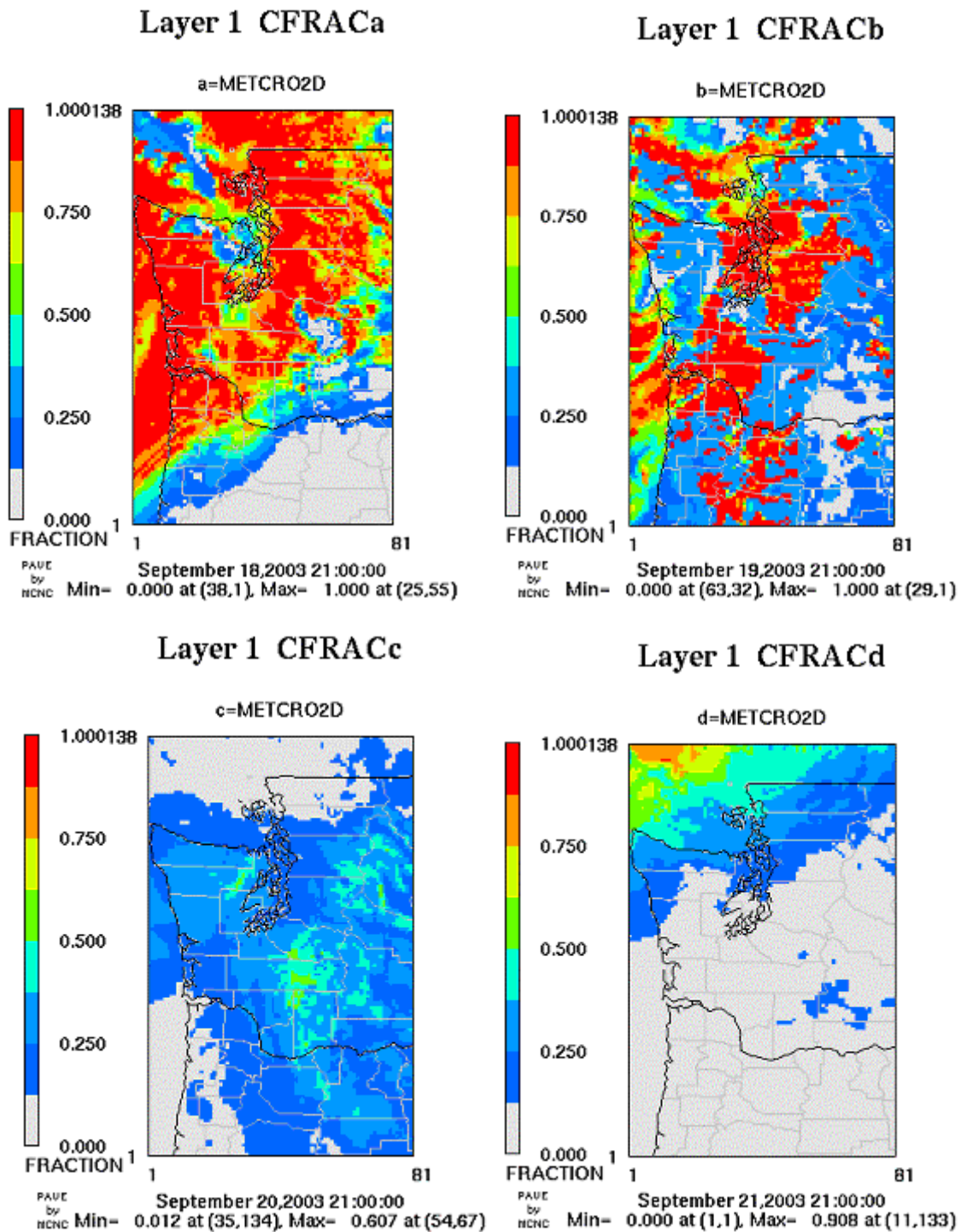


Figure 11: Modeled cloud cover during a non-episode period (September 18-21, 2003) at 1200 PST; outputs were taken from MM5-MCIP cloud fraction calculations.

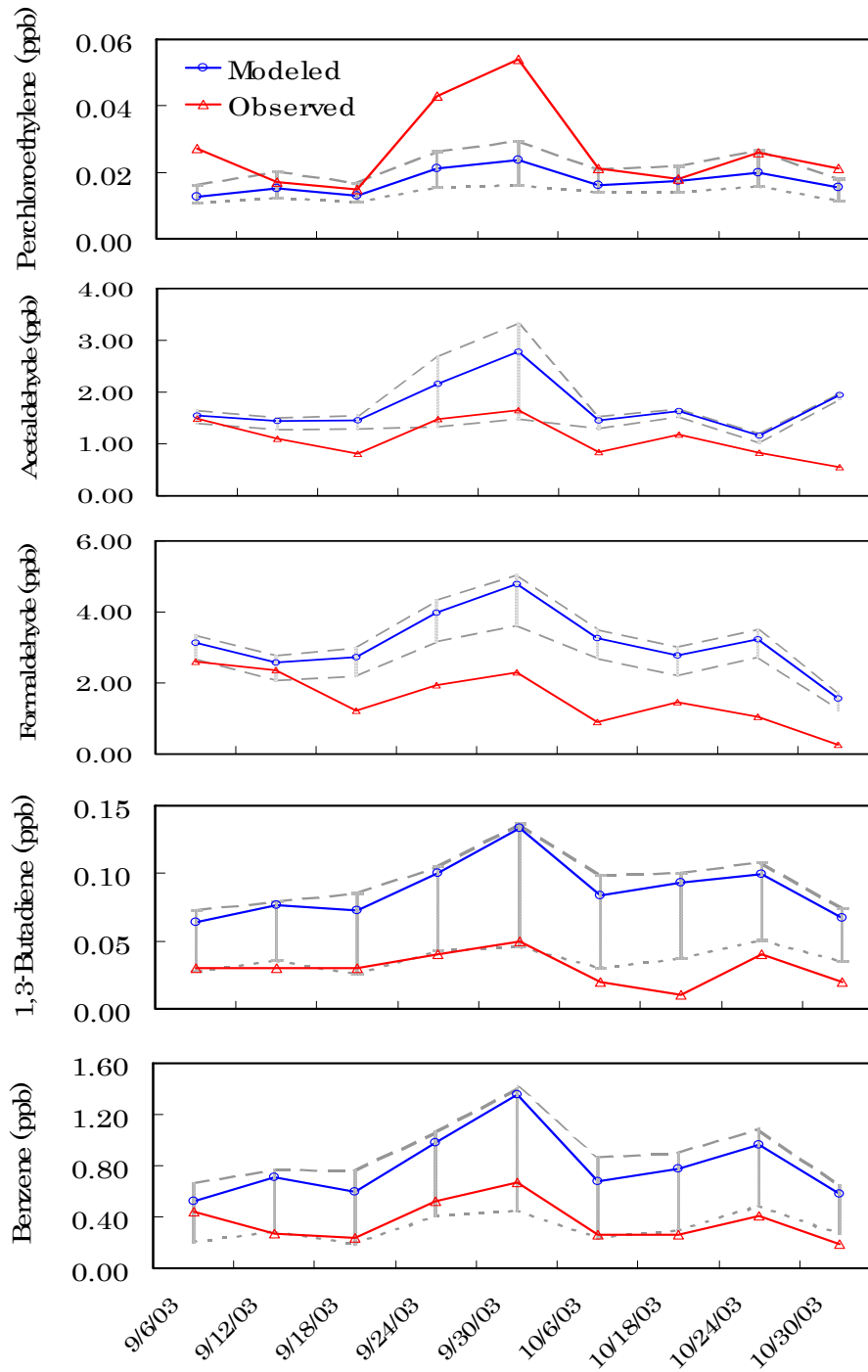


Figure 12: 24-hr average modeled and observed air toxics mixing ratios for selected days in September and October 2003 at Seattle Beacon Hill site. Error bars associated with the modeled air toxics represent the maximum and minimum levels within the 3 x 3 grid-cell matrix.

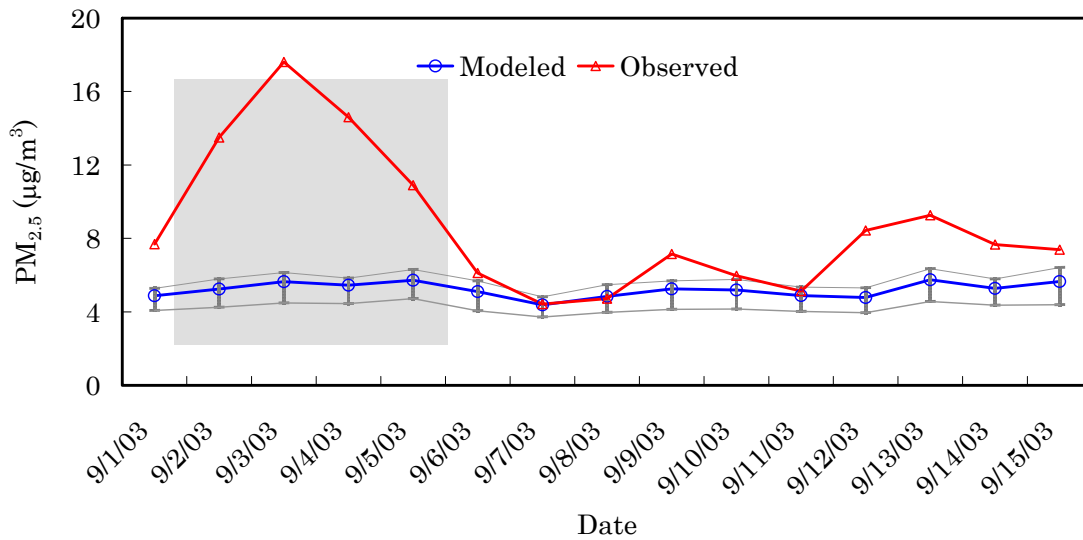


Figure 13: Time series of 24-hr average PM_{2.5} modeled and observed concentrations. The error bars associated with the modeled concentration represent the maximum and minimum modeled concentrations of PM_{2.5} within the 3x3 grid-cell matrix. The shaded time period corresponds to an observed high O₃ period.

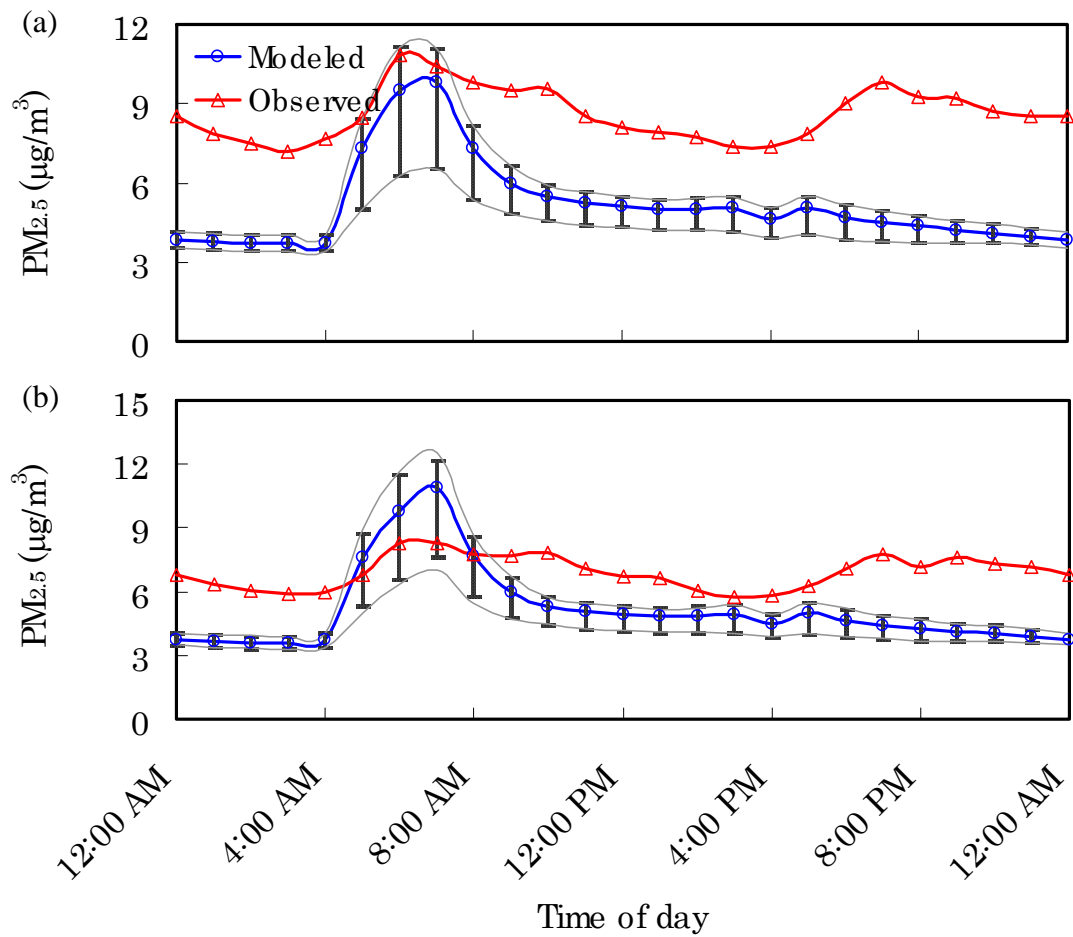


Figure 14: (a) Modeled and observed average hourly concentrations of $PM_{2.5}$ using data from 12 sites for September 1-15, 2003, and (b) for September 8-15, 2003. Error bars are showing the maximum and minimum modeled concentrations within the 3x3 grid-cell matrix.

Table 1: Performance statistics for CALMET wind speed predictions using data obtained from September 4-30, 2003. Max and min represent statistics based on the maximum and minimum wind speeds within the 3 x 3 grid-cell matrix.

SITE	Observed daily mean WS (m/s)	MB (m/s)			FB (%)			ME (m/s)			FE (%)		
		Max	Monitor	Min	Max	Monitor	Min	Max	Monitor	Min	Max	Monitor	Min
Enumclaw 212	1.66	1.12	0.23	-0.20	50	13	-16	1.14	0.39	0.32	51	22	22
Marysville	1.53	1.00	0.59	0.24	50	31	12	1.00	0.61	0.39	50	32	22
Mt Zion	2.12	1.90	1.19	0.36	57	36	4	1.90	1.24	0.71	57	39	28
North Bend	1.6	1.47	0.69	-0.09	57	32	-9	1.47	0.75	0.37	57	35	25
Seattle Beacon Hill	2.78	0.19	-0.20	-0.52	8	-6	-20	0.42	0.37	0.58	16	14	23
Tacoma South	1.31	1.73	1.36	1.06	79	66	53	1.73	1.38	1.10	79	68	58
Vancouver High Way 99	1.31	1.21	0.69	0.13	47	28	1	1.21	0.77	0.46	47	34	27
Wishram High Way 14	5.48	-1.73	-2.21	-2.84	-34	-49	-70	1.92	2.28	2.84	40	51	70
<i>Average</i>	2.22	0.86	0.14	-0.23	39	19	-6	1.35	1.06	0.85	50	37	34

Table 2: Performance statistics for predictions of temperature of CALMET based on the data obtained from September 4 to September 30, 2003.

Site	Observed daily mean temperature (°F)	MB (°F)			FB (%)			ME (°F)			FE (%)		
		Max	Monitor	Min	Max	Monitor	Min	Max	Monitor	Min	Max	Monitor	Min
Enumclaw	58	5	4	2	8	6	2	5	4	3	8	6	5
Mt Zion	63	1	-1	-3	2	-1	-5	2	2	3	3	3	5
North Bend	59	2	-1	-4	3	-2	-6	4	4	5	5	7	9
Seattle Beacon Hill	60	2	2	1	4	3	1	3	2	2	4	3	3
Vancouver	63	2	1	0	3	1	0	4	2	2	3	3	3
Wishram	67	-3	-5	-6	-5	-8	-9	4	5	6	5	8	9
<i>Average</i>	62	1	0	-2	2	1	-3	3	3	3	5	5	6

Table 3: O₃ prediction performance statistics for September 2003 based on 8-hr daily maximum mixing ratios. Results in max and min columns represent performance statistics based on the maximum and minimum O₃ mixing ratios predicted within the 3 x 3 grid-cell around the monitor.

	Observed 8-hr daily max (ppb)	MB (ppb)			FB (%)			ME (ppb)			FE (%)		
		Max	Monitor	Min	Max	Monitor	Min	Max	Monitor	Min	Max	Monitor	Min
Urban Sites													
Issaquah, WA	45	23	19	14	58	51	41	23	19	14	58	51	41
Milwaukie, OR	57	18	15	11	45	39	30	19	16	13	46	41	36
Seattle Beacon Hill, WA	35	20	16	15	58	49	46	20	16	15	58	49	46
Vancouver, WA	77	11	7	4	29	21	14	13	11	10	33	30	28
<i>Average</i>	<i>60</i>	<i>18</i>	<i>14</i>	<i>11</i>	<i>48</i>	<i>40</i>	<i>33</i>	<i>19</i>	<i>16</i>	<i>13</i>	<i>49</i>	<i>43</i>	<i>38</i>
Semi-urban/ Rural Sites													
Belfair, WA	61	11	9	6	29	23	18	12	10	8	29	25	21
Carus, OR	84	15	12	9	38	33	25	16	14	12	40	36	31
Custer, WA	56	11	8	6	30	24	17	12	10	8	31	27	23
Enumclaw, WA	73	9	4	0	23	14	5	12	10	10	29	25	24
Mt. Rainier, WA	89	6	0	-7	14	2	-15	11	9	9	24	19	19
North Bend, WA	72	15	12	9	41	34	27	15	13	11	41	36	32
Pack Forest, WA	76	11	8	5	29	23	16	12	10	9	29	25	22
Sauvie Island, OR	73	14	11	8	37	31	25	14	12	10	37	32	27
Turner, OR	81	15	11	9	35	28	23	17	15	13	39	34	32
Wishram, WA	71	2	0	-2	6	2	-4	7	7	7	15	15	15
Yelm, WA	76	15	13	10	36	32	26	15	14	11	37	33	27
<i>Average</i>	<i>74</i>	<i>11</i>	<i>8</i>	<i>5</i>	<i>29</i>	<i>22</i>	<i>15</i>	<i>13</i>	<i>11</i>	<i>10</i>	<i>32</i>	<i>28</i>	<i>25</i>

Table 4: Performance statistics for O₃ predictions during an episode (September 2-5, 2003) and a non-episode (September 18-21, 2003) periods.

Site	8-hr daily max observed (ppb)		MB (ppb)		FB (%)		ME (ppb)		FE (%)	
	Episode	Non-episode	Episode	Non-episode	Episode	Non-episode	Episode	Non-episode	Episode	Non-episode
Belfair, WA	61	36	-1	11	-2	32	8	11	15	32
Carus, OR	84	35	4	14	8	35	8	14	12	35
Custer, WA	56	36	2	8	10	22	7	8	18	22
Enumclaw, WA	73	42	-12	8	-22	19	12	8	22	19
Mt. Rainier, WA	89	43	-26	3	-47	7	26	5	47	12
North Bend, WA	72	32	-1	16	-3	46	5	16	9	46
Pack Forest, WA	76	42	-6	6	-9	15	6	6	9	15
Sauvie Island, OR	73	35	7	12	16	31	9	12	20	31
Turner, OR	81	39	4	8	10	19	19	8	30	19
Wishram, WA	71	49	-14	0	-24	2	14	6	24	15
Yelm, WA	76	38	9	7	18	19	14	7	25	19
<i>Average</i>			-3	8	-4	23	11	9	21	24

Table 5: Ratio analysis of air toxics relative to benzene measured at Seattle Beacon Hill site.

Ratio with respect to benzene	Emissions	Mixing ratios	
		Modeled	Observed
Acetaldehyde	0.28	2.34	3.20
Formaldehyde	1.03	4.03	4.43
1,3-Butadiene	0.12	0.11	0.09
Perchloroethylene	0.01	0.02	0.07

Table 6: Performance statistics for AIRPACT2 for PM_{2.5} predictions (September 1-15, 2003).

Site	Daily mean observed (µg/m ³)	MB (µg/m ³)			FB (%)			ME (µg/m ³)			FE (%)		
		Max	Monitor	Min	Max	Monitor	Min	Max	Monitor	Min	Max	Monitor	Min
Bellevue	8	-1	-1	-3	-7	-11	-37	3	3	3	34	35	39
Kent	10	-3	-4	-5	-26	-32	-49	4	4	5	34	39	51
Lacey	7	-2	-3	-3	-38	-44	-56	2	3	3	38	44	56
Lake Forest Park	7	-2	-2	-3	-18	-31	-40	2	2	3	34	33	40
Lynwood	8	-3	-4	-4	-29	-42	-57	3	4	4	35	44	57
Marysville	9	-4	-5	-5	-58	-62	-78	4	5	5	58	62	78
North Bend	7	-3	-4	-4	-36	-40	-49	4	4	4	48	50	55
Seattle Beacon Hill	9	-3	-4	-5	-13	-18	-52	4	4	5	35	35	52
Seattle Duwamish Valley	12	-5	-5	-7	-43	-54	-82	5	5	7	43	54	82
Tacoma Port	12	-5	-6	-7	-43	-55	-68	5	6	7	44	55	68
Tacoma South St.	9	-3	-4	-4	-31	-41	-56	3	4	4	38	43	56
Vancouver	8	-2	-3	-4	-15	-29	-52	3	3	4	34	36	53
<i>Average</i>	9	-3	-4	-5	-30	-38	-56	4	4	5	39	44	57

CHAPTER 3

EVALUATION OF THE AIRPACT2 AIR QUALITY FORECAST SYSTEM AND THE COMMUNITY MULTI-SCALE AIR QUALITY (CMAQ) MODEL FOR THE PACIFIC NORTHWEST

Abdullah Mahmud, Joe Vaughan, Jack Chen, Jeremy Avise, Brian Lamb and Hal Westberg

Laboratory for Atmospheric Research

Department of Civil & Environmental Engineering

Washington State University, WA 99164-2910

Abstract

The second-generation CALGRID photochemical model in the AIRPACT2 air quality forecast system was replaced with the state-of-the-science third-generation Models-3 CMAQ photochemical model. The performance of the AIRPACT2 system using CMAQ was evaluated, and the results from this study were compared with the simulations using CALGRID for the current AIRPACT2 modeling domain. A comparative performance analysis between the CALGRID and CMAQ models was carried out using observations from the months of September and October 2003.

CMAQ predicted the 8-hr daily maximum O₃ more accurately than CALGRID. Both models predicted high O₃ reasonably well; however, CMAQ performed better than CALGRID in predicting low O₃, and O₃ at urban sites. For urban sites, CALGRID predicted O₃ with average mean bias (MB) of 14 ppb, mean error (ME) of 16 ppb, fractional bias (FB) of 40% and fractional error (FE) of 43% as compared to MB of 0 ppb, ME of 8 ppb, FB of -4% and FE of 28% for CMAQ. For semi-urban/rural sites these measures were lower for CMAQ than CALGRID. Neither of the models captured completely the nighttime O₃ titration phenomenon. Both CALGRID and CMAQ captured air toxics trends quite well. 24-hr mixing ratios of benzene, 1,3-butadiene, and perchloroethylene predicted by these models were in agreement with each other; however, the models differed in predicting formaldehyde and acetaldehyde. CMAQ predicted both formaldehyde and acetaldehyde close to observations as compared to CALGRID. For the PM_{2.5} prediction, 24-hr average PM_{2.5} concentrations were better predicted by CMAQ than CALGRID, although both models missed high levels of PM_{2.5} during a period of high ozone from September 2 to September 4, 2003. The better performance, however, was expected from CMAQ as it handles secondary formation of PM_{2.5} aerosols in the atmosphere. It was found that

the un-specified mass from anthropogenic sources (A25) was the biggest (31.9%) contributor followed by the sulfate (ASO4) (29.8%) and the water (AH2O) (24.7%) aerosols to the total PM_{2.5}. Both CALGRID and CMAQ captured the morning rush hour PM_{2.5} concentrations quite well.

3.1 Introduction

The third-generation Community Multiscale Air Quality (CMAQ) model was developed under the Models-3 project by the United States Environmental Protection Agency (USEPA) in 1998 (Ching and Byun, 1999). CMAQ is a multi-component, multi-scale Eulerian air quality model that contains sophisticated modules for simulating all atmospheric and land processes that affect the transport, transformation, and deposition of atmospheric pollutants and/or their precursors on both urban and regional scales. The modeling system can address tropospheric ozone, acid deposition, visibility, fine particulate and other pollutant issues in the context of a ‘one atmosphere’ perspective where complex interactions between atmospheric pollutants and urban and regional scales are confronted (Ching and Byun, 1999). Scientists and regulatory agencies have been using CMAQ as the-state-of-the-art modeling tool to study gas-phase chemistry and particulate chemistry and dynamics at urban to regional scales (e.g., O’Neill and Lamb, 2005; US EPA AIRNow, 2005; Jun and Stein, 2004; Arnold *et al.*, 2003; O’Neill 2002; Chen, 2002; Bullock and Brehme, 2002). Near real-time air quality forecast using the CMAQ photochemical model is also becoming a significant use of the model (e.g., US EPA AIRNow, 2005). The Air Indicator Report for Public Access and Community Tracking version 2 (AIRPACT2) (Vaughan *et al.*, 2004), a numerical air quality forecast system developed for the Pacific Northwest, is also being upgraded to take the advantages of the latest air quality science incorporated in the CMAQ model by replacing the second-generation CALGRID (Yamartino, 1992) model. As part of this upgrade to AIRPACT2, the objectives of this study were to evaluate the performance of the AIRPACT2 system using CMAQ, and to compare the results from this study with simulations using CALGRID. The results from this study would outline the

strengths and weaknesses of the AIRPACT2 system, and hence, provide a basis for improving the forecast system.

Discussions on model performance evaluation techniques, the AIRPACT2 system design, and the results of the current AIRPACT2 evaluation have been presented in the previous chapters of this thesis. A number of air quality studies using CMAQ have been carried out for the Pacific Northwest (e.g., O'Neill and Lamb, 2005; O'Neill, 2002; Chen, 2002). The performance of CMAQ as a photochemical model has also been studied for other locations (e.g., Hogrefe *et al.*, 2004; Arnold *et al.*, 2003; Mebust *et al.*, 2003). O'Neill and Lamb (2005) also carried out a comparative performance study between the CALGRID and the CMAQ models using statistical measures and process analysis technique. However, these evaluations were carried out for short periods of historic pollution episodes. In contrast, this study presents the CMAQ model evaluation, and compares the results with those from the CALGRID model for a month long simulation from an operational forecast system.

3.2 System design, modeling domain, and observation network

A schematic diagram of the modified version of the AIRPACT2 system is shown in Figure 1. In the modified system, the PSU/NCAR fifth generation mesoscale meteorological model, MM5 version 3 (Dudhia *et al.*, 2002) remains the main meteorological model with MCIP version 2.2 (Byun *et al.*, 1999) as the interface processor for the CMAQ model. SMOKE version 2.0 (Houyoux *et al.*, 2004) is also used as the emission processor in the modified system. However, the SAPRC99 (Carter, 2000) instead of the SAPRC97 (Carter *et al.*, 1997) chemical mechanism is utilized in the emission processing. Emission rates are expressed in mole/s/cell as per the requirements of the CMAQ model. Descriptions of the meteorological model, the interface processor, and the emission processor can be found in Chapter 1 of this thesis.

Figure 2 shows the major components and their relationships in the CMAQ modeling system. The CMAQ modeling system includes interface processors to incorporate the outputs of the meteorology and emissions processors and to prepare the requisite input information for initial and boundary conditions and photolysis rates to the CMAQ Chemical Transport Model (CCTM). One of the main advantages of the Model-3 CMAQ model is that the emissions processing and the meteorological modeling systems can be replaced with alternative processors (Ching and Byun, 1999). In the modified AIRPACT2 system, CMAQ used SMOKE as the emission processor instead of the Models-3 Emission Projection and Processing System (MEPPS). SMOKE produces hourly gridded and speciated emissions that can be directly used in the CMAQ system.

The Meteorology-Chemistry interface Processor (MCIP) translates and processes model outputs from the Mesoscale Meteorological model, MM5 for the CCTM. In the modified AIRPACT2 system, MCIP interpolates the MM5 vertical profile data to match the corresponding layers in the CCTM. MCIP uses landuse information from the Landuse Processor (LUPROC) to calculate the planetary boundary layer (PBL) and the surface parameters. The following PBL parameters are extracted by MCIP: friction velocity, convective velocity scale, PBL height, air temperature, Monin-Obukhov length, roughness length, and terrain elevation.

The Initial Condition (ICON) and Boundary Condition (BCON) processors provide concentration fields for individual chemical species for the beginning of a simulation and for the grid-cells surrounding the modeling domain, respectively. The ICON and BCON processors use data provided from previous three-dimensional model simulations or from clean-troposphere vertical profiles. In this work, the ICON file provided initial profile concentrations of RADM2 chemical species listed in Table 1 for the first day of simulation for the entire domain. Later, the

ICON file was generated using the previous day last hour of three-dimensional simulation results for each simulation day. The initial profile concentrations at the boundary grid-cells from the ICON file were used in the BCON file, which was used at the beginning of each simulation for the entire period. The IC and BC concentrations of the model species were adapted from Jiang (2001) and the literature.

The photolysis processor (JPROC) calculates temporally varying photolysis rates. JPROC requires vertical O₃ profiles, temperature profiles, a profile of the aerosol number density, and the earth's surface albedo to produce the photolysis rates for the CCTM. The photolysis rates were generated for each day of simulation.

The CCTM simulates the relevant atmospheric chemistry, transport and deposition processes involved throughout the modeling domain. The CCTM solves atmospheric advection and diffusion equations using the Asymmetric Convective Model (ACM) by Pleim and Chang (1992) method. CMAQ includes both the Regional Acid Deposition Model 2 (RADM2) (Stockwell *et al.*, 1990) and Carbon Bonding IV (CBIV) (Gery *et al.*, 1989) chemical mechanisms with an option to incorporate the SAPRC99 chemical mechanism. In this study, the SAPRC99 is utilized. Both the quasi-steady-state-approximation (QSSA) and the Sparse Matrix Vectorized Gear (SMVGEAR) (Jacobson and Turco, 1994) algorithm options are available in the CCTM. In the modified AIRPACT2 system, CMAQ uses the QSSA method option. The CCTM uses an aerosol module by Binkowski and Roselle (2003) that uses a modal approach. The CCTM also uses an explicit cloud process scheme that plays an important role in calculating pollutant concentrations that depend on temperature and solar radiation levels. CMAQ models deep convective clouds and shallow clouds using the algorithms as implemented in the RADM model.

The modified AIRPACT2 used the same domain of the current AIRPACT2 system. In order to carry out the model evaluation, data from the same network of observation stations discussed in Chapter 2 were used.

3.3 Results and discussions

CMAQ simulations were carried out using the same MM5 meteorology, and the NET96 emission inventory as were used for CALGRID simulations. Therefore, it is expected that the differences between the current and the modified AIRPACT2 in predicting mixing ratios of gas-phase species and concentrations of particulates will be primarily due to different processes in the CALGRID and CMAQ models. Thus results presented in this section ultimately reflect the performances of the two photochemical models.

3.3.1 Simulations of O₃

The performance of CMAQ was evaluated for 8-hr daily maximum O₃ mixing ratios using statistical measures and by interpreting hourly episode and non-episode time series. Statistical measures were applied to data points with a cutoff value of 20 ppb of observed O₃ following the work of Jiang *et al.* (1998). The performance was studied at each of the 15 sites over the entire month of September 2003. Additionally, average statistics for urban and semi-urban/rural sites were also generated.

Table 2 contains the performance statistics of the CMAQ model in predicting O₃. The model showed variable performance at different monitoring sites. The highest 8-hr daily maximum of 89 ppb of O₃ was measured at Paradise located at an elevation of 1700 m above mean sea level on the side of Mt Rainier, which is approximately 120 km downwind of the Seattle metropolitan area. Sites located within the Vancouver/Portland area in the southern part of the domain, which includes Sauvie Island, Vancouver, Wishram, Milwaukie, Carus, and

Turner, usually showed higher levels of O₃ compared to other monitoring sites near Seattle in the middle and northern parts of the domain. CMAQ also predicted high O₃ at and around these sites. Although the model over-estimated O₃ at most semi-urban/rural sites, the performance at urban sites was mixed: O₃ was over-estimated at the Issaquah and Milwaukie sites and under-estimated at the Seattle Beacon Hill and Vancouver sites. Average MB of 0 ppb and 2 ppb for the entire month of September 2003 were found at urban and semi-urban/rural sites, respectively. This indicates that the model simulated observations quite well both at urban and semi-urban/rural sites. FB, ME and FE for urban and semi-urban/rural sites were also comparable. The highest FB of 16% was found at Issaquah, an urban site, and at two sites in the semi-urban/rural areas: Mt Rainier in WA and Sauvie Island in OR.

Statistics between CALGRID and CMAQ have also been included in Table 3. The performance of CMAQ was better than that of CALGRID as indicated by the lower biases and errors associated with CMAQ simulations. CMAQ simulated O₃ better for urban sites than CALGRID, which mostly over-estimated O₃ at urban sites. To further investigate system performance, a four-day O₃ episode from September 2 through to September 5, 2003, and a non-episode period from September 18 through to September 21, 2003 were selected for analysis. In general, both the CALGRID and the CMAQ models performed relatively better during the O₃ episode than during the non-episode period. Figure 3 depicts time series of the episode and the non-episode cases of hourly modeled and measured O₃ at each site. These plots show that both the models captured the diurnal patterns quite well, and predicted the 1-hr daily peak O₃ reasonably accurately at most sites during the episode period. However, it is interesting to see that neither the CALGRID nor the CMAQ predicted the 1-hr daily peak O₃ correctly at Paradise on Mt Rainier site during the episode. This was, perhaps, caused due to the influences of the

local topography that was not resolved in either of the models. The 1-hr peak O₃ predicted with CMAQ rarely exceeded the observations even at urban sites. On the other hand, CALGRID estimated O₃ was greater than observations at most urban sites including Seattle Beacon Hill, Issaquah and Milwaukie for most days during the episode. For the non-episode period, CALGRID over-estimated O₃ at most sites. Unlike CALGRID, CMAQ estimated the peak 1-hr O₃ quite close to observations during the non-episode period. The CMAQ model utilizes a comprehensive cloud processes scheme in the CCTM, whereas the CALGRID model has no cloud scheme. This partly explains why the CALGRID model performed poorly during the non-episode period as opposed to the CMAQ model. It was reported in Chapter 2 that most parts of the domain were overcast at noon on the 18th and 19th September 2003 creating unfavorable conditions for O₃ production. However, the CALGRID model did not see this cloud process and eventually over-estimated O₃ mixing ratios at almost all sites.

The time series plots of 1-hr O₃ also reveal that although CMAQ showed better performances at low O₃, neither of the models could capture the nighttime O₃ titration phenomenon as it was seen at the Issaquah and North Bend sites. Jiang *et al.* (2003) also reported similar findings using CALGRID photochemical model for the Pacific Northwest. Pleim *et al.* (2005) described similar behavior and suggested a modification of the vertical diffusivity as a function of landuse to correct this problem. The observed nighttime O₃ levels during September were not significant from a regulatory standpoint; however, the large differences between CALGRID modeled and observed mixing ratios contributed to bias and errors and degraded the overall model performance

A Q-Q plot of ranked (unpaired in time and space) modeled and observed 8-hr daily max O₃ in Figure 4 shows that both the models performed quite well in predicting high O₃. On the

other hand, CMAQ predicted low O₃ relatively better than CALGRID. The plot of the 8-hr daily max observed versus modeled O₃ within the 15 sites in Figure 5 shows that CMAQ is likely to predict observations more accurately than CALGRID. The high R² of 0.91 for CMAQ predictions indicate better linear correlation with observations than the R² of 0.75 for CALGRID. A scatter plot of modeled versus observed 8-hr daily max O₃ in Figure 6 shows good model performance. The CMAQ model showed better ability to predict 8-hr max O₃ mixing ratios at the right time and place compared to the CALGRID model.

3.3.2 Simulations of air toxics

There has been growing interest in air toxics in recent years because of the potential adverse health effects. In the current AIRPACT2 system, benzene, 1,3-butadiene, and perchloroethylene are added as primary pollutants to the SAPRC97 chemical mechanism in CALGRID, and are treated as reactive tracers with first order loss only and no treatment of subsequent products. Formaldehyde and acetaldehyde, which are also air toxics, treated as explicit compounds in the chemical mechanism so that the secondary formation of air toxics is included in the current AIRPACT2. Air toxics are also treated similarly in the CMAQ model using the SAPRC99 chemical mechanism. However, the loss processes of primary air toxics in the SAPRC99 mechanism included more reactions than for the SAPRC97 mechanism in CALGRID. Table 4 includes the loss mechanisms of primary air toxics incorporated in CMAQ and CALGRID models.

Modeled gas-phase air toxics mixing ratios were extracted for those days when observations were available. Ambient toxics mixing ratios were obtained over a 24-hr period on every sixth day from an urban site in Seattle Beacon Hill, WA. To increase the size of the comparison data set for air toxics, modeled data were also extracted for October 2003. Both the

CMAQ and the CALGRID models captured the trends of the air toxic compounds quite accurately as shown in Figure 7. The predicted mixing ratios differed between these models. CMAQ predicted formaldehyde and acetaldehyde close to observations as compared to CALGRID. However, predicted mixing ratios of benzene, 1,3-butadiene, and perchloroethylene by the models are quite comparable. It is noteworthy, however, that the observed mixing ratios generally fall within the max-min range of modeled mixing ratios for the 3 x 3 matrix of grid cells around the Beacon Hill site. This level of agreement suggests that CMAQ, including the emission inventory, generally captures the correct behavior of air toxics and also suggests that wind direction variability and the terrain feature of the site are not completely resolved in the model. This systematic discrepancy was further investigated by a ratio analysis. As benzene is relatively non-reactive and both models predicted the same level of benzene mixing ratios, emission, modeled and ambient ratios of formaldehyde, acetaldehyde, perchloroethylene, and 1,3-butadiene were calculated with respect to benzene. Table 5 contains ratios of the air toxics compounds to benzene. The modeled and the ambient ratios were calculated using the mixing ratio of an air toxic compound to the mixing ratio of benzene.

For 1-3 butadiene, the emission ratio is essentially identical to the modeled ratio for both models and also nearly equal to the ambient ratio. This indicates consistency between the emission inventory and both the modeled and observed ambient mixing ratios. For perchloroethylene, there is some consistency between the emission inventory ratio and the modeled ratios, but both are significantly less than the ambient ratios. This suggests that the loss of perchloroethylene due to chemistry is not significant in the models. The emission inventory may also be under-estimated or local sub-grid scale sources may be influencing the observations. For acetaldehyde and formaldehyde, the difference between emission ratios and modeled ratios

suggest that both models reflect significant secondary formation. As both models predicted the same level of benzene mixing ratio as compared to formaldehyde and acetaldehyde, which were significantly lower in CMAQ than in CALGRID, the modeled ambient ratios for CALGRID was significantly higher than for CMAQ. Hence, it is hard to compare the modeled ratios of formaldehyde and acetaldehyde with their ambient ratios for CMAQ, and draw any conclusion from that. Nevertheless, the time-series of modeled and observed 24-hr average mixing ratios of formaldehyde and acetaldehyde showed better agreement for CMAQ than CALGRID.

In general, the performance of both CALGRID and CMAQ were quite comparable in predicting air toxics. Both models captured the trends and chemistry of the air toxic compound. However, predictions for formaldehyde and acetaldehyde are much better in CMAQ than these are in CALGRID.

3.3.3 PM_{2.5} prediction

In the CMAQ photochemical model, fine particulate matter (PM_{2.5}) is treated through an aerosol module that utilizes a modal approach. The aerosol module of the CMAQ is designed to be an efficient and economical depiction of aerosol dynamics in the atmosphere (Binkowski, 1999). The smaller Aitken (*i* th) mode represents fresh particles either from nucleation or from direct emission, while the larger accumulation mode (*j* th) mode represents aged particles. Primary emissions may also be distributed between these two modes. The two modes interact with each other through coagulation. Each mode can grow through condensation of gaseous precursors; and they are also subject to dry and wet deposition. The smaller mode may grow into the larger mode and partially merge with it.

The chemical species treated in the aerosol mode are fine sulfate, nitrate, ammonium, water, anthropogenic and biogenic carbon, elemental carbon and other un-specified material of

anthropogenic origin. Table 6 lists the aerosol species treated in the CMAQ aerosol module. The sum of these species account for the total mass of PM_{2.5}. A detailed description of the CMAQ aerosol component can be found in Binkowski and Roselle (2003). As CALGRID does not account for particle growth or the secondary formation of particulates in the atmosphere, modeled concentrations of PM_{2.5} in the current AIRPACT2 system accounted for the primary emissions mostly from diesel particulate matter (DSPM) in the month of September 2003.

Hourly measured concentrations from 12 monitoring sites in WA and corresponding modeled concentrations were considered to calculate a 24-hr average performance statistics. Table 7 contains the performance statistics of CMAQ for predictions of PM_{2.5} concentrations. The model showed variable performance, although it underestimated PM_{2.5} concentrations at all sites. It showed an average MB of -1 µg/m³ and FB of -12% during the study period. The model performed relatively well at the Bellevue site as indicated by a low negative MB and FB, where average measured PM_{2.5} concentration was 8 µg/m³. The highest 24-hr average concentrations of 12 µg/m³ of PM_{2.5} were measured at sites in Seattle Duwamish Valley and Tacoma areas, and the model performed poorly for these sites. The performance results, however, were better for CMAQ than for CALGRID as indicated by the errors and biases depicted in Table 8.

Figure 8 shows the 24-hr average time-series plot of modeled and observed PM_{2.5} concentrations from 12 sites in the domain for September 1-14, 2003. It is interesting to notice that although CMAQ predicted higher concentrations of PM_{2.5} than CALGRID, neither of the models could capture the high levels of PM_{2.5} concentrations observed during September 2-4, 2003. The figure also shows that CMAQ captured PM_{2.5} concentrations for later days quite well as observed 24-hr average fell within the maximum and minimum range of concentrations within the 3 x 3 grid-cell matrix. In order to understand how the models behaved during the day, the

diurnal patterns of modeled and observed $PM_{2.5}$ were also constructed. Using data from all sites from September 1 through to September 14, 2003 average hourly concentrations of $PM_{2.5}$ were calculated. Figure 9 shows that both CMAQ and CALGRID predicted the early rush hour $PM_{2.5}$ peak concentrations between 5 AM and 8 AM quite close to the measured levels. As CALGRID treats primary $PM_{2.5}$ only, it failed to capture the late afternoon peak $PM_{2.5}$ as opposed to CMAQ, which captured the peak, but under-estimated the concentration. It could be argued that the emission inventory used in AIRPACT2 is correct, and both the models performed reasonably well in predicting primary emissions, which are freshly emitted from traffic sources, during morning hours. Figure 10 shows that the most dominant aerosol species in the $PM_{2.5}$ mass is the un-specified materials from anthropogenic sources (31.9%) followed by sulfate (29.8%) and water (24.7%). The secondary biogenic and anthropogenic organic masses contribute the least to the $PM_{2.5}$ concentration.

To summarize, CMAQ showed better capabilities in predicting $PM_{2.5}$ concentrations as opposed to CALGRID. Although CMAQ under-estimated 24-hr average $PM_{2.5}$ concentrations at most sites, it showed good performance in depicting the diurnal pattern. The choice of CMAQ over CALGRID in the AIRPACT2 system would certainly be a good option in improving the forecast accuracies for $PM_{2.5}$ predictions.

3.4 Conclusion

Results from this study indicated that the forecasting ability of the AIRPACT2 was better with the CMAQ model than with the CALGRID model. Although both models predicted high O_3 quite well, the overall prediction accuracies are much better for CMAQ compare to CALGRID. As for the air toxic compounds, both models captured the temporal trends of most toxics. However, CMAQ predicted observed formaldehyde and acetaldehyde better than did

CALGRID. Mixing ratios of benzene and 1,3-butadiene were generally over-predicted by the models; yet, the observed mixing ratios were within the maximum-minimum range of the 3 x 3 grid-cell matrix. Both CMAQ and CALGRID under-estimated 24-hr average PM_{2.5} concentrations; but simulated the primary PM_{2.5} in the morning rush hours quite well. CMAQ also captured the pattern of PM_{2.5} for afternoon periods as it handles the secondary formations of aerosols. The forecast ability and accuracy of the AIRPACT2 system are likely to improve by when the CALGRID model will be replaced with the CMAQ model for operational purpose.

3.5 Acknowledgments

The authors would like to thank the NW-AIRQUEST for funding this study. Support was also provided from Boeing Corporation endowment funds to Washington State University. The authors thank Sally Otterson and colleagues from the Washington Department of Ecology and staffs from the Oregon Department of Environmental Quality for collaboration to compile the AIRPACT2 emission inventory and Cliff Mass and colleagues at the University of Washington for assistance in accessing the MM5 forecast system.

References

- Arnold, J., Dennis, R., and Tonnesen, G., 2003. Diagnostic evaluation of numerical air quality models with specialized ambient observations: testing the Community Multiscale Air Quality modeling system (CMAQ) at selected SOS 95 ground sites. *Atmospheric Environment* **37**, 1185–1198.
- Atlas, E., and Ridley, B. 1996. The Mauna Loa Observatory Photochemistry Experiment: Introduction, *Journal of Geophysical Research* **101 (D9)**, 14531-14541.
- Binkowski, F and Roselle, S., 2003. Models-3 Community Multiscale Air Quality (CMAQ) model aerosol component: 1. Model description. *Journal of Geophysical Research* **108 (D6)**, 4183.
- Binkowski, F., 1999. Aerosols in Models-3 CMAQ. CMAQ Science Documentation, Chapter 10. United States Environmental Protection Agency (USEPA). EPA/600/R-99/030..
- Bullock Jr., O., and Brehme, K., 2002. Atmospheric mercury simulation using the CMAQ model formulation description and analysis of wet deposition results. *Atmospheric Environment* **36**, 2135-2146.
- Byun, D., Pleim, J., Tang, R., and Bourgeois, A. 1999. Meteorology Chemistry Interface Processor (MCIP) for MODEL-3 Community Multiscale Air Quality (CMAQ) Modeling System. United States Environment Protection Agency, EPA/600/R-99/030.
- Carter, W, Luo, D., and Malkina, I., 1997. Environmental chamber studies for development of an updated photochemical mechanism for VOC reactivity assessment. Final report prepared for California Air Resources Board under Contract 92-345 by Center for Environmental Research and Technology, University of California, Riverside, pp-213.
- Carter, W., 2000. Documentation of the SAPRC99 chemical mechanisms for VOC reactivity assessment. Report submitted to the California Air Resources Board under Contract 92-329, and contract 92-3209 by the Center for Environmental Research and Technology, University of California, Riverside, CA.
- Chen, J., 2002. Aerosol and ozone sensitivity analysis with the Community Multi-scale Air Quality (CMAQ) model for the Pacific Northwest. M.S. Thesis. Department of Civil & Environmental Engineering, Washington State University, Pullman, WA.
- Ching, J., and Byun, D., 1999. Introduction to the Models-3 framework and the Community Multiscale Air Quality (CMAQ) model. CMAQ science documents. EPA/600/R-99/030.
- Dudhia, J., Gill, D., Guo, Y., Manning, K., Bourgeois, A., Wang, W., and Bruyere, C. 2002. PSU/NCAR Mesoscale Modeling System Tutorial Class Notes and User's Guide: *MM5 Modeling System Version 3*. Mesoscale and Microscale Meteorology Division, National Center for Atmospheric Research, Boulder, CO.
- Finlayson-Pitts, B., and Pitts, J. 2000. Chemistry of the upper and lower atmosphere. Academic Press, USA.
- Gery, M., Whitten, G., Killus, J., and Dodge M., 1989. A photochemical kinetics mechanism for urban and regional scale computer modeling. *Journal of Geophysical Research* **104(D3)**, 3555-3576.
- Heubert, B., Howell, S., Zhuang, L., Heath, J., Litchy, L., Wylie, D., Kreidler-Moss, J., Coppicus, S. and Pfeiffer, J., 1998. Filter and impactor measurements of anions and cations during the First Aerosol Characterization Experiment (ACE I). *Journal of Geophysical Research* **103 (D13)**, 16,493-16,509.

- Hogrefe, C., Rao, S., Kasibhatla, P., Kallos, G., Tremback, C., Haoe, W., Olerud, D., Xiu, A., McHenry, J., and Alapaty, K., 2001. Evaluating the performance of regional-scale photochemical modeling systems: Part I-meteorological predictions. *Atmospheric Environment* **35**, 4159-4174.
- Houyoux, M., Vukovich, J., Brandmeyer, J., Seppanen, C., and Holland, A. 2004. SMOKE user manual version 2. Carolina Environmental Program, NC.
- Jacobson, M., and Turco, R., 1994. SMVGear: A sparse matrix, vectorized gear code for atmospheric models. *Atmospheric Environment* **28**, 273-284.
- Jiang, G., 2001. Photochemical air quality modeling in the Puget Sound region. PhD dissertation, Washington State University, Department of Chemistry, Pullman, WA.
- Jiang, W., Hedley, M., and Singleton, D., 1998. Comparison of the MC2/CALGRID and SAIMM/UAM-V photochemical modeling systems in the Lower Fraser Valley, British Columbia. *Atmospheric Environment* **32(17)**, 2969-2980.
- Jun, M., and Stein, M., 2004. Statistical comparison of observed and CMAQ modeled daily sulfate levels. *Atmospheric Environment* **38**, 4427-4436.
- Killin, R., Simonich, S., Jaffe, D., DeForest, C., and Wilson, G., 2004. Transpacific and regional atmospheric transport of anthropogenic semi-volatile organic compounds to Cheeka Peak Observatory during the spring of 2002. *Journal of Geophysical Research* **109**, D23S24
- McInnes, L., Quinn, P., Covert, D., and Anderson, T., 1996. Gravimetric analysis, ionic composition, and associated water mass of the marine aerosol. *Atmospheric Environment* **30 (6)**, 869-884.
- Mebust, M., Eder, B., Binkowski, F., and Roselle, S., 2003. Models-3 community Multiscale Air Quality (CMAQ) model aerosol component: 2. model evaluation. *Journal of Geophysical Research* **108 (D6)**, 4184.
- Millet, D., Goldstein, A., Allan, J., Bates, T., Boudries, H., Bower, K., Coe, H., Ma, Y., McKay, M., Quinn, P., Sullivan, A., Weber, R., and Worsnop, D., 2004. Volatile organic compound measurements at Trinidad Head, California, during ITCT 2K2: analysis of sources, atmospheric composition, and aerosol residence times. *Journal of Geophysical Research* **109**, D23S16.
- O'Neill, S. 2002. Modeling ozone and aerosol formation and transport in the Pacific Northwest and calculating fractional source contributions to downwind receptors. PhD dissertation, Department of Civil and Environmental Engineering, Washington State University.
- O'Neill, S., and Lamb, B., 2005. Intercomparison of the Community Multi-Scale Air Quality model and CALGRID using process analysis. *Environmental Science and Technology* **39**, 5742-5753.
- Pleim, J., and Chang, J., 1992. A non-local closure model in the convective boundary layer. *Atmospheric Environment* **26A**, 965-981.
- Pleim, J., and Mathur, R., 2005. Diagnostic evaluation, sensitivity analyses, and new development in the Eta/CMAQ air quality forecast system. Paper presented at the 7th Conference on Atmospheric Chemistry organized by the American Meteorological Society. January 10-13, 2005. San Diego, CA.
- Quinn, P., Marshall, S., Bates T., Covert, D., and Kapustin, V., 1995. Comparison of measured and calculated aerosol properties relevant to the direct radiative forcing of tropospheric sulfate aerosol on climate. *Journal of Geophysical Research* **100 (D5)**, 8977-8991.

- Stockwell, W., Middleton, P., Chang, J., and Tang, X., 1990. The second-generation regional acid deposition model chemical mechanism for regional air quality modeling. *Journal of Geophysical Research* **95 (D10)**, 16,343-16,367.
- United States Environmental Protection Agency (USEPA), 2005. AIRNow air quality forecast project (<http://airnow.gov/>).
- Vaughan, J., Lamb, B., Frei, C., Wilson, R., Bowman, C., Figueroa-Kaminsky, C., Otteson, S., Boyer, M., Mass, C., Albright, M., Koenig, J., Collingwood, A., Gilroy, M., and Maykut, N. 2004. A numerical daily air quality forecast for the Pacific Northwest. *Bulletin of the American Meteorological Society* **85**, 549-561.
- Yamartino, R., Scire, J., Carmichael, G., Chang, Y., 1992. The CALGRID mesoscale photochemical grid model CI, Model formulation. *Atmospheric Environment* **26**, 1493-1512.

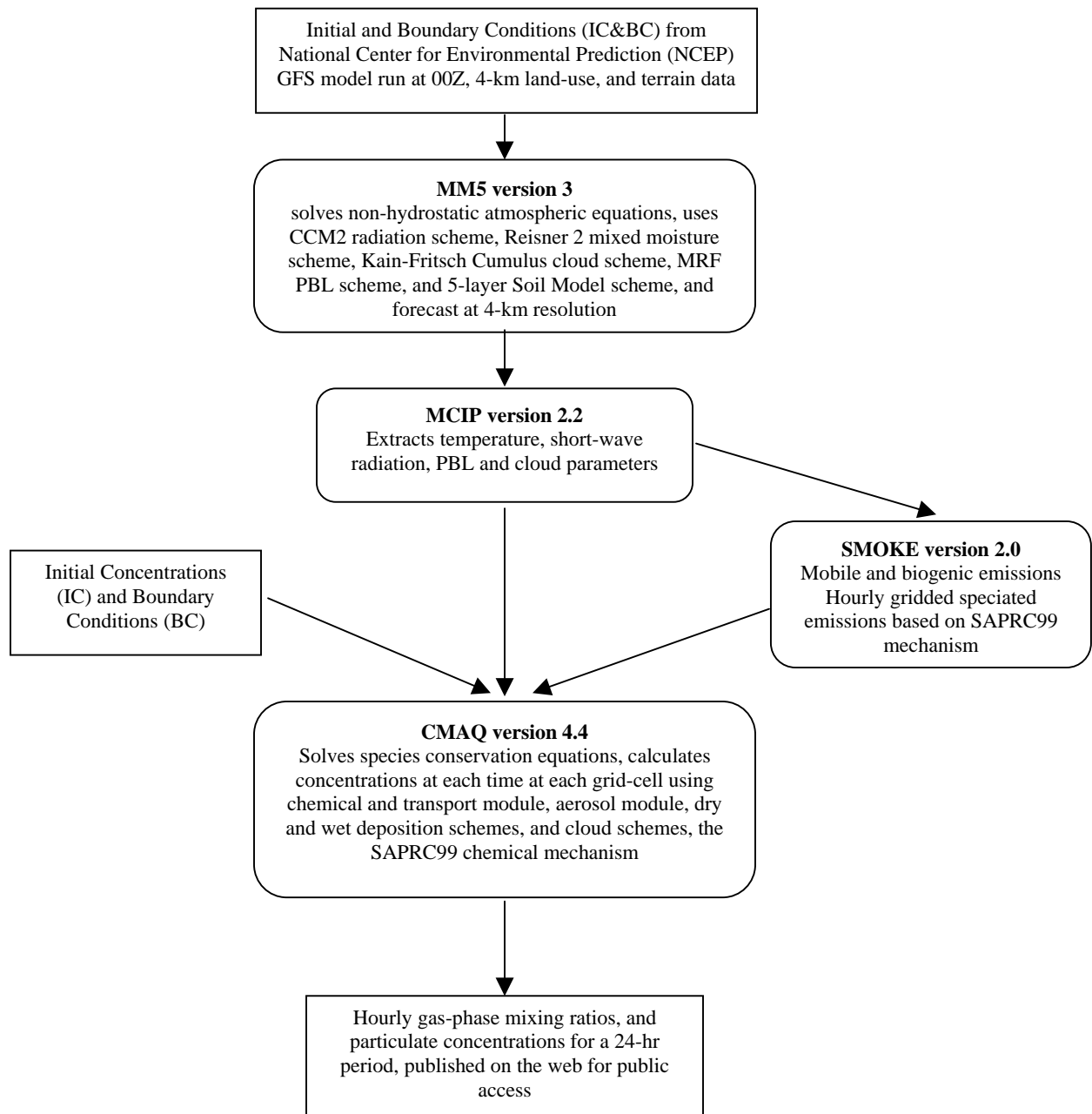


Figure 1: Schematic diagram of the modified AIRPACT2 forecast system. Rounded boxes represent main models/processors and square boxes represent input/output files.

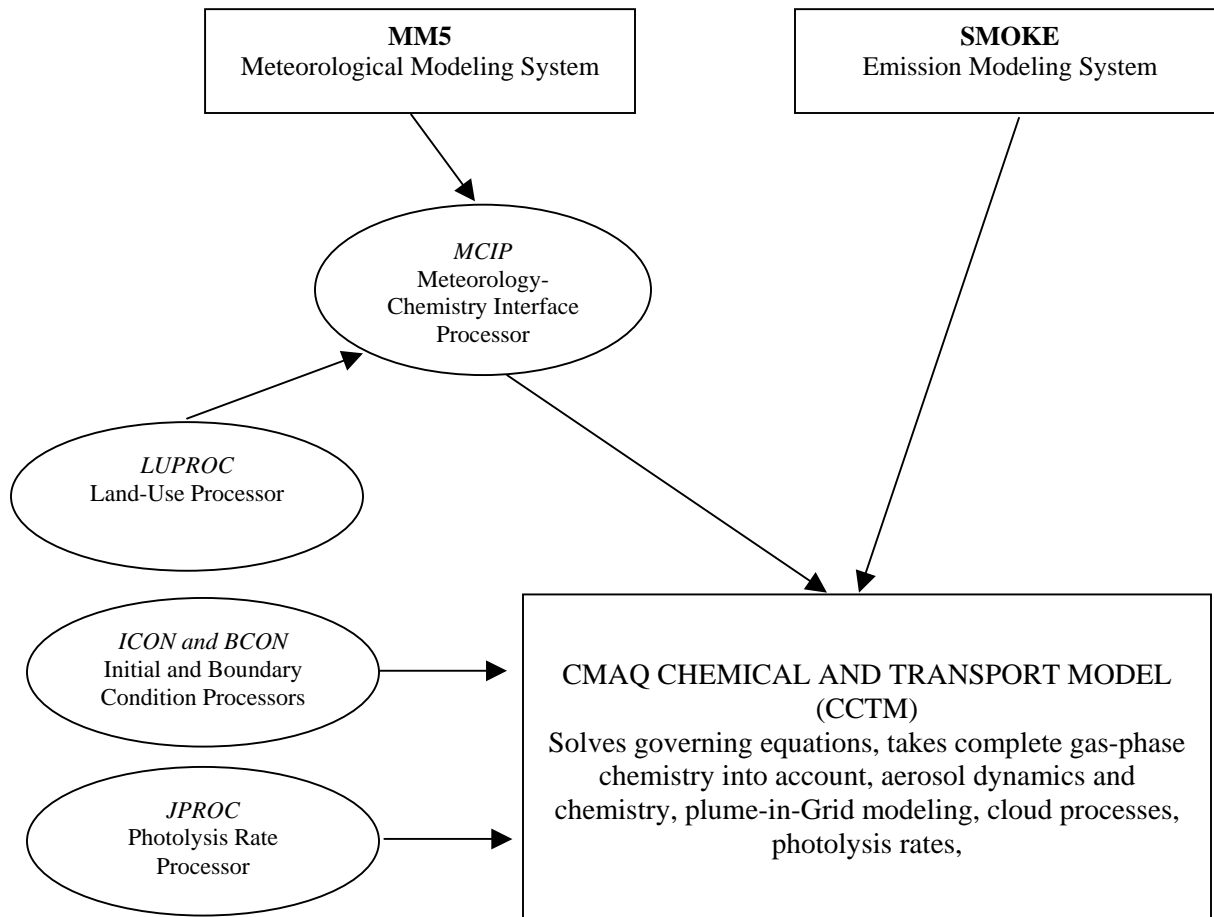


Figure 2: Major components in the CMAQ modeling system (*adapted from Ching and Byun, 1999*). Circles represent processors and boxes represent main models.

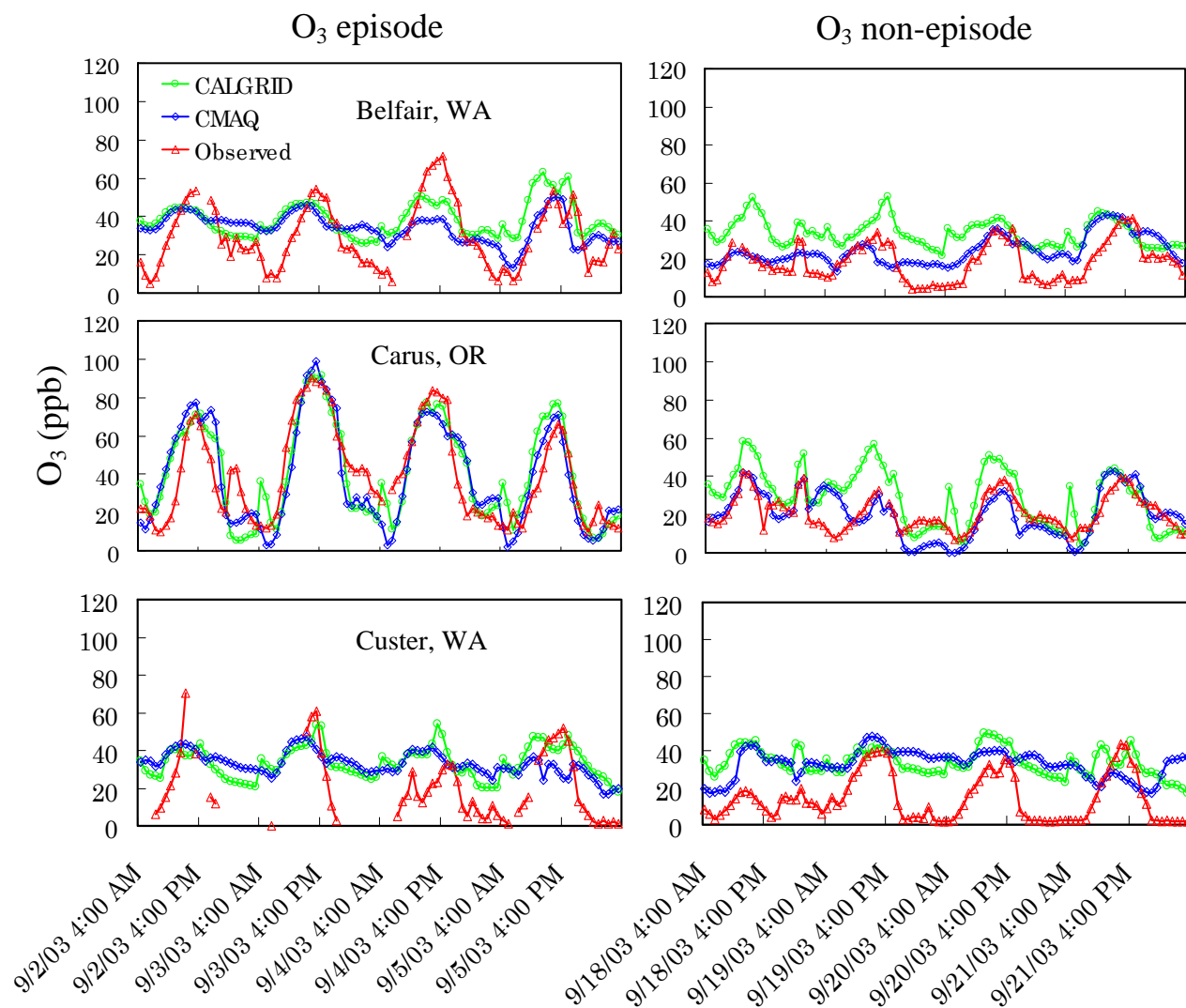


Figure 3 (cont.): Hourly O₃ mixing ratios during the episode (September 2-5, 2003), and the non-episode (September 18-21, 2003) periods for sites in WA and OR.

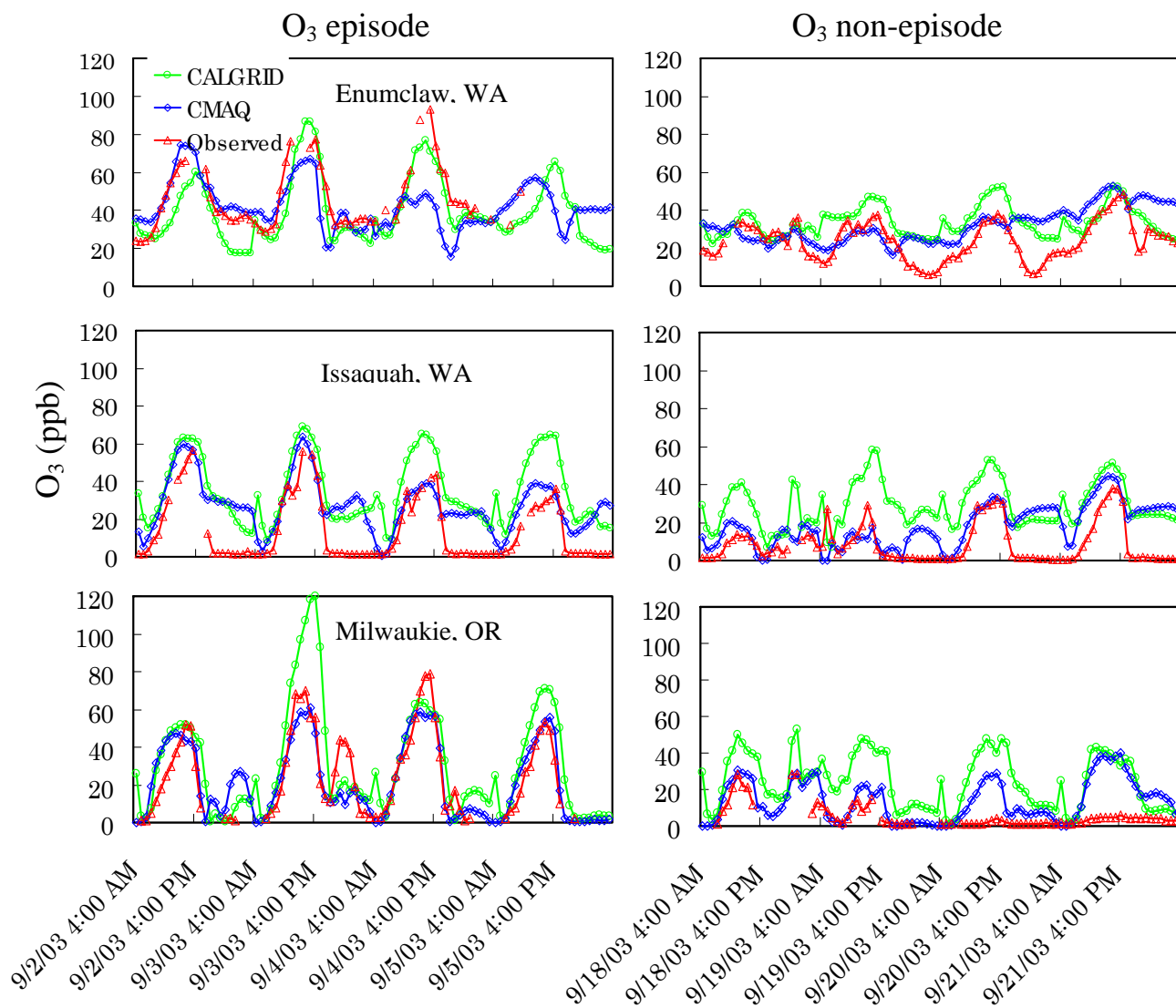


Figure 3 (cont.): Hourly O₃ mixing ratios during the episode (September 2-5, 2003), and the non-episode (September 18-21, 2003) periods for sites in WA and OR.

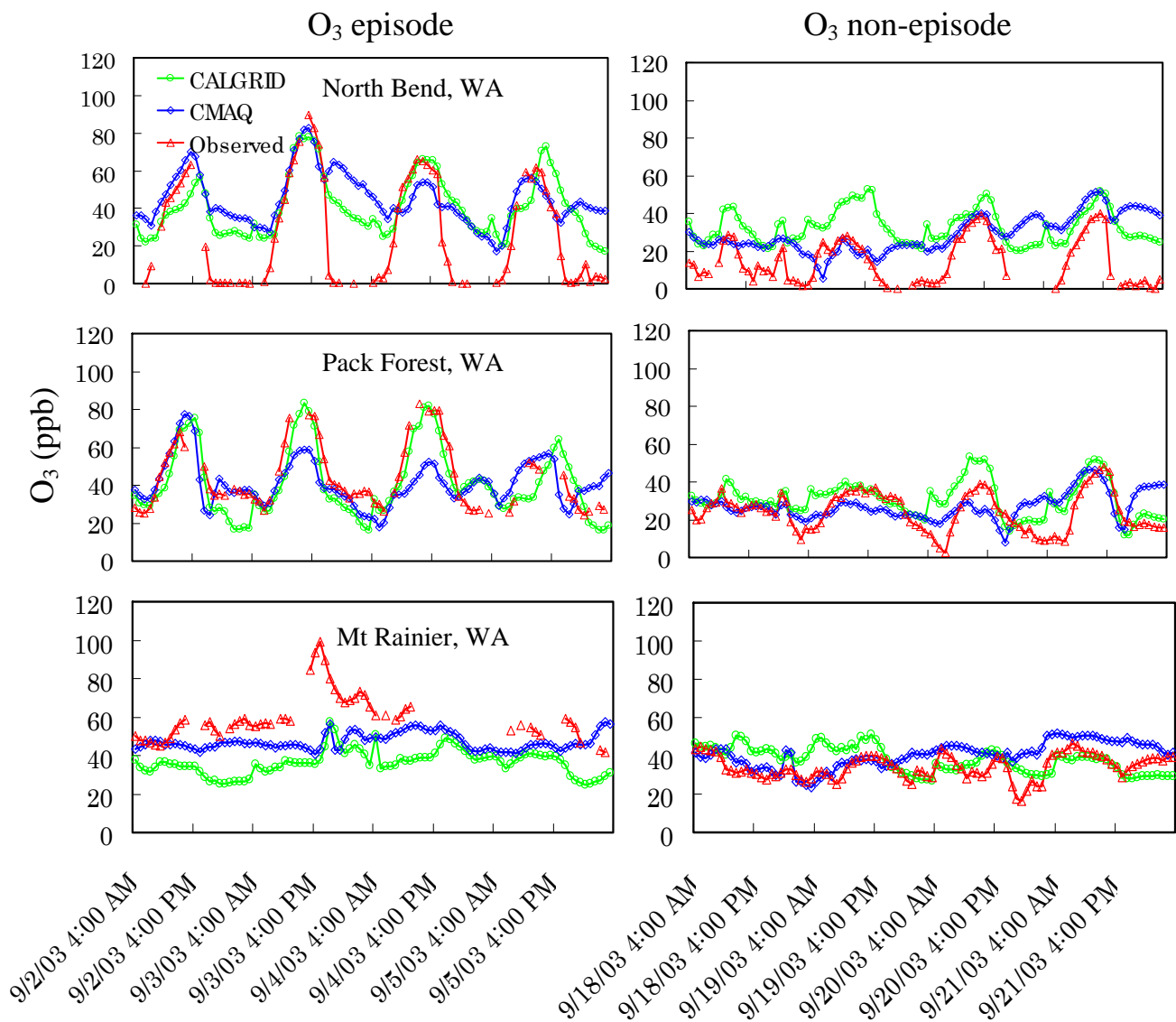


Figure 3 (cont.): Hourly O₃ mixing ratios during the episode (September 2-5, 2003), and the non-episode (September 18-21, 2003) periods for sites in WA and OR.

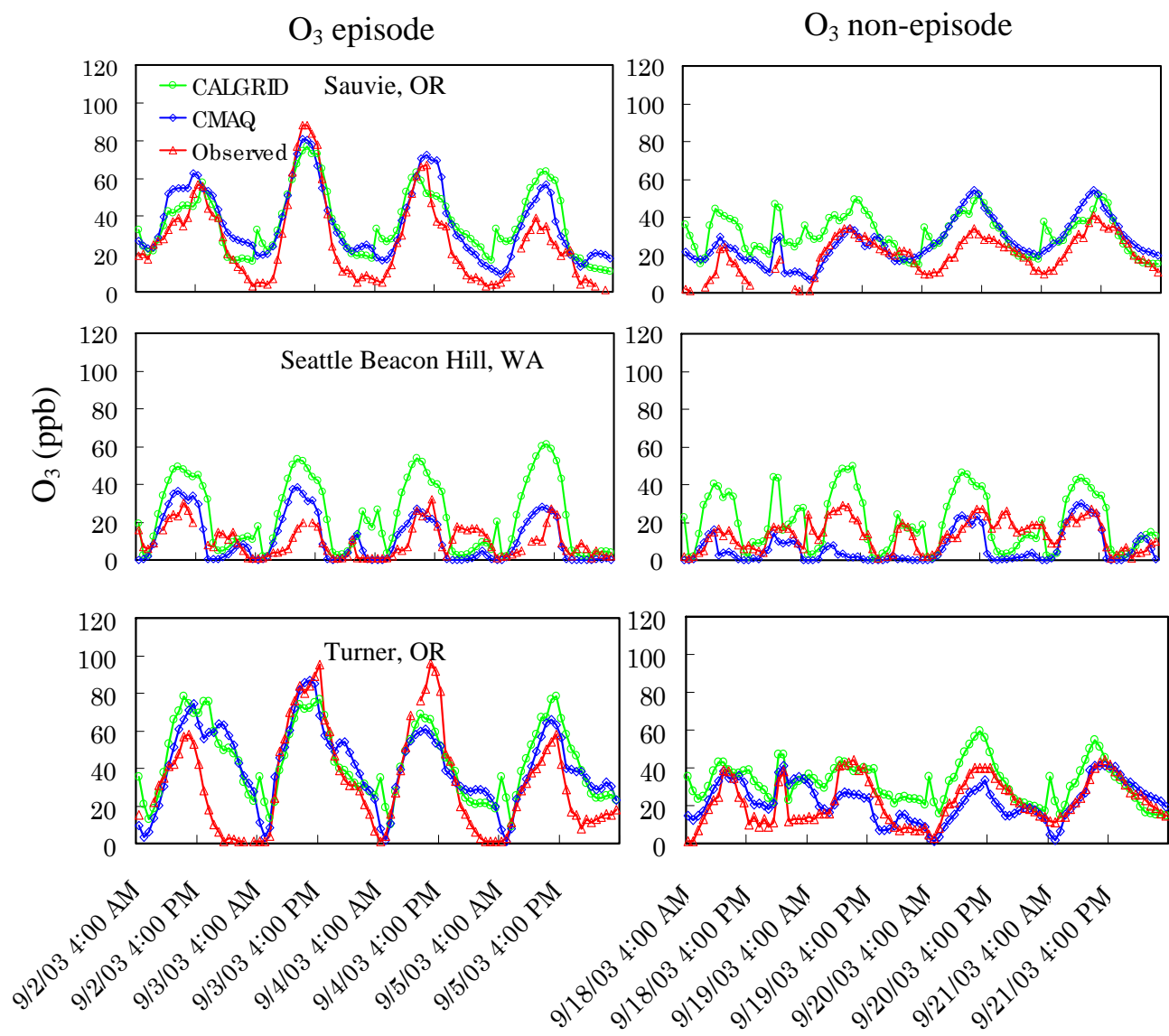


Figure 3 (cont.): Hourly O₃ mixing ratios during the episode (September 2-5, 2003), and the non-episode (September 18-21, 2003) periods for sites in WA and OR.

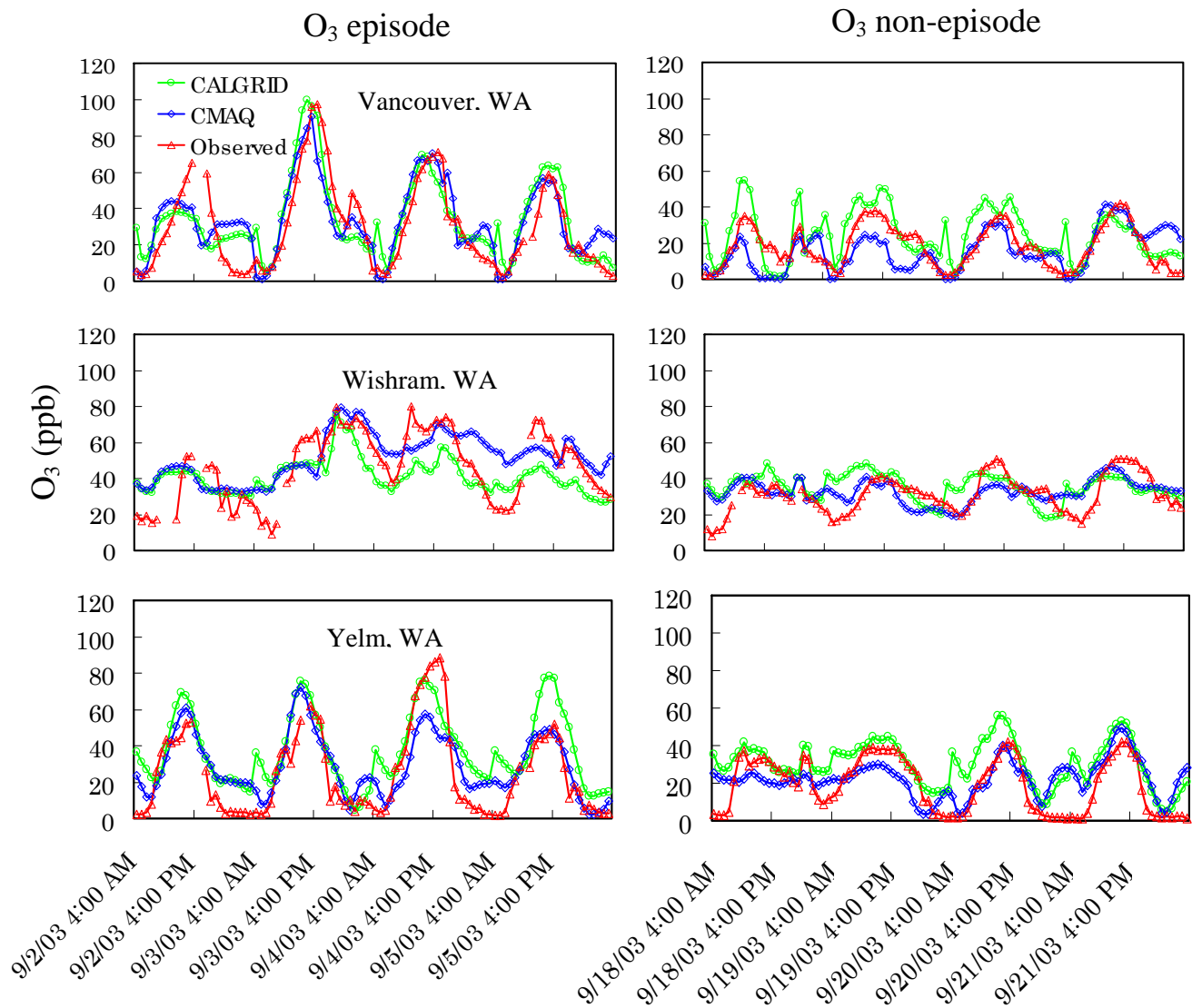


Figure 3: Hourly O₃ mixing ratios during the episode (September 2-5, 2003), and the non-episode (September 18-21, 2003) periods for sites in WA and OR.

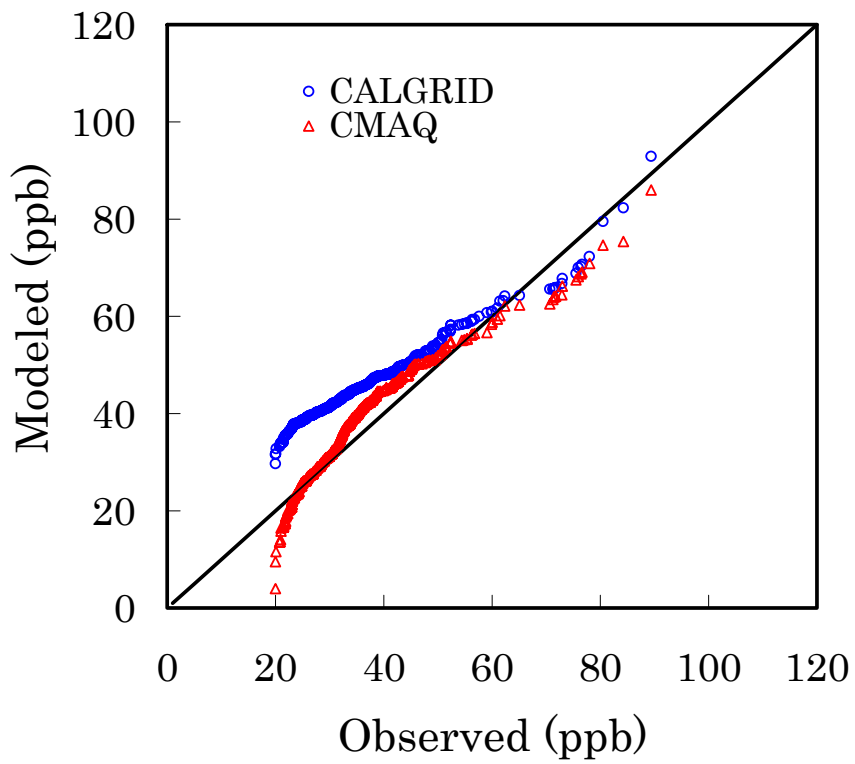


Figure 4: A Q-Q plot of O₃ modeled and observed data points (unpaired in time and space) for September 2003. The solid line represents 1:1 relationship between modeled and observed O₃.

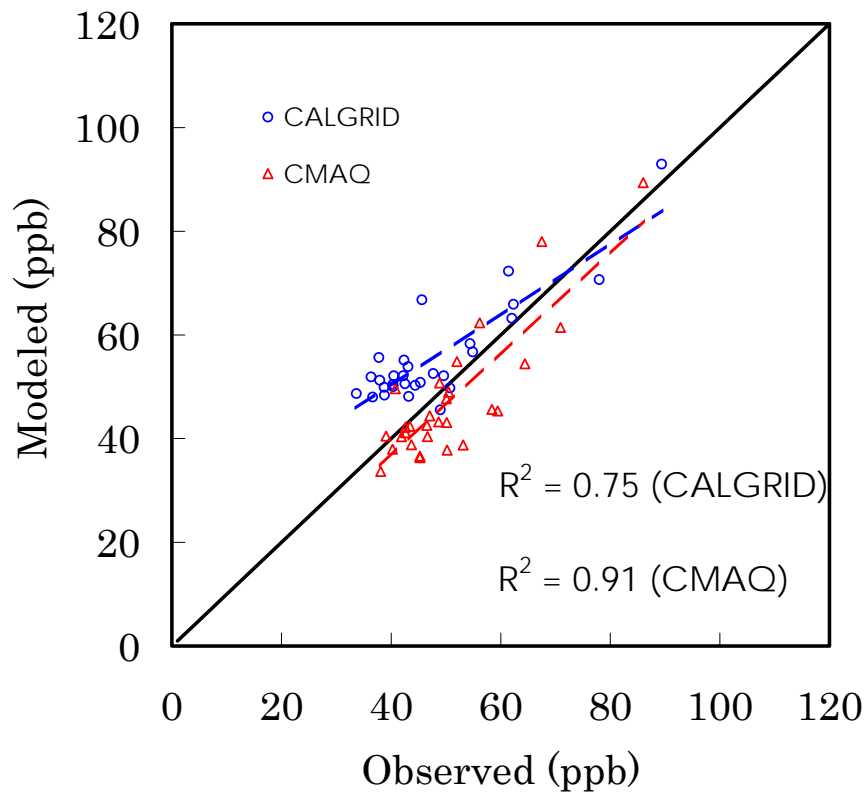


Figure 5: 8-hr daily maximum observed and corresponding modeled 8-hr daily maximum O₃ within 15 sites (paired in time). Dashed lines represent linear trend lines for CALGRID (open circles) and CMAQ (open triangles)

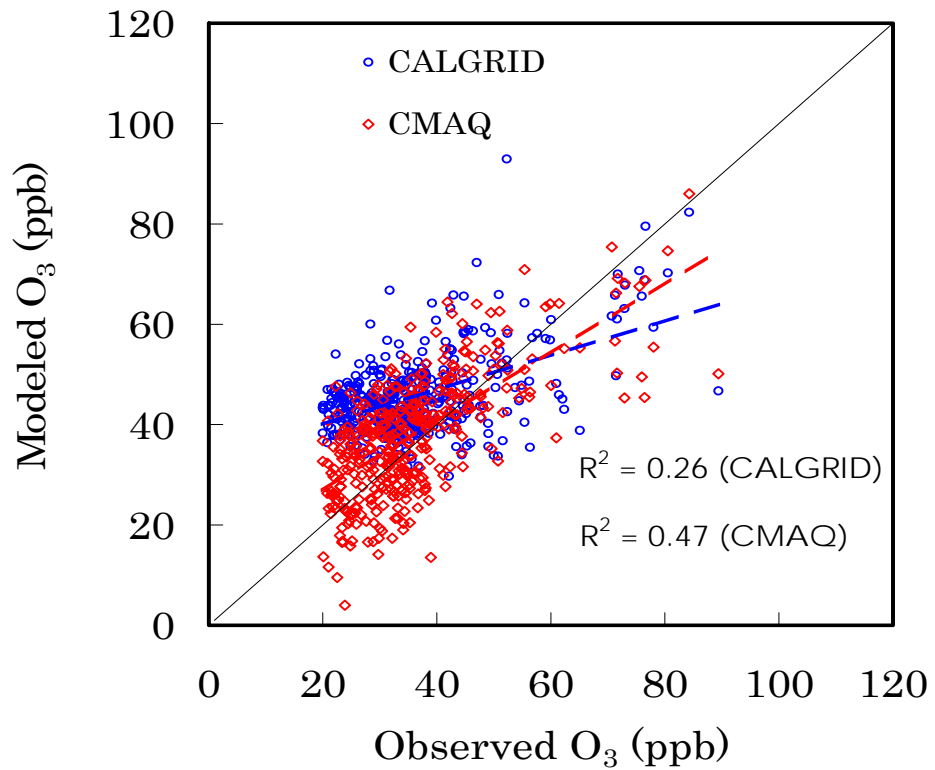


Figure 6: Scatter plot of observed versus modeled data points: CALGRID (open circles) and CMAQ (open diamonds). Note that the data are paired in time and space. Dashed lines represent linear trend lines of modeled O₃.

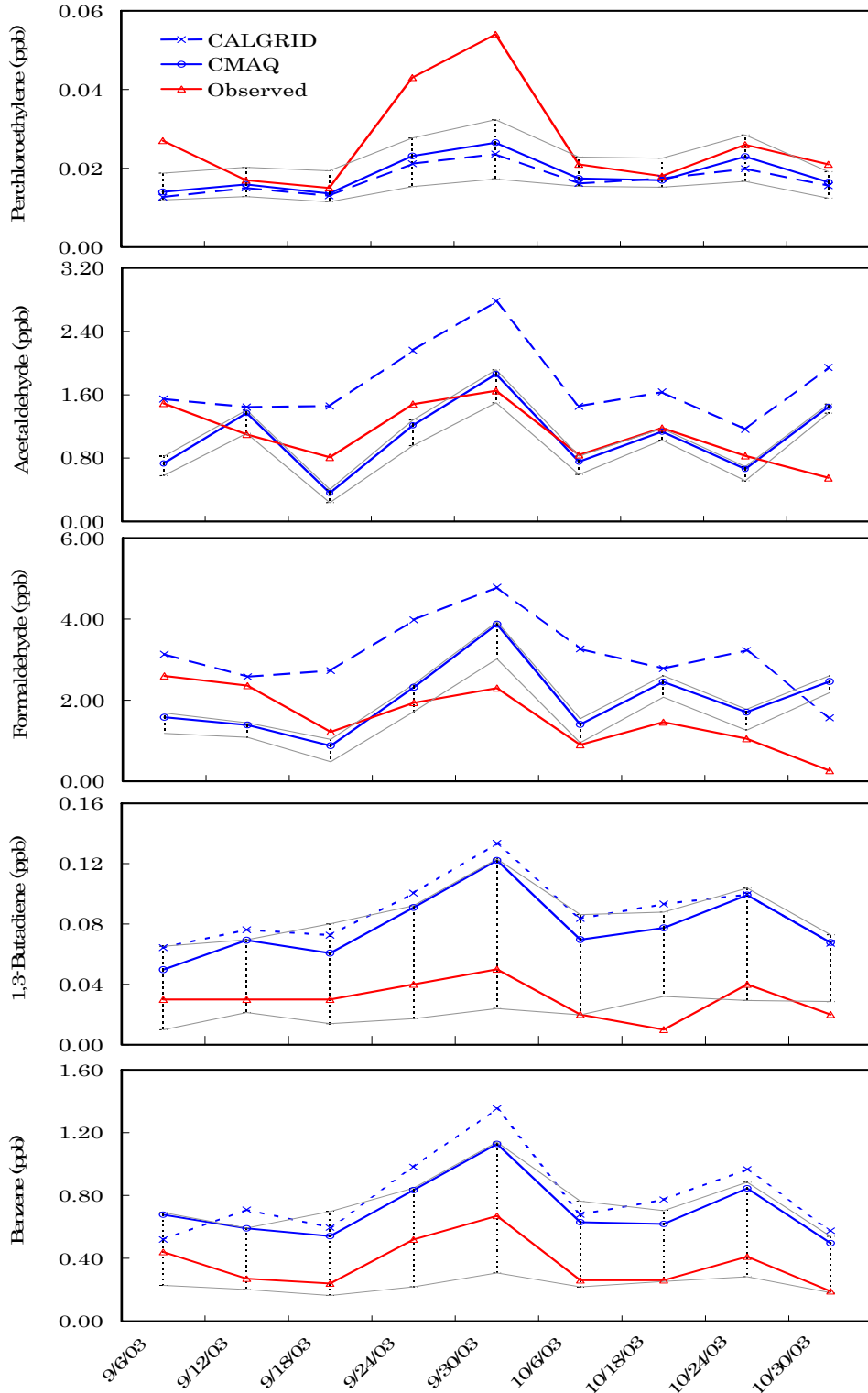


Figure 7: 24-hr average modeled and observed air toxics mixing ratios at Seattle Beacon Hill. Error bars associated with CMAQ modeled air toxics represent the maximum and the minimum levels within the 3 x 3 grid-cell matrix.

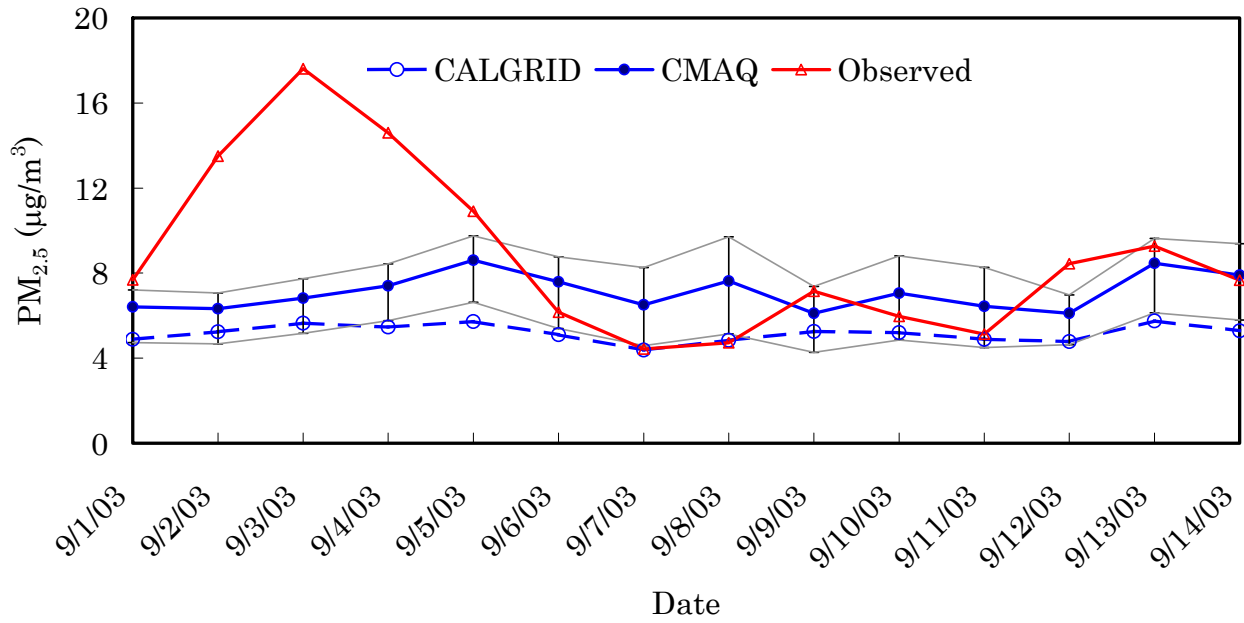


Figure 8: Time series of 24-hr average $PM_{2.5}$ modeled and observed concentrations. The plot is based on average data obtained from 12 monitoring stations in WA during September 1-14, 2003. The error bars associated with the modeled concentrations represent the maximum and the minimum modeled concentrations of $PM_{2.5}$ within the 3 x 3 grid-cell matrix.

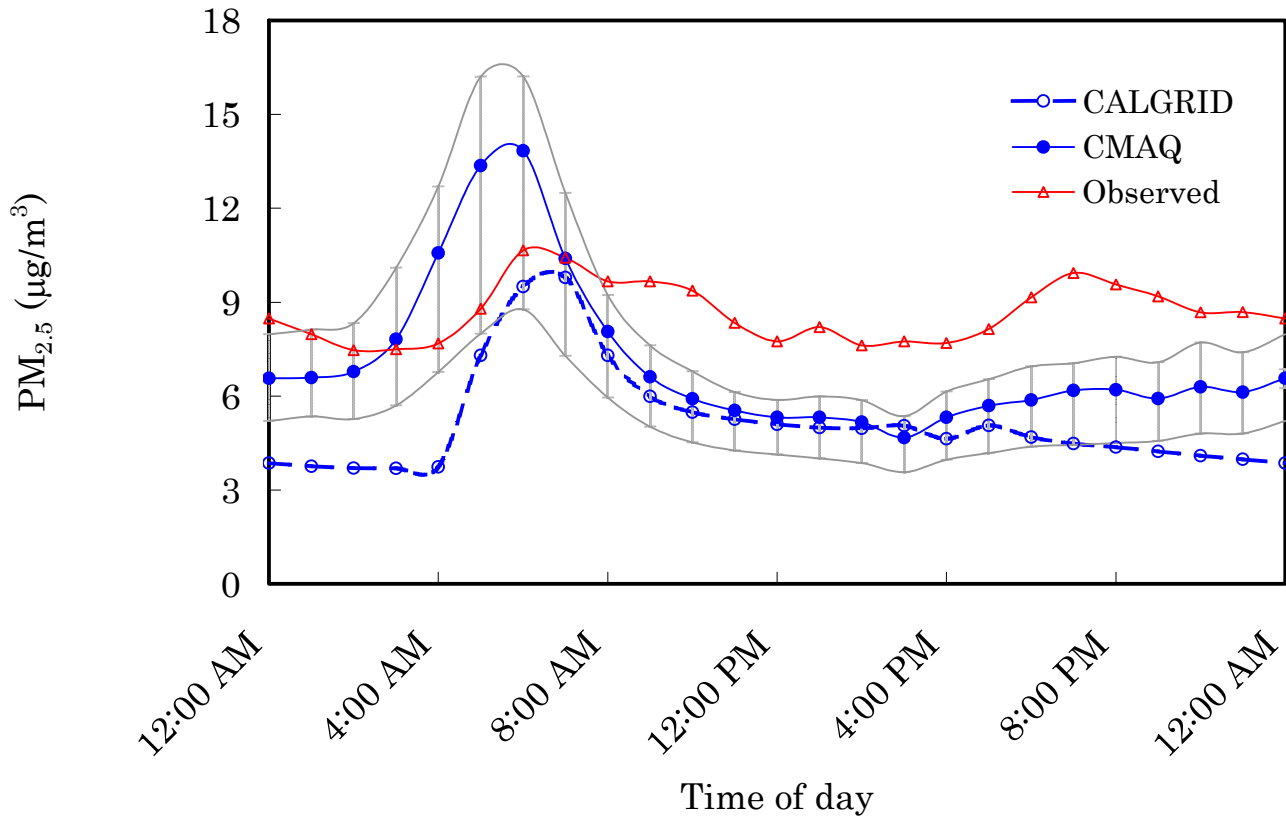
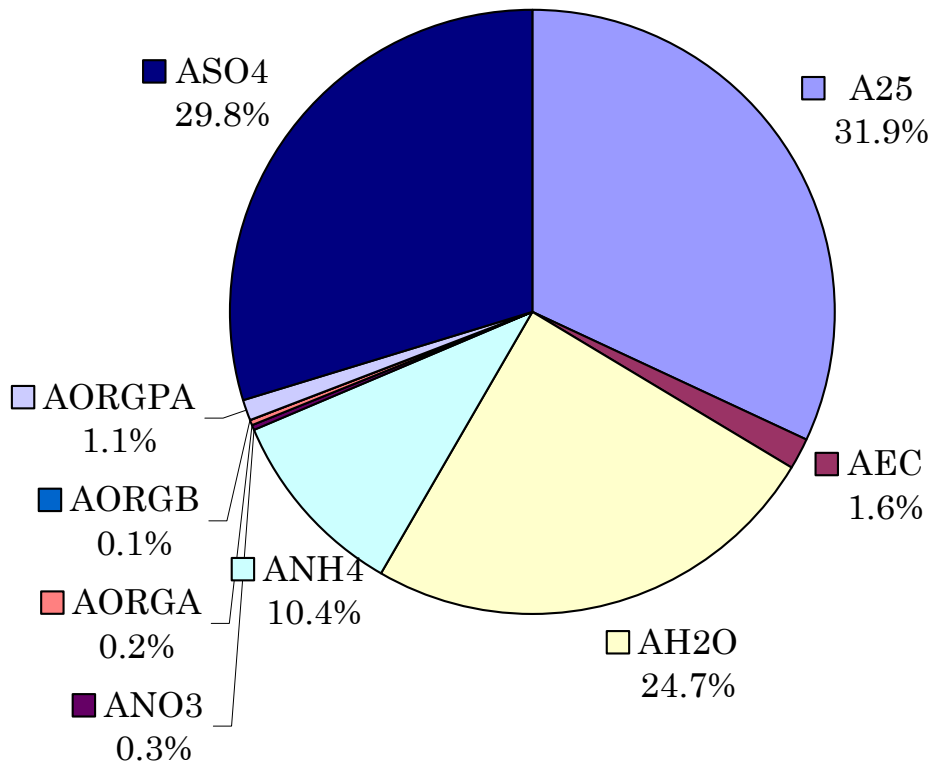


Figure 9: Diurnal patterns of modeled and observed concentrations of PM_{2.5}. Error bars show the maximum and the minimum modeled concentrations of PM_{2.5} within the 3 x 3 grid-cell matrix.



Legend description:

A25	Unspecified anthropogenic mass
AEC	Elemental carbon mass
AH2O	Water mass
ANH4	Ammonium mass
ANO3	Nitrate mass
AORGA	Secondary anthropogenic organic mass
AORGB	Secondary biogenic organic mass
AORGPA	Primary organic mass
ASO4	Sulfate mass

Figure 10: Partial contributions of aerosol species to the fine particulate mass ($PM_{2.5}$). Note that each species includes both the Aitkin (*i* th) mode and the accumulation (*j* th) mode particles.

Table 1: CMAQ Initial Conditions (ICON) and Boundary Conditions (BCON) for the western boundary.

CMAQ Species	Initial Concentrations	Reference
AECJ	0.050 $\mu\text{g}/\text{m}^3$	McInnes <i>et al.</i> , 1996
AH2OJ	0.510 $\mu\text{g}/\text{m}^3$	McInnes <i>et al.</i> , 1996
ALD	0.001 $\mu\text{g}/\text{m}^3$	Jiang (2001)
ANH4I	0.018 $\mu\text{g}/\text{m}^3$	Quinn <i>et al.</i> , 1995
ANH4J	0.114 $\mu\text{g}/\text{m}^3$	Heubert <i>et al.</i> , 1998
ANO3J	0.063 $\mu\text{g}/\text{m}^3$	Heubert <i>et al.</i> , 1998
ASO4I	0.292 $\mu\text{g}/\text{m}^3$	Quinn <i>et al.</i> , 1995
ASO4J	0.648 $\mu\text{g}/\text{m}^3$	Heubert <i>et al.</i> , 1998
BENZENE	0.00008 ppm	Millet <i>et al.</i> , 2004
BUTADIENE13	0.00002 ppm	Finlayson-Pitts and Pitts, 2000
C2Cl4	0.00001 ppm	Killin <i>et al.</i> , 2004
CH2O	0.00016 ppm	Atlas and Ridley, 1996
CO	0.170 ppm	Millet <i>et al.</i> , 2004
H2O2	0.002 ppm	Jiang (2001)
HC5	0.003 ppm	Jiang (2001)
HC8	0.001 ppm	Jiang (2001)
HCHO	0.002 ppm	Jiang (2001)
HNO3	0.002 ppm	Jiang (2001)
ISO	0.004 ppm	Jiang (2001)
KET	0.008 ppm	Jiang (2001)
NO2	0.001 ppm	Jiang (2001)
NUMACC	8.6E+07 #/ m^3	Quinn <i>et al.</i> , 1995
NUMATKN	3.5E+08 #/ m^3	Quinn <i>et al.</i> , 1995
NUMCOR	5.6E+06 #/ m^3	Quinn <i>et al.</i> , 1995
O3	0.0400 ppm	Jiang (2001)
OL2	0.0005 ppm	Jiang (2001)
OLI	0.0004 ppm	Jiang (2001)
OLT	0.0002 ppm	Jiang (2001)
TOL	0.0004 ppm	Jiang (2001)
XYL	0.0005 ppm	Jiang (2001)

Table 2: CMAQ O₃ prediction performance statistics for September 2003. Statistical measures were calculated using 8-hr daily maximum mixing ratios with a 20 ppb of observed O₃ cutoff. Results in max and min columns represent the statistics for the maximum and the minimum O₃ mixing ratios predicted within the 3 x 3 grid-cell matrix.

	8-hr daily max observed (ppb)	MB (ppb)			FB (%)			ME (ppb)			FE (%)		
		Max	Monitor	Min	Max	Monitor	Min	Max	Monitor	Min	Max	Monitor	Min
Urban Sites													
Issaquah	45	12	6	-1	32	16	-5	12	8	6	36	24	21
Milwaukie	57	7	1	-3	18	0	-12	11	7	8	30	23	29
Seattle Beacon Hill	35	9	-4	-5	23	-23	-28	11	7	8	34	37	40
Vancouver	77	3	-2	-5	7	-11	-20	9	8	8	25	28	31
<i>Average</i>	<i>53</i>	<i>8</i>	<i>0</i>	<i>-3</i>	<i>20</i>	<i>-4</i>	<i>-16</i>	<i>11</i>	<i>8</i>	<i>7</i>	<i>31</i>	<i>28</i>	<i>30</i>
Semi-urban/ Rural Sites													
Belfair	61	2	0	-1	4	0	-4	5	5	5	13	13	14
Carus	84	6	4	0	16	11	-2	9	8	7	24	23	24
Custer	56	5	4	1	14	10	4	9	8	8	25	25	26
Enumclaw	73	5	3	-1	14	9	-2	8	7	8	19	18	20
Mt. Rainier	72	9	6	3	26	16	10	11	10	9	30	28	25
North Bend	76	5	2	-1	12	6	-1	9	8	7	21	20	19
Pack Forest	89	4	3	-2	10	8	-2	9	8	7	19	17	15
Sauvie Island	73	9	7	3	21	16	7	10	9	8	27	25	24
Turner	81	6	0	-1	13	1	-4	11	9	9	27	25	25
Wishram	71	-1	-2	-3	-3	-5	-8	5	5	5	11	12	13
Yelm	76	2	0	-2	5	-1	-7	9	8	7	24	23	23
<i>Average</i>	<i>74</i>	<i>5</i>	<i>2</i>	<i>0</i>	<i>12</i>	<i>6</i>	<i>-1</i>	<i>8</i>	<i>8</i>	<i>7</i>	<i>22</i>	<i>21</i>	<i>21</i>

Table 3: Performance statistics for CALGRID and CMAQ for O₃ prediction.

Urban Sites	Observed daily 8-hr max (ppb)	MB (ppb)		FB (%)		ME (ppb)		FE (%)	
		CALGRID	CMAQ	CALGRID	CMAQ	CALGRID	CMAQ	CALGRID	CMAQ
Issaquah	45	19	6	51	16	19	8	51	24
Milwaukie	57	15	1	39	0	16	7	41	23
Seattle Beacon Hill	35	16	-4	49	-23	16	7	49	37
Vancouver	77	7	-2	21	-11	11	8	30	28
Average	63	14	0	40	-4	16	8	43	28
Semi-urban/ Rural Sites									
Belfair	61	9	0	23	0	10	5	25	13
Carus	84	12	4	33	11	14	8	36	23
Custer	56	8	4	24	10	10	8	27	25
Enumclaw	73	4	3	14	9	10	7	25	18
Mt. Rainier	89	0	6	2	16	9	10	19	28
North Bend	72	12	2	34	6	13	8	36	20
Pack Forest	76	8	3	23	8	10	8	25	17
Sauvie Island	73	11	7	31	16	12	9	32	25
Turner	81	11	0	28	1	15	9	34	25
Wishram	71	0	-2	2	-5	7	5	15	12
Yelm	76	13	0	32	-1	14	8	33	23
Average	74	8	1	22	6	11	8	28	21

Table 4: First order reactions for primary air toxics, and their rate constants incorporated in the CMAQ chemical mechanisms.

Model	Reactions of air toxics	Rates
CMAQ	<p>1,3-Butadiene</p> ¹ BUTADIENE13 + HO = PRODUCTS ¹ BUTADIENE13 + O3 = PRODUCTS ¹ BUTADIENE13 + NO3 = PRODUCTS ¹ BUTADIENE13 + O3P = PRODUCTS	$k = 1.48 \times 10^{-11} \exp[4.48 \times 10^2/T]$ $k = 1.34 \times 10^{-14} \exp[-2.283 \times 10^3/T]$ $k = 1.00 \times 10^{-13}$ $k = 1.98 \times 10^{-11}$
	<p>Benzene</p> ¹ BENZENE + HO = PRODUCTS ² BENZENE + NO3 = PRODUCTS ³ BENZENE + O3 = PRODUCTS	$k = 2.47 \times 10^{-12} \exp[-2.07 \times 10^2/T]$ $k = 3.01 \times 10^{-17}$ $k = 7.01 \times 10^{-23}$
	<p>Perchloroethylene</p> ¹ C2Cl4 + HO = PRODUCTS ⁴ C2Cl4 + NO3 = PRODUCTS ⁵ C2Cl4 + O3 = PRODUCTS	$k = 9.64 \times 10^{-12} \exp[-1.209 \times 10^3/T]$ $k = 1.79 \times 10^{-16}$ $k = 1.00 \times 10^{-21}$
CALGRID	<p>1,3-Butadiene</p> ¹ BUTD + HO = PRODUCTS	$k = 1.48 \times 10^{-11} \exp[4.48 \times 10^2/T]$
	<p>Benzene</p> ¹ BENZ + HO = PRODUCTS	$k = 2.47 \times 10^{-12} \exp[-2.07 \times 10^2/T]$
	<p>Perchloroethylene</p> ¹ PERC + HO = PRODUCTS	$k = 9.64 \times 10^{-12} \exp[-1.209 \times 10^3/T]$

¹Rate constants from toxic CMAQ provided by EPA (via Idaho Dept. of Ecology)

²Atkinson, R., Kinetics and mechanisms of the gas-phase reactions of the NO₃ radical with organic compounds, *J. Phys. Chem. Ref. Data*, 20, 459-507, 1991.

³Pate, C.T., Atkinson, R., and Pitts, J.N., Jr., The Gas Phase Reaction of O₃ with a Series of Aromatic Hydrocarbons, *J. Environ. Sci. Health Part A*, 11, --, 1976.

⁴Chew, A.A., Atkinson, R., and Aschmann, S.M., Kinetics of the gas-phase reactions of NO₃ radicals with a series of alcohols, glycol ethers, ethers and chloro-alkenes, *J. Chem. Soc. Faraday Trans.*, 94, 1083-1089, 1998.

⁵Atkinson, R., Baulch, D.L., Cox, R.A., Hampson, R.F., Kerr, J.A., Rossi, M.J., and Troe, J., Evaluated kinetic, photochemical and heterogeneous data for atmospheric chemistry: supplement V, IUPAC subcommittee on gas kinetic data evaluation for atmospheric chemistry, *J. Phys. Chem. Ref. Data*, 26, 521-1011, 1997.

Table 5: Ratio of air toxics compounds relative to benzene at Seattle Beacon Hill, WA.

Species	Emission ratio	Modeled ratio		Ambient ratio
		CALGRID	CMAQ	
Acetaldehyde	0.28	2.28	1.54	3.20
Formaldehyde	1.03	4.03	2.85	4.43
1,3-Butadiene	0.12	0.11	0.11	0.09
Perchloroethylene	0.01	0.02	0.03	0.07

Table 6: List of aerosol species treated in CMAQ that account for total PM_{2.5} concentration.

Species	Name
A25I	Aitken mode unspecified anthropogenic mass
A25J	Accumulation mode unspecified anthropogenic mass
AECI	Aitken mode elemental carbon mass
AECJ	Accumulation mode elemental carbon mass
AH2OI	Aitken mode water mass
AH2OJ	Accumulation mode water mass
ANH4I	Aitken mode ammonium mass
ANH4J	Accumulation mode ammonium mass
ANO3I	Aitken mode nitrate mass
ANO3J	Accumulation mode nitrate mass
AORGAI	Aitken mode secondary anthropogenic organic mass
AORGAJ	Accumulation mode secondary anthropogenic organic mass
AORGBI	Aitken mode secondary biogenic organic mass
AORGBJ	Accumulation mode secondary biogenic organic mass
AORGPAI	Aitken mode primary organic mass
AORGPAJ	Accumulation mode primary organic mass
ASO4I	Aitken mode sulfate mass
ASO4J	Accumulation mode sulfate mass

Table 7: Performance statistics of CMAQ for PM_{2.5} predictions. Note that 24-hr average data were calculated using hourly PM_{2.5} concentration from September 1 to September 14, 2003).

Sites	24-hr average observed ($\mu\text{g}/\text{m}^3$)	MB ($\mu\text{g}/\text{m}^3$)			FB (%)			ME ($\mu\text{g}/\text{m}^3$)			FE (%)		
		Max	Monitor	Min	Max	Monitor	Min	Max	Monitor	Min	Max	Monitor	Min
Bellevue	8	1	0	-2	22	14	-19	3	3	3	44	39	34
Kent	10	0	-2	-4	12	-5	-32	4	5	5	54	47	48
Lacey	7	0	-1	-3	-5	-20	-42	2	2	3	35	35	45
Lake Forest Park	7	0	-2	-2	2	-19	-33	2	2	2	38	33	36
Lynwood	8	-1	-3	-4	-4	-25	-51	3	3	4	37	38	51
Marysville	9	-2	-3	-5	-25	-35	-65	4	4	5	43	43	65
North Bend	7	1	-1	-3	14	-9	-36	4	5	5	65	69	66
Seattle Beacon Hill	9	-1	-2	-4	21	13	-34	4	4	4	41	37	38
Seattle Duwamish Valley	12	-1	-2	-6	-6	-17	-58	5	3	6	27	28	58
Tacoma Port	12	-3	-4	-6	-11	-29	-48	5	5	6	36	41	52
Tacoma South St.	9	-1	-2	-4	3	-12	-40	3	3	4	36	31	44
Vancouver	8	0	-1	-3	11	-4	-29	3	3	3	39	34	38
<i>Average</i>	9	-1	-2	-4	3	-12	-41	4	4	4	41	40	48

Table 8: Performances of CALGRID and CMAQ models in predicting PM_{2.5} concentrations.

Site	24-hr average observed (µg/m ³)	MB (µg/m ³)		FB (%)		ME (µg/m ³)		FE (%)	
		CALGRID	CMAQ	CALGRID	CMAQ	CALGRID	CMAQ	CALGRID	CMAQ
Bellevue	8	-1	0	-11	14	3	3	35	39
Kent	10	-4	-2	-32	-5	4	5	39	47
Lacey	7	-3	-1	-44	-20	3	2	44	35
Lake Forest Park	7	-2	-2	-31	-19	2	2	33	33
Lynwood	8	-4	-3	-42	-25	4	3	44	38
Marysville	9	-5	-3	-62	-35	5	4	62	43
North Bend	7	-4	-1	-40	-9	4	5	50	69
Seattle Beacon Hill	9	-4	-2	-18	13	4	4	35	37
Seattle Duwamish Valley	12	-5	-2	-54	-17	5	3	54	28
Tacoma Port	12	-6	-4	-55	-29	6	5	55	41
Tacoma South St.	9	-4	-2	-41	-12	4	3	43	31
Vancouver	8	-3	-1	-29	-4	3	3	36	34
Average	9	-4	-2	-38	-12	4	4	44	40

APPENDIX I

Table 1: List of air quality monitoring stations

SL No.	Acronym	Location	Species
1	Belfair	71 E Campus Dr, Belfair, WA	O ₃
2	Bellevue	Aquatic Center, 601 143rd Ave NE, Bellevue, WA	PM _{2.5}
3	Carus	Spangler Road, Carus, OR	O ₃
4	Custer	1330 Loomis Trail Rd, Custer, WA	O ₃
5	Duwamish Valley	4752 E Marginal Way S, Seattle Duwamish Valley, WA	PM _{2.5}
6	Enumclaw	30525 SE Mud Mountain Road, Enumclaw, WA	O ₃
7	Issaquah	20050 SE 56th, Lake Sammamish State Park, Issaquah, WA	O ₃
8	Kent	James St and Central Ave, Kent, WA	PM _{2.5}
9	Lacey	Mt View Elem School, 1900 College St SE, Lacey, WA	PM _{2.5}
10	Lake Forest Park	17171 Bothell Way NE, Lake Forest Park, WA	PM _{2.5}
11	Lynnwood	6120 212th St, SW Lynnwood, WA	PM _{2.5}
12	Marysville	Marysville JHS, 1605 7th St, Marysville, WA	PM _{2.5}
13	Milwaukie	23rd St. St. Johns Church, Milwaukie, OR	O ₃
14	Mt. Rainier	Mt Rainier National Park, Jackson Visitor Center, WA	O ₃
15	North Bend	42404 SE North Bend Way, North Bend, WA	O ₃ , PM _{2.5}
16	Pack Forest	Charles L Pack Forest, La Grande, WA	O ₃
17	Savie Island	Rte. 1, Box 442 -Soc. Sec Beach, Sauvie Island, OR	O ₃
18	Seattle Beacon Hill	15th S and Charlestown, Seattle Beacon Hill, WA	O ₃ , PM _{2.5} , air toxics
19	Tacoma	7802 South L St, Tacoma, WA	PM _{2.5}
20	Tacoma Port	2301 Alexander Ave, Tacoma Port, WA	PM _{2.5}
21	Turner	Turner, OR	O ₃
22	Vancouver Blairmount Dr	Mt View HS, 1500 SE Blairmount Dr, Vancouver, WA	O ₃
23	Vancouver Plain Blvd	8205 E 4th Plain Blv, Vancouver, WA	PM _{2.5}
24	Wishram	Hwy 14, Wishram, WA	O ₃
25	Yelm	709 Mill Road SE, Yelm	O ₃